"Until a few years ago meteorologists were not conscious of any problems regarding the change from cloud particles to rain drops. In their opinion the cloud particle, having once been formed, grows by continued condensation and coagulation until it is sufficiently large to fall as a raindrop."

Sir George Simpson, K.C.B., F.R.S.

Presidential Address,
Royal Meteorological Society.

January, 1941.

THE COLLISION AND COALESCENCE OF WATER DROPLETS

by

JOHN DAVID WOODS
Department of Physics
Imperial College of Science and Technology

A Thesis submitted for the
Degree of Doctor of Philosophy at the
University of London

January 1965

ABSTRACT

This thesis describes experimental investigations into the factors which influence the collision and coalescence of cloud drops. Experimental values have been obtained for the collection efficiencies of drops of up to 100μ radius colliding with (a) much smaller droplets, and (b) drops of the same size.

The results for dissimilar drops agree well with the theoretical values of Shafrir and Neiburger, and a subsidiary experiment confirmed Hocking's prediction that drops of smaller than 18μ radius do not capture droplets of any size.

Streak photographs of equal drops falling freely under gravity show that those with radii greater than 40μ collide spontaneously with collection efficiencies of nearly unity. This result is in conflict with theoretical computations by Pearcey and Hill, who predicted larger collection efficiencies, and by Shafrir and Neiburger, who predicted collection efficiencies of zero. The only previous experiment, by Telford et al., supported the former theory. It is suggested that Telford's results were interpreted incorrectly. A tentative collection efficiency diagram, based upon the experimental data, is proposed.

Perturbations to the drop trajectories caused by turbulent motions in the air are clearly visible in the streak photographs. It is suggested that this micro-turbulence caused the majority of collisions between equal drops of radii from 35 to 40μ . Similar collisions have been observed in a horizontal air jet which gave a wind shear of 10 sec^{-1} .

Streak photographs of equal drops carrying equal and opposite electric charges show how the drop trajectories are influenced by the electrical attraction. The increase in coalescence rate with drop charges is shown for collisions between equal drops of 16μ, 36μ and 40μ radius. The results are in good agreement with those obtained by Telford et al for 65μ radius drops.

CONTENTS

		Page
Abstract		3
Acknowledgements		11
Publications		12
CHAPTER 1	INTRODUCTION	13
1.1	A general statement of the problem	13
1.2	Historical introduction	14
1.3	Notation A. Theoretical	22
	B. Experimental	27
	C. Coalescence rate	28
	D. Coalescence efficiency	29
CHAPTER 2	A SURVEY OF PREVIOUS WORK	36
2.1	Theoretical analysis	
	A. Flow round an isolated drop	37
	B. Collision efficiency computations	49
2.2	Experimental investigations	62
	A. Indirect methods	63
	B. Direct observations	74
	C. Model experiments	79

		Page
2.3	Perturbations to gravitational coalescence	86
	A. Electrification	87
	B. Turbulence	95
CHAPTER 3	COLLECTION EFFICIENCIES FOR DROPS OF DISSIMILAR SIZES	100
3.1	Outline of the experiment	100
3.2	Theory	101
3.3	The experiment	
	A. Apparatus	105
	B. Procedure	119
	C. Subsidiary experiment	122
3.4	Results	126
3.5	Comparison of experimental and theoretical results	131
CHAPTER 4	COLLECTION EFFICIENCIES FOR DROPS OF SIMILAR SIZES	140
4.1	Outline of the experiment	140
4.2	The experiment A. Apparatus	141
	B. Procedure	146
4.3	Analysis of the streak photographs	147

		Page
4.4	Results	158
4.5	Discussion	169
4.6	The effect of turbulence	172
	A. Air motions within the stream	172
	B. Collisions caused by an artificial wind shear	176
4.7	The effect of electrification	181
CHAPTER 5	CONCLUDING DISCUSSION	191
References		195
Appendix A	"An improved vibrating capillary device for producing uniform water droplets of 15 to 500μm radius."	200
Appendix B	"Experimental determination of collection efficiencies for small water droplets in air."	201

ILLUSTRATIONS

		Page
1.1	Typical droplet spectrum for a fine weather cumulus	17
1.2	Trajectories of a 10μ radius droplet relative to a 20μ radius collector drop	23
1.3	Grazing trajectories	26
1.4	Coalescence efficiency	31
2.1	Flow round a sphere - potential flow . . .	40
2.2	" " " - Stokes	42
2.3	" " " - Pearcey and McHugh . .	44
2.4	" " " - Jenson	47
2.5	Collision efficiency diagram - Mason . . .	52
2.6	" " " - Pearcey & Hill	54
2.7	Indirect capture	56
2.8	Collision efficiency diagram - Hocking . . .	58
2.9	" " " - Mason . . .	60
2.10	" " " - Shafrir and Neiburger . .	61
2.11	Experimental collection efficiency curve - Kinzer & Cobb	67
2.12	" " efficiency curve - Picknett . .	73

		Page
2.13	Experimental collection efficiency curve - Schotland	84
2.14	" " efficiency curve - Schotland	85
2.15	Effect of electrification - Telford et al	92
3.1	The apparatus - photograph	106
3.2	" " - diagram	107
3.3	Typical droplet size distribution	109
3.4	Production of a stream of satellite drops	112
3.5	Captured droplet size distributions . . .	121
3.6	Equilibrium drop size as a function of humidity	124
3.7	Experimental collection efficiency curves	127
3.8	Experimental and Theoretical curves	132
3.9	" " "	133
3.10	Effect of reducing delay between cloud injection and collector injection (a) . .	135
	(b) . .	136
4.1	The apparatus - photograph	142
4.2	" " - diagram	143
4.3	Illumination of the drops	145

		Page
4.4	Coalescence of two 130μ drops	150
4.5	Calculation of impact parameter	152
4.6	Experimental determination of distance k between the streak highlight and the drop centre	155
4.7	Period of natural oscillation	157
4.8	Collisions between equal 62μ drops . . .	159
4.9	Collision between equal 64μ drops followed by an unequal collision	161
4.10	Unequal collisions	162
4.11	Fall speeds of two colliding drops of radius 62μ	164
4.12	Tentative experimental collection efficiency diagram	168
4.13	Steady air motion in a drop stream . . .	173
4.14	Turbulent motions in a drop stream . . .	175
4.15	Angled collision between 36μ radius drops	177
4.16	Angled collision in an air jet	179
4.17	Effect of drop charges on coalescence rate	184
4.18	Photograph of collisions between charged drops	185

ACKNOWLEDGEMENTS

The research described in this thesis was carried out at the Cloud Physics Laboratory, Imperial College, under the supervision of Professor B.J. Mason. It is a pleasure to acknowledge the constant help and encouragement of Professor Mason during the past three years. I would also like to thank my colleagues for many stimulating discussions and the workshop and office staff for their technical assistance.

The following establishments loaned equipment:-

A.E.R.E., Harwell : radiation meter

C.D.E.E., Porton : Eastman high speed camera

The Arsenal, Woolwich : Fastax high speed camera

The Department of Scientific and Industrial Research provided a research studentship.

PUBLICATIONS

Part of the work described in this thesis has been published in the following papers.

1. "An improved vibrating capillary device for the production of uniform drops."
   Journal of Scientific Instruments, 40, 247, 1963.
2. "Experimental determination of collection efficiencies for small water droplets in air."
   Quarterly Journal of the Royal Meteorological Society, 90, 373, 1964.
3. "The wake capture of water drops in air."
   Quarterly Journal of the Royal Meteorological Society - (in press).

Copies of the first two papers are included at the end of the thesis.

Figures 4.4. and 4.8a and a summary of the experiments presented in chapters 3 and 4 have appeared in the following paper by Professor Mason.

"The collision, coalescence and disruption of drops."
Endeavour, 23, 136, 1964.

CHAPTER 1

INTRODUCTION

1.1 A GENERAL STATEMENT OF THE PROBLEM

Since the war it has become generally accepted that heavy rain may be generated in tropical clouds by the "coalescence mechanism". The small water droplets formed by condensation collide with one another and coalesce to form larger drops which grow at an ever increasing rate until they eventually fall through the base of the cloud as raindrops. It is easy to see how these collisions are caused by differences in the terminal velocities of drops of different sizes falling under gravity. However, difficulties appear when one seeks to predict the rate at which the coalescence mechanism will proceed and hence how rapidly raindrops can form under a given set of conditions.

The problem hinges upon the precise way in which cloud droplets collide; it is necessary to predict what fraction of these collisions will result in coalescence. During the past twenty years, several attempts have been made theoretically to analyse the motion of two colliding cloud droplets, but they have met with only limited success. The complexity of the

equations requiring solution has forced investigators to make approximations which are only valid for certain drop sizes and produce conflicting results elsewhere. Experimental investigations have met with similarly limited success because of the difficulty in producing and controlling very small water droplets.

The laboratory experiments described in this thesis were designed to investigate droplet collisions over a wide range of drop sizes and under conditions which closely match those found in the atmosphere.

1.2 HISTORICAL INTRODUCTION

The subject of Sir George Simpson's presidential address to the Royal Meteorological Society on the 22nd January, 1941, was "The formation of cloud and rain". In it he admirably summarized the disturbed state of cloud physics which had resulted from the pioneer work of Aitken, Shaw, Wegener, Bergeron, Findeison and others. During the prewar years these meteorologists had sought to establish quantitative theories for the growth of cloud particles and so determine why rain falls from some clouds and not from others. Previously, raindrops were assumed to form by the

aggregation of tiny water droplets which make up a cloud (and similarly snowflakes were assumed to form by the aggregation of ice crystals), but the theories were purely qualitative.

In a classic paper presented to the Meteorological Association of the International Union of Geodesy and Geophysics at their Lisbon meeting in 1933, Bergeron had cast doubt upon the efficacy of the coalescence mechanism. He considered the various mechanisms that were available to cause collisions between droplets in a monodisperse cloud; (1) electrical charges on the drops, (2) capillary and hygroscopic forces, (3) temperature differences, (4) turbulence. Each of these was dismissed as being quite unable to produce raindrops in the brief life-span of a cloud. Bergeron did not discuss the effects of polarization in the intense electric fields found in clouds, nor did he consider a polydisperse cloud.

Findeisen (1939), in a paper entitled "The problem of the formation of rain-drops in clouds which are entirely composed of water", agreed with Bergeron's conclusions for homogeneous clouds, but pointed out that in his experience clouds and fogs contain particles

of very different sizes (see Fig. 1.1) with different terminal velocities and that, in consequence, the larger drops will overtake and collide with smaller ones. He then proceeded to develop a mathematical theory for this "gravitational accretion" and to compute the growth of particles in typical clouds. The computations suggested that fairly large raindrops could fall from moderate cumulus, but Findeisen believed that this contradicted the observed behaviour of natural clouds. He remained convinced that only drizzle falls from water clouds, however thick they are, and explained the discrepancy between his opinion and his results by predicting that the large cloud drops sweep aside smaller ones and so do not collide with them. Thus, although he had no evidence for it, Findeisen had isolated the crucial problem requiring solution before the coalescence mechanism could be described quantitatively.

In his survey of the subject, Simpson criticized Findeisen's dogmatic attitude and quoted in evidence for the coalescence mechanism a variety of field observations of heavy rain falling from wholly liquid clouds. He suggested that a vigorous updraught provides all the conditions necessary for copious rainfall, namely

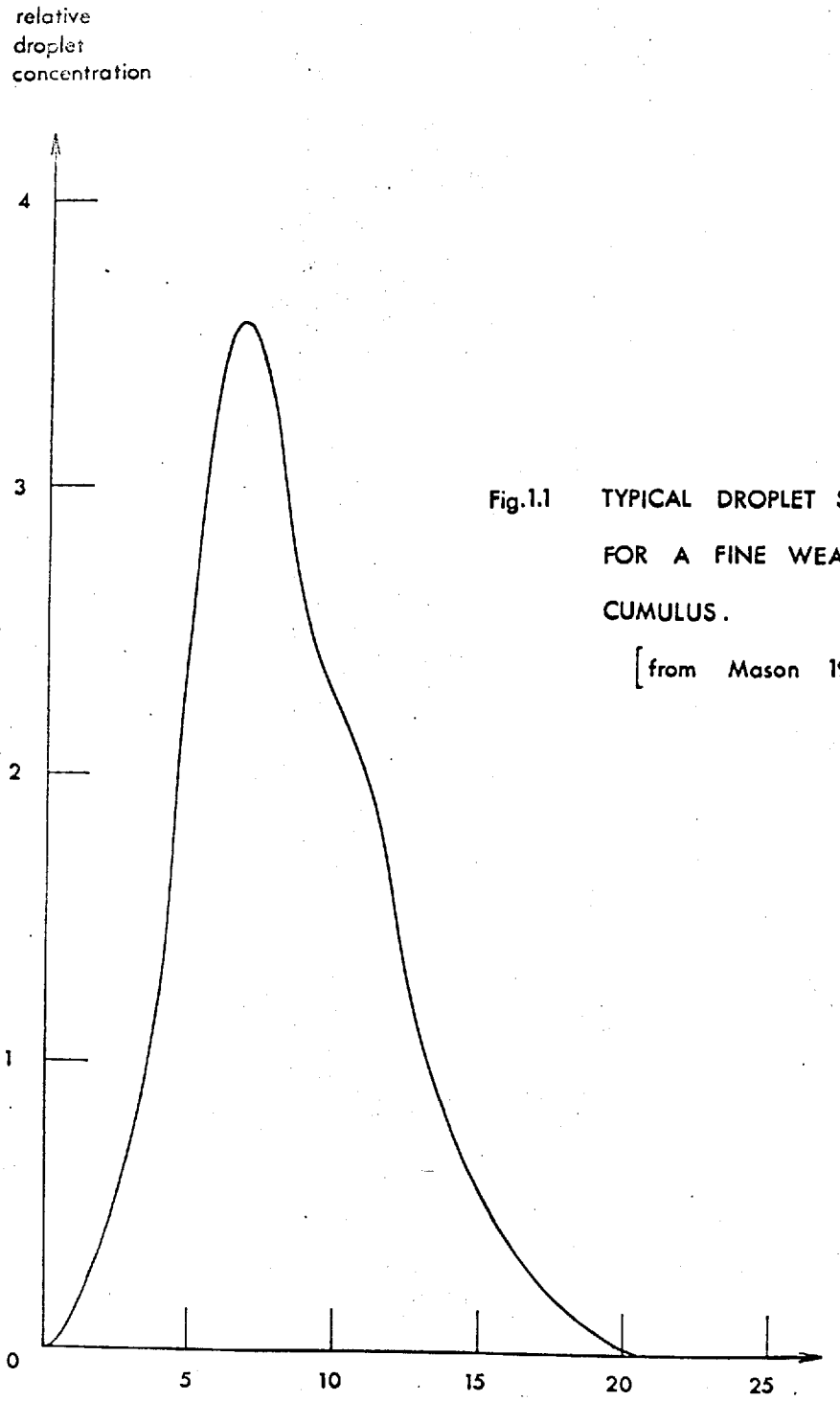

Fig.1.1 TYPICAL DROPLET SPECTRUM FOR A FINE WEATHER CUMULUS.

[from Mason 1957]

(1) the release of large quantities of water, (2) a wide variation in cloud drop size, (3) a considerable depth of cloud. Later in his address, Simpson stated that "There is no reason to doubt that with clouds of sufficient depth, copious rain in large drops would be produced in this way by ascending currents without the formation of ice". The force of Simpson's advocacy for the coalescence mechanism is a sign of the doubts that had formed in the minds of meteorologists following the success of the Findeisen-Bergeron ice mechanism* for raindrop formation. The final proof only came after the war, when radar was applied to studying precipitating clouds (Bowen, 1950).

The next major step in developing a theory for the coalescence mechanism came in 1948 when Langmuir published calculations which made allowance for the hydrodynamic

---

* These authors proposed that all raindrops result from the melting of snowflakes as they fall below the $0^{\circ}C$ isotherm. The snowflakes are aggregates of ice crystals which grow rapidly at the expense of the surrounding supercooled cloud drops as the result of the difference between the equilibrium vapour pressures over ice and water.

sweeping aside of small droplets, as predicted by Findeisen. He showed that, despite the reduced capture efficiency of cloud particles, they could still grow very rapidly by gravitational accretion and so produce large raindrops in deep cumulus clouds. Langmuir's publication was soon followed by important theoretical papers from Australia (Bowen, 1950) and England (Ludlam, 1951), which finally established the coalescence mechanism in its present form.

Bowen used Langmuir's data to calculate the trajectories of drops growing by coalescence in cumulus clouds having various updraughts, liquid water contents, and initial drop sizes. In his paper, Bowen quotes a series of observations made from aeroplanes and on ground radar which provide ample evidence that heavy showers fall from warm cumulus in Australia. He quotes raindrops with a mean diameter of 0.5 mm falling from clouds 3,000 feet in depth. Ludlam's paper contains many similar computations and derives a variety of general expressions for droplet growth. Both authors conclude that the coalescence mechanism will only get going if drops of radius greater than 20μ are present in the cloud; Ludlam suggested that these grow

by condensation on large sea-salt nuclei. He also predicted a minimum cloud depth of 1.5 to 2 km if these 20μ drops are to grow to raindrop size. Further modification to the theory came from Telford (1955), who included in his calculations the probability of a few droplets making very frequent collisions and hence predicted that the process may work even faster than had been estimated by Langmuir, Bowen and Ludlam.

The main effort during the past ten years has been aimed at improving upon Langmuir's analysis of droplet collisions and so deriving reliable data for inclusion in cloud development computations. Recently the availability of high speed electronic computors has been exploited, notably by Hocking (1958) and by Shafrir and Neiburger (1963), to carry out lengthy calculations on the trajectories of colliding cloud drops. None of these, however, has obtained satisfactory data for drops of larger than 30μ radius, where differences in the various solutions reflect the different approximations made by each author.

Experimental data becomes crucial in this situation, where theoretical analyses produce a variety of conflicting results. Unfortunately the production,

control and observation of very small water drops in the laboratory have also produced great difficulties. A dozen or more workers in America, Australia and the United Kingdom have designed experiments to test the theoretical predictions of Langmuir and his successors, without complete success. The serious limitations to the available experimental techniques have forced some workers to adopt an indirect approach with the result that their conclusions are even more open to doubt than the theories that they were testing. The more direct experiments (notably by Picknett, 1960) have been restricted to small ranges of drop sizes.

The present work was initiated with the object of testing the theoretical predictions over the widest possible range of drop sizes. It was found that two different techniques were required, each a logical extension of one or more of the earlier experiments. They are described in Chapters 3 and 4 after a critical survey of both theoretical and experimental work carried out during the past twenty years.

1.3 NOTATION

The theory of gravity coalescence has been developed piecemeal by a number of workers, each of whom has used his own notation. So, in order to avoid confusion, it is necessary to establish from the start which notation will be used here. Wherever necessary, the differences between the chosen notation and that of other workers will be explained and, in general, the results of other authors quoted in Chapter 2 will be modified to conform to the present scheme.

A. Theoretical

Figure 1.2 illustrates a collision between a "collector" drop of radius R and a droplet of radius r. The flow of air round the leading surface of the collector deflects the droplet sideways, but the latter's inertia prevents it from following the streamlines precisely, as would an infinitely small particle. The droplet therefore crosses the streamlines round the front of the collector and it will either hit or miss the latter depending upon the impact parameter, b, of the collision. There will be a grazing impact parameter, b_g, which leads to a

Fig. 1.2 TRAJECTORIES OF A 10μ RADIUS DROPLET RELATIVE TO A 20μ RADIUS COLLECTOR DROP. [from Hocking 1958]

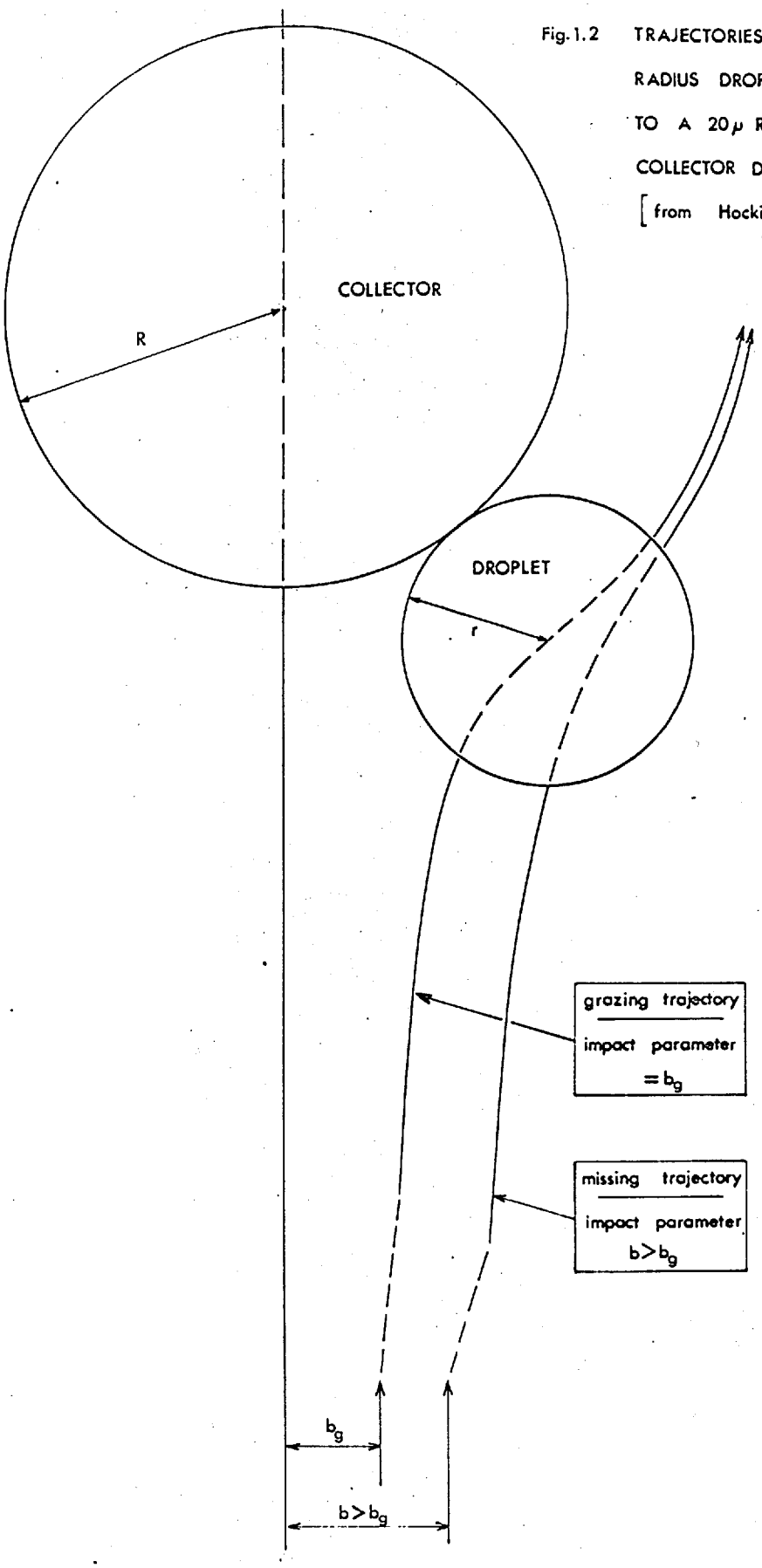

grazing trajectory. Collision will result if the drops approach one another with $b<b_g$, but if $b>b_g$ then the droplet will pass right round the collector without touching it and they will separate*. The value of b_g will be a unique function of the radii (R and r) of the two drops provided that they approach one another at terminal velocity and under the action of no other force but gravity. The effects of electrification and turbulence on b_g will be discussed later.

The object of theoretical investigations during the past twenty years has been to determine values of b_g for all combinations of drop sizes. It has become customary to divide b_g by (R + r) to obtain a dimensionless factor called the linear collision efficiency. More useful still is the square of this value, which will be called the collision efficiency, E_o, which is

---

* A further possibility "indirect collision" will be discussed in Chapter 2.

also a unique* function of R and r.

$$E_o = \frac{b_g^2}{(R+r)^2}$$

This is also the ratio of the collision cross-section to the geometric cross-section for a given collision (see Fig 1.3).

An alternative nomenclature, in which b_g is normalized by dividing it by R instead of (R + r) will not be used here. For the purpose of clarity the fractions so obtained will be referred to as the linear collision ratio and the collision ratio, E_o', respectively.

$$E_o' = \frac{b_g^2}{R^2}$$

The object of theoretical investigations is, therefore, to obtain values of E_o for all combinations of R and r. It is convenient to display these values in the form of graphs of $E_o(R,r)\big|_R : {}^r/_R$. A family of such curves of constant R will be called a Collision Efficiency Diagram. Examples will be found in the next chapter. This display has been selected because it provides directly the information required for cloud

---

* As the viscosity and density of the air change with altitude there will be a corresponding change in E_o.

Fig.1.3 GRAZING TRAJECTORIES

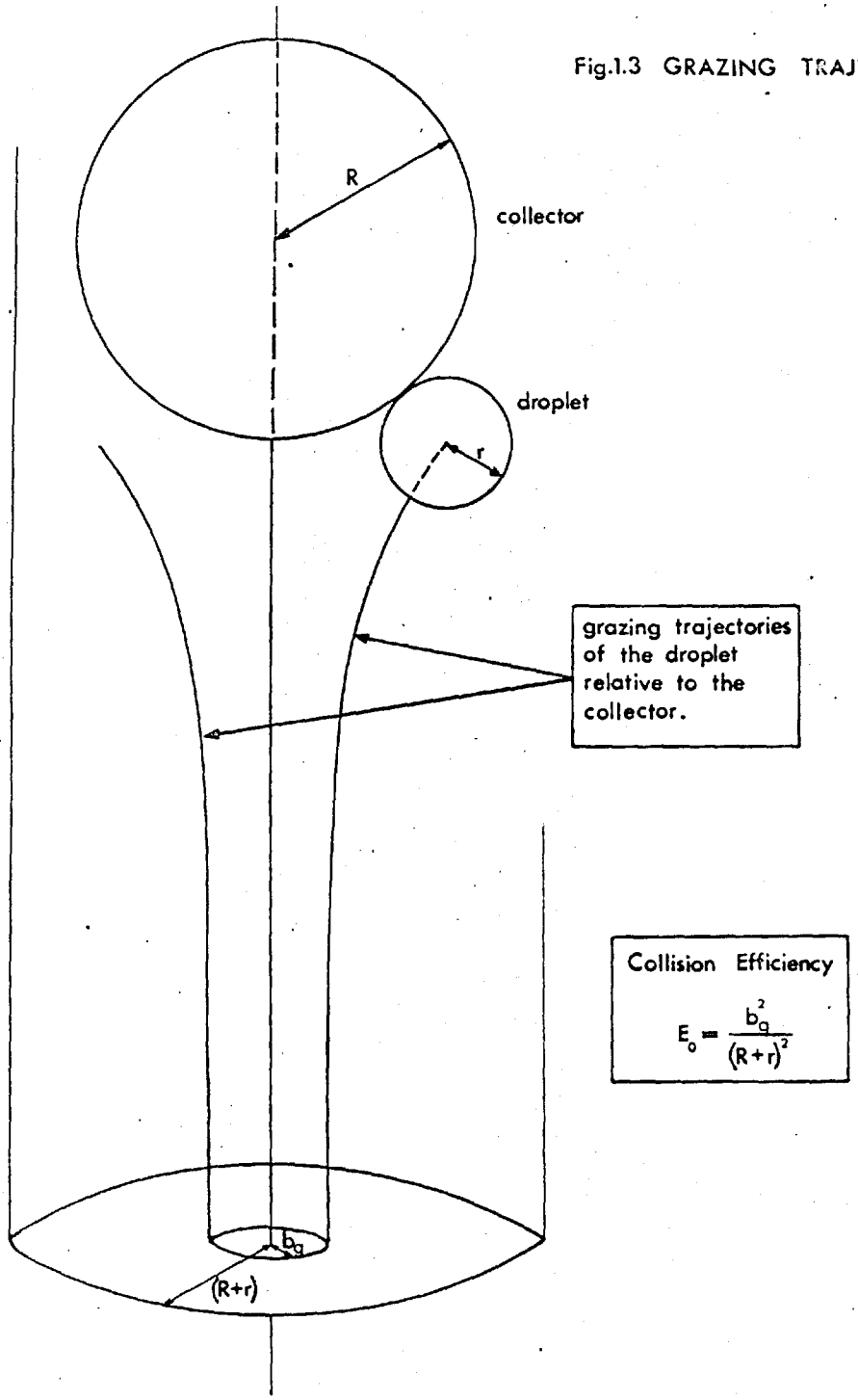

development computations. It also leads to a rectangular plot, which is more convenient than the trapezoidal or triangular plots of other workers.

B. Experimental

The majority of experiments do not investigate the actual trajectories of colliding drops, but measure the number of droplets captured by a collector in given circumstances. It is convenient to define a Collection Efficiency, E, equal to the fraction of droplets actually captured out of those droplets with centres lying directly below the collector in a column of gometric cross-section $\pi(R+r)^2$. It is assumed that the others are swept round the collector.

This definition is very similar to that for the collision efficiency, E_o, which may be defined as the fraction of droplets that actually collide with the collector out of those lying within a column of radius $\pi(R+r)^2$ directly below it. It is convenient therefore to invent a parameter b_c defined by the equation

$$E = \frac{b_c^2}{(R+r)^2}$$

The ratio of the collision efficiency, E_o, to the

collection efficiency, E, is called the coalescence efficiency, ϵ. Thus,

$$E = \epsilon . E_o$$

C. Coalescence rate

Using the established definition for collection efficiency it is possible to introduce the basic equation for the rate at which the coalescence mechanism proceeds. This equation will be used in the chapters that follow.

Consider a polydisperse cloud divided into narrow size ranges. One of these ranges contains the collectors, radius $R \rightarrow R + dR$ and the other the droplets, radius $r \rightarrow r + dr$. The number concentrations of each are $N(R)dR$ and $N(r)dr$ and the fall speeds of the drop are V and v respectively.

In unit time a collector will capture those droplets lying within a column of area $E(R,r) . \pi (R+r)^2$ and length $(V-v)$ directly below it. The number of droplets in this volume is $N(r)dr . E(R,r) . \pi (R+r)^2 . (V-v)$. This is the number of droplets captured by a single collector in unit time. There are $N(R)dR$ collectors per unit volume, so the number of such coalescence events occurring per unit volume per second is given by the expression

$$\frac{d\,N(R,r)_{dR.dr}}{dt} = N(R).\,N(r).\,E(R,r).\pi(R+r)^2\,(V-v)\;dR.dr. \qquad (1.1)$$

This is the general coalescence rate equation. The instantaneous rate at which selected classes of drops are mutually coalescing is obtained by integration over finite ranges of R and r.

D. Coalescence efficiency

Many early workers (e.g. Rayleigh, 1879) considered the possibility that cloud drops may collide and bounce apart without coalescing. Contemporary theories reject the concept of cloud drops bouncing elastically from one another because the approach velocities are too small to supply the energy required for deformation of the drop surfaces. However, it is still pertinent to question whether all those drops that collide (i.e. $b < b_g$) do actually coalesce, or whether they slide round each other to separate when the droplet gets above the collector.

Jayaratne (1964) has studied the impact of water drops of radius $100\mu < R < 200\mu$ with a water meniscus of 5 mm radius. He found that coalescence only resulted when the drops hit the surface with impact angles and impact velocities lying within certain ranges. While

Jayaratne's experiments do not match the conditions prevailing in rain clouds, they provide a warning that coalescence may result from drop collisions with some impact parameters and not for others. Furthermore, it may not be possible to state categorically that a given impact parameter will or will not result in coalescence. There may be a certain probability of coalescence, $P_c(b)$, which varies with impact parameter, b. In Fig. 1.4 are plotted examples illustrating the three possibilities, namely (1) Coalescence for all values of $b < b_g$, (2) Coalescence for all values of b within certain zones, and (3) Some finite probability of coalescence for all values of $b < b_g$. In the first case the coalescence efficiency is unity and the collection and collision efficiencies are identical. In consequence $b_g = b_c$ and the capture cross-section, πb_c^2, equals the collision cross-section. In the other two cases the coalescence efficiency is less than unity $\left[\epsilon = \int_0^{b_g} P_c(b)db \,/\, b_g \right]$ so $E < E_o$ and $b_c < b_g$. In these cases it is clear that the parameter b_g represents not a critical impact parameter (as in case (1)), but a statistical average.

Jayaratne explains his coalescence zones in terms of the draining away of a thin film of air trapped between

Fig. 1.4 COALESCENCE EFFICIENCY

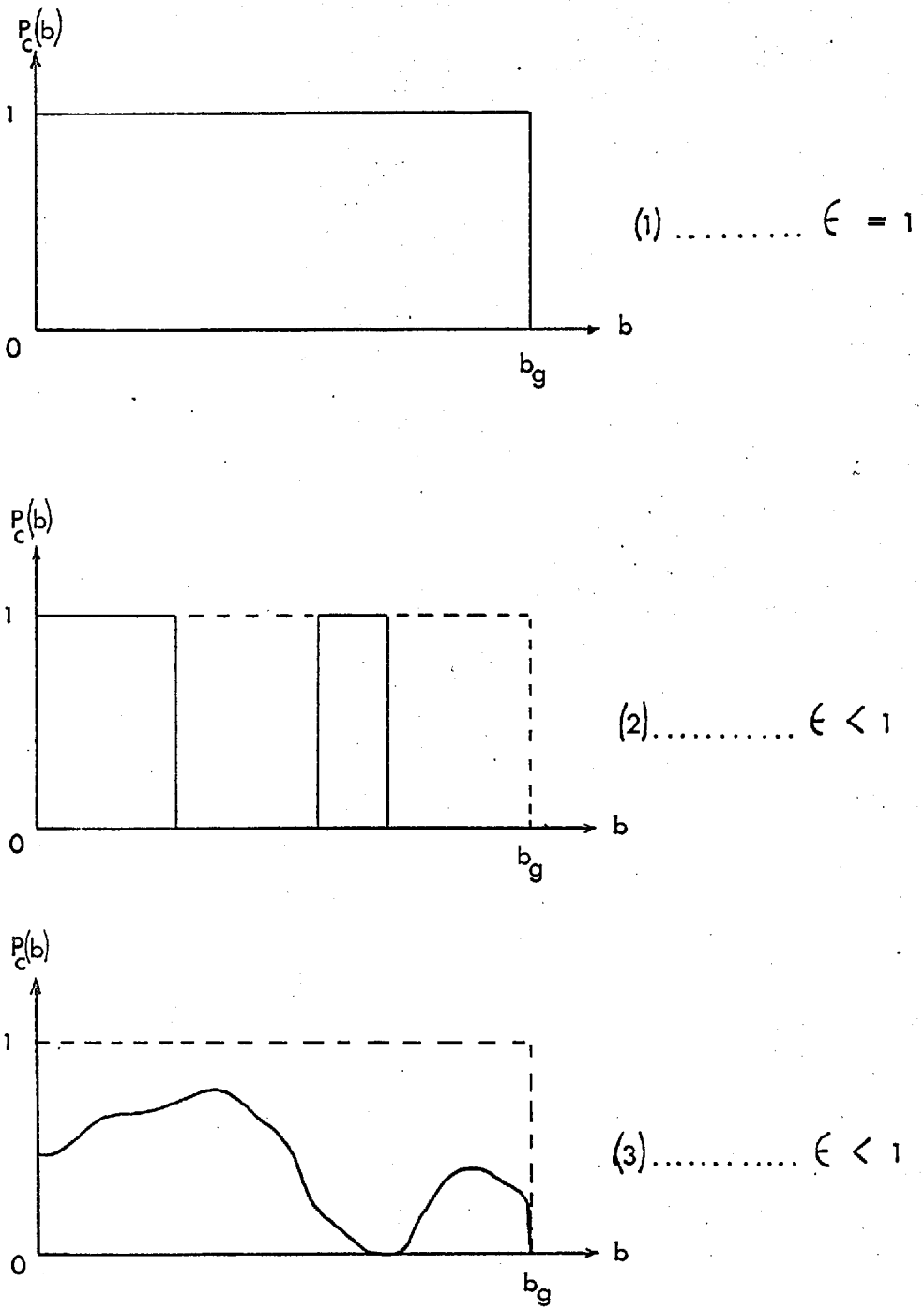

the two impacting surfaces. The initial impact energy is absorbed in compressing the trapped air, which escapes relatively slowly because of the thinness of the gap. As the air escapes the two water surfaces gradually approach one another until Van der Waals forces become sufficiently large to provide an attraction which draws them together. Eventually a continuous liquid neck is formed between the surfaces and grows rapidly, decreasing the surface energy of the drops. The time that elapses between the initial impact and the final coalescence is called the coalescence time. Prokhorov (1954) showed that it may be increased if the surfaces meet in a very undersaturated environment. (This is not likely to occur in a cloud). On the other hand, the coalescence time may be considerably reduced if the water surfaces are electrified. In Jayaratne's experiment an electric field of about 100v/cm. was sufficient to ensure coalescence for all impact parameters and angles. It is probable that the electrification caused micro-distortion of the water surfaces and so formed a connecting liquid neck before Van der Waals forces could act.

In the case of cloud drop collisions the high curvature if the impinging drop surfaces will assist

drainage of the air film and a very short coalescence time is to be expected. This will be further reduced by the electrical polarization of the drops in the cloud's electric field. The magnitude of this field will increase from the fine weather value of about 300 V/m. to several thousand V/m in a growing cumulus.

These factors will almost certainly combine to ensure that the coalescence efficiency of pairs of cloud drops of every combination of sizes will be unity (Fuchs, 1955).

A SUMMARY OF DEFINITIONS USED IN THE THESIS

DROP - the general term used for any water sphere.

COLLECTOR - radius R - the upper drop in a collision.

DROPLET - radius r - the lower drop in a collision.

DROP RATIO - r/R

IMPACT PARAMETER - b - the horizontal separation of collector and droplet before they interact with one another.

GRAZING IMPACT PARAMETER - b_g - the maximum impact parameter which results in collision between collector and droplet.

CRITICAL IMPACT PARAMETER - b_c - (see Section 1.3 D).

COLLISION EFFICIENCY - $E_o = \dfrac{b_g^2}{(R+r)^2}$

COLLISION RATIO - $E_o' = \frac{b_g^2}{R^2}$

COLLECTION EFFICIENCY - $E = \frac{b_c^2}{(R+r)^2}$

COLLECTION RATIO - $E' = \frac{b_c^2}{R^2}$

COLLISION CROSS-SECTION - πb_g^2

CAPTURE CROSS-SECTION - πb_c^2

GEOMETRIC CROSS-SECTION - $\pi(R + r)^2$

COLLECTION EFFICIENCY DIAGRAM - curves of E for constant R plotted against r/R.

COLLISION EFFICIENCY DIAGRAM - curves of E_o for constant R plotted against r/R.

COALESCENCE DISPLAYS USED BY VARIOUS AUTHORS

DATE	AUTHOR	ORDINATE	ABSCISSA	FAMILY CONSTANT
	THEORETICAL			
1948	LANGMUIR	E_o'	K^*	R
1956	PEARCEY and HILL	E_o'	$\frac{R-r}{r}$	R
1958	HOCKING	E_o'	r/R	R
1963	SHAFRIR and NEIBURGER	$\sqrt{E_o'}$	r/R	R
1963	LINBLAD and SEMONIN	E_o'	volts	R,r
1962	MASON	E_o'	r/R	R
	EXPERIMENTAL			
1951	HITSCHFELD and GUNN	E'	r	R
1956 /58	KINZER and COBB	E'	R	$\bar{r}$
1960	PICKNETT	E	r/R	R
1956	TELFORD et al	E'	r=R	-
1961	TELFORD and THORNDIKE	E'	r=R	-
1957	SCHOTLAND	E'	r=R	-
1958	SCHOTLAND	E'	r	R

$^*K = \frac{2 r^2 \rho (V - v)}{9 R \eta}$ where η = air viscosity

CHAPTER 2

A SURVEY OF PREVIOUS WORK

2.1 THEORETICAL ANALYSIS

Undoubtedly the theoretical approach provides the most promising method of obtaining quantitative data for the coalescence mechanism. The ideal approach is easily outlined. The interaction between colliding drops is divided into a series of brief time steps. At each step the flow pattern round the two spheres is computed and the hydrodynamic force on each deduced. The drops are then allowed to move in response to the forces for a brief interval of time, after which their new positions are calculated. The air flow pattern round the drops in their new positions is then computed and the cycle is repeated. In this way, the motion of the drops may be followed throughout their interaction. If at some stage the drops "overlap", then they are said to have collided; if not, they are said to have missed one another. Each collision is followed from a large initial separation of the drops, where the air flow round each is not perturbed by the other. The trajectories resulting from a series of impact parameters are computed and by a limiting process

the grazing impact parameter, b_g, is obtained to the required accuracy. The collision efficiency $E_o = \frac{b_g^2}{(R+r)^2}$ follows directly.

The difficulty lies in computing the airflow pattern round the two drops and even, it turns out, round one isolated drop when its Reynolds number is greater than unity. In principle it is possible to apply the appropriate boundary conditions to the Navier-Stokes equations and hence to obtain the velocity of the air at every point round the drops. However, it is easy to demonstrate that the equations requiring solution are non-linear and cannot be solved analytically.

A. Flow round an isolated drop

The simplest example is an isolated sphere of radius R falling at terminal velocity V through a fluid of kinematic viscosity ν, density ρ and pressure p. The equations of motion for an incompressible steady-state flow round the sphere are

$$\underline{u} \cdot \nabla \underline{u} = -\frac{1}{\rho} \nabla p + \nu \nabla^2 \underline{u} \qquad 2.1\ (a)$$

$$\nabla \cdot \underline{u} = 0 \qquad (b)$$

with the boundary conditions

$$\underline{U}(\infty, \theta) = 0 \qquad 2.2\ (a)$$

$$\underline{U}(R, \theta) = 0 \qquad (b)$$

The conditions state that the fluid is at rest at large distances from the sphere (a) and that there is no slipping at the sphere's surface (b).

An alternative formulation may be obtained by introducing the stream function ψ and the vorticity ξ, given by

$$\underline{u} = (u_r, u_\theta) = \left[\frac{1}{r^2 \sin\theta} \cdot \frac{\partial \psi}{\partial \theta} - \frac{1}{r \sin\theta} \cdot \frac{\partial \psi}{\partial r}\right]$$

and $$\xi = \frac{1}{r}\left[\frac{\partial (r u_\theta)}{\partial r} - \frac{\partial u_r}{\partial \theta}\right]$$

It is also usual to transform to a co-ordinate system in which the following sphere is at rest. The boundary conditions then become

$$\underline{u}(\infty, \theta) = \underline{V}_\infty$$

$$\underline{u}(R, \theta) = 0$$

The two velocity components u_r (radial) and u_θ (tangential) are obtained by differentiating the stream function field. A brief account will now be given of the more important approximate analytical solutions and numerical solutions

obtained by various authors.

When the sphere moves with a high velocity (large Reynolds number) the air round its leading surface may be treated as non-viscous and having no vorticity.

$$\text{i.e. } \text{curl } \underline{U} = 0$$

This is the condition for a conservative field which may always be described as the gradient of some scalar potential at any point.

$$\text{i.e. } \underline{U} = \text{grad } \phi$$

The velocity round the falling sphere is now defined in terms of a scalar field ϕ. As the flow is also incompressible we have

$$\text{div } \underline{U} = 0$$

$$\text{i.e. } \nabla^2\phi = 0$$

This is the condition for potential flow, which gives a useful approximation to the flow round the front of a sphere at large Reynolds numbers. (The presence of a boundary layer and a wake make it invalid behind the sphere). The potential flow round a sphere is shown in fig. 2.1.

At the opposite end of the scale, Stokes (1851) considered the case of "creeping motion" which occurs at

Fig. 2.1 POTENTIAL FLOW ROUND A SPHERE.

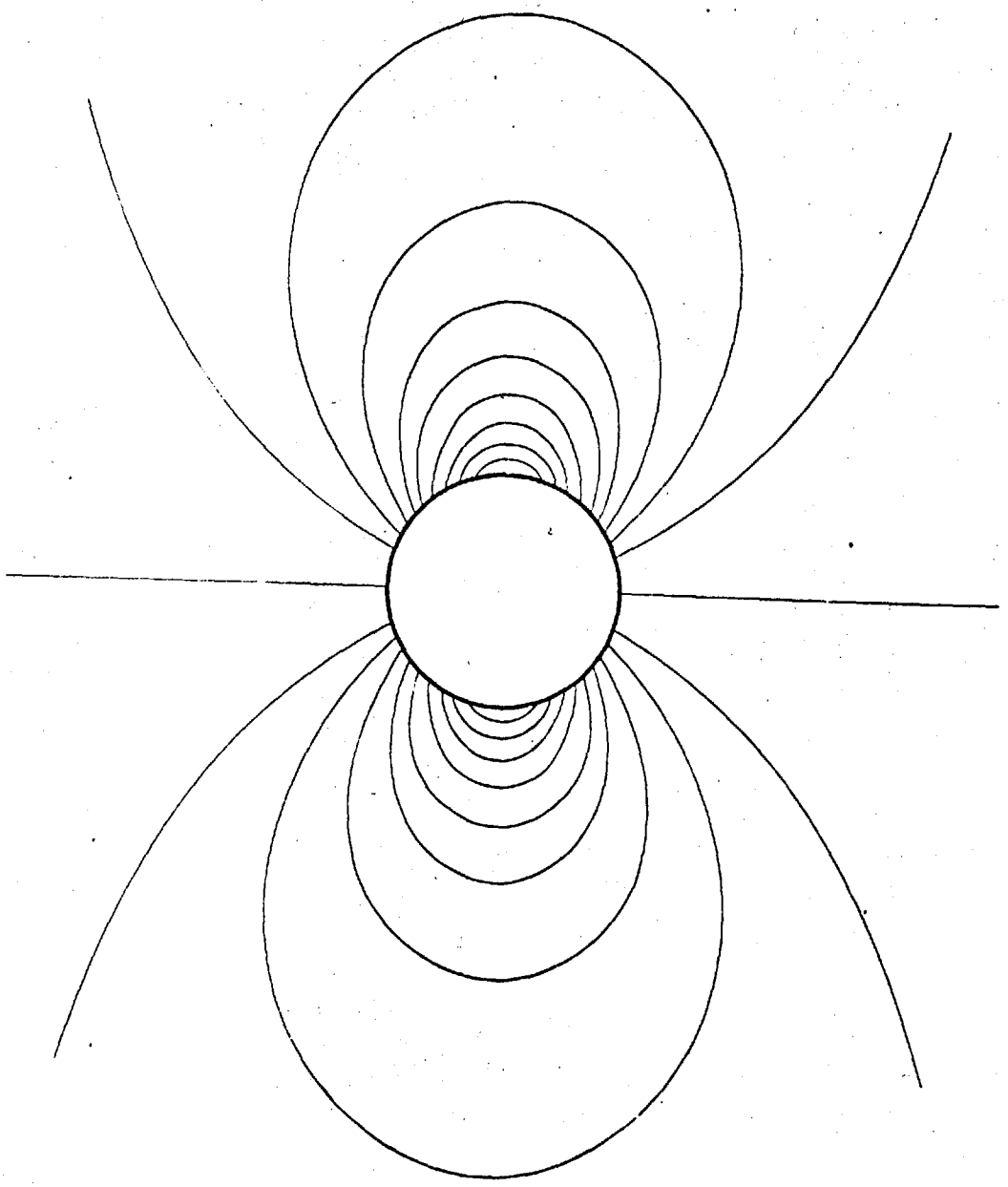

very low Reynolds numbers ($Re \ll 1$). In this case the rate of change of the inertia of the fluid is negligible when compared with the viscous forces near the sphere, and equation 2.1a reduces to

$$0 = \frac{1}{\rho}\nabla p + \nu \nabla^2 \underline{U} \qquad 2.3$$

The equation is now linear and may be solved analytically (see, for example, Lamb 1932) to give values of U_r and U_θ at all points round the sphere. The flow diagram so obtained (see Fig. 2.2) is typified by a symmetry either side of the horizontal diameter. This solution has been most successful, but is restricted to small drops ($R_e < \frac{1}{2}$, $R < 30\mu$). Furthermore, the viscous forces decrease with range from the drop at a greater rate than do the inertial forces until eventually they become comparable. Thus, even for small droplets, the Stokes equation fails to give the correct flow at large distances from the drop.

Oseen (1911) overcame this difficulty by including a linearized inertia term $\underline{V}_\infty . \nabla \underline{U}$ in place of the $\underline{U} . \nabla \underline{U}$ of equation 2.1a As $\lim_{r \to \infty} \underline{U} = \underline{V}_\infty$, this makes the equation correct at large distances from the drop. Close to it, at low Reynolds numbers, the inertia term is negligible in comparison with the viscous term, so the

Fig. 2.2 FLOW ROUND A SPHERE. after Stokes.

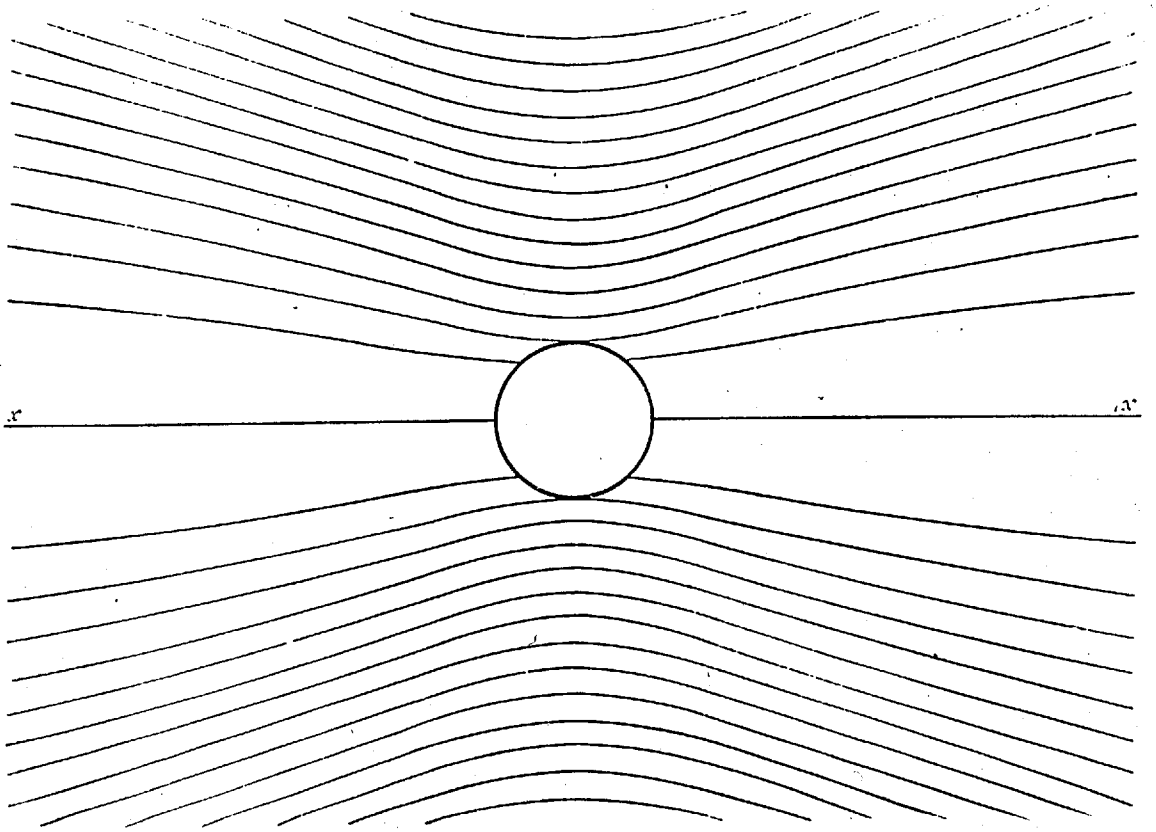

error introduced by linearizing the viscous term is no greater than ignoring it, as in the Stokes formula. However, at larger Reynolds numbers the inertia forces close to the drop become comparable with the viscous forces and both Stokes and Oseen approximations fail, although one would expect the latter to be closer to the correct value.

Pearcey and McHugh (1955) have used the complete analytical solution of Oseen's approximation given by Goldstein (1929 a,b) to carry out detailed computations of the flow round a sphere for Re = 1, 4 and 10 and approximately for Re = 40. Their flow diagrams for Re = 1,4 and 10 are reproduced in Fig. 2.3. Even at Re = 1 there is a marked asymmetry in the flow, with the contour of $U_\theta = 0$ providing a rough division between the rotational flow behind the sphere and the irrotational flow in front of it. The authors introduce a "wake", defined as the region of vorticity (rotational flow), but they emphasise that this does not require a stationary vortex or eddy behind the drop. In fact they found no such eddy, even at Re = 10. The profile of the wake is governed by the fall speed of the drop and the rate of diffusion of the vorticity outwards and forwards. Thus the wake extends round to the front of the smaller drops, but is left

Fig. 4

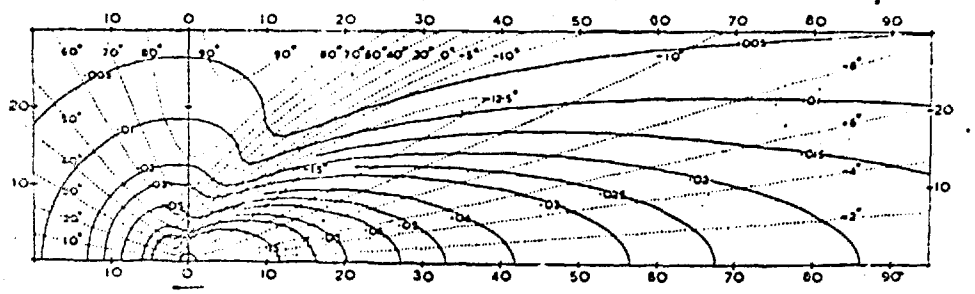

Flow around a sphere at great distances at $R=1$. Contours of constant magnitude and direction of flow velocities. The magnitude, full lines, is referred to the velocity of the sphere ; the lines of constant direction, dotted, indicate direction away from the axis of motion. Dimensions are referred to the radius of the sphere, which moves from right to left.

Fig. 5

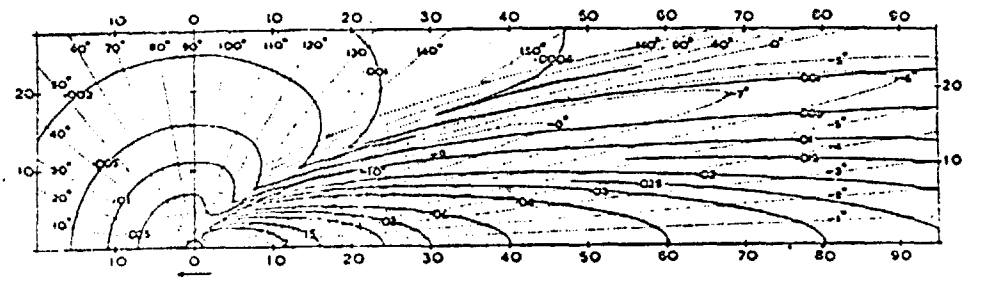

Flow around a sphere at great distances at $R=4$. Contours of constant magnitude and direction of flow velocities. The magnitude, full lines, is referred to the velocity of the sphere ; the lines of constant direction, dotted, indicate direction away from the axis of motion. Dimensions are referred to the radius of the sphere, which moves from right to left.

Fig. 6

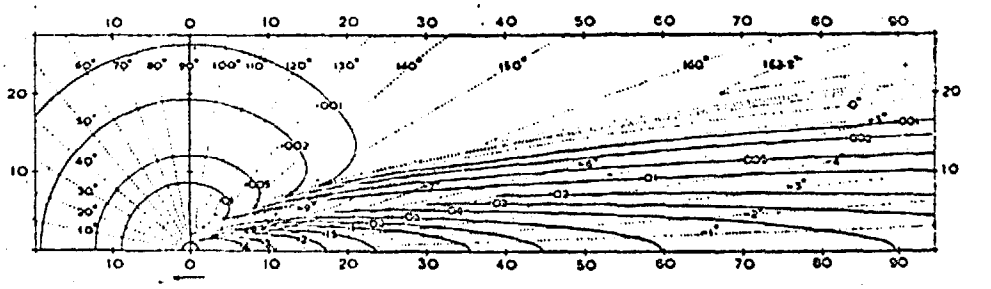

Flow around a sphere at great distances at $R=10$. Contours of constant magnitude and direction of flow velocities. The magnitude, full lines, is referred to the velocity of the sphere ; the lines of constant direction, dotted, indicate direction away from the axis of motion. Dimensions are referred to the radius of the sphere, which moves from right to left.

Fig.2.3 FLOW ROUND A SPHERE Pearcey & McHugh

behind the fast moving, larger drops (see Fig. 2.3). The authors find clear indication for a boundary layer at Reynolds numbers as low as 10. At large distances behind the drop, the flow is directed towards the drop with a velocity which falls off exponentially as $1/z$, where z is the distance behind the drop.

Pearcey and McHugh do not make any estimate of the errors due to the use of Oseen's approximation, but point out that these are likely to be greatest near the drop surface, where the inertia term $\underline{u}.\nabla\underline{u}$ dropped from equation 2.1 becomes large when the Reynolds number is large. The authors suggest that the error introduced by their approximation might affect the solution "so far as to fail to show a separation which could be indicated by a solution of the complete equations of motion".

Proudman and Pearson (1957) went one step further than Oseen, replacing the Navier-Stokes equation by two linear equations, one valid near the drop and the other valid at large distances from it. Using a "matching" system they determined the values given by the two equations at each point and hence obtained an interpolated value. Their equations are carefully compared with the Stokes

and Oseen approximations and relationships between the three are discussed in considerable detail. Unfortunately, however, the authors do not plot any example of the flow pattern nor do they give tabulated values of the air velocity. Nevertheless they do quote one point of disagreement with Pearcey and McHugh's results. The latter workers found no closed eddy in the wake, even at Re = 10, but Proudman and Pearson find a closed eddy at Re = 8. They point out, however, that their theory cannot be extended to such high Reynolds numbers. Jenson (1959) suggests limits of Re = 5 on Proudman and Pearson's theory and Re = 2 on Pearcey and McHugh's theory, beyond which they become unreliable.

Seeking to obtain flow diagrams for higher Reynolds numbers, Jenson (1959) used a completely different technique. He employed a relaxation method to compute, step by step, values for the stream function and vorticity from the complete Navier-Stokes equations. This technique makes no approximations beyond those inherent in the numerical technique itself. Jenson's diagrams of streamlines and vorticity for drops with Reynolds numbers of 5, 10, 20 and 40 are reproduced in Fig. 2.4; he also includes a comprehensive set of tabulated values. A closed eddy is first

Fig. 2.4 FLOW ROUND SPHERE. after Jenson.

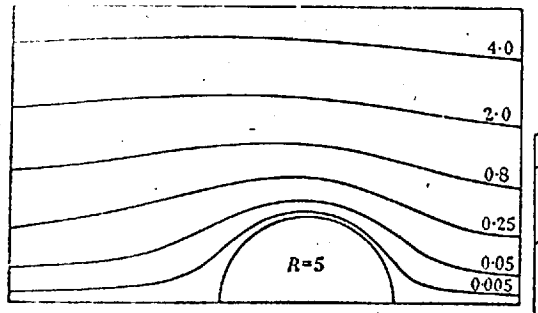

3

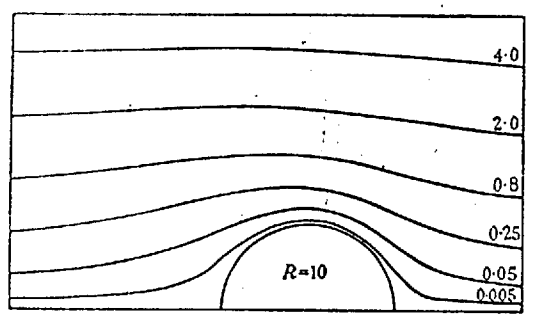

4

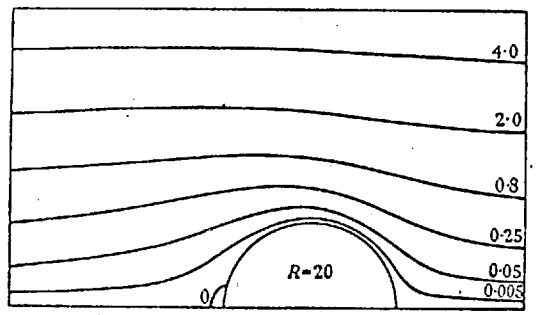

5

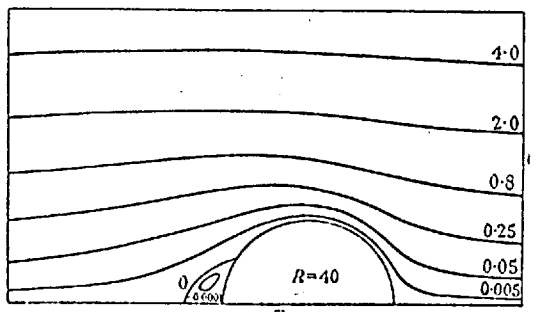

6 ← flow

FIGURES 3 TO 6. Streamlines.

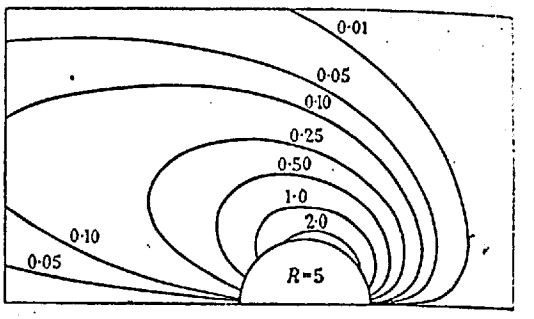

7

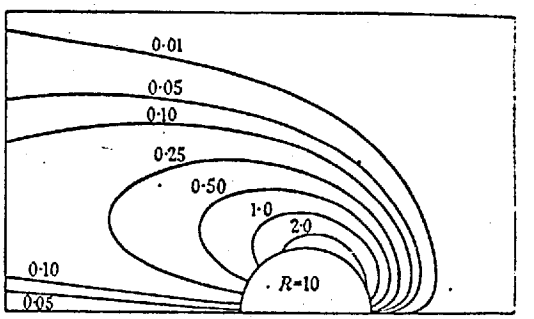

8

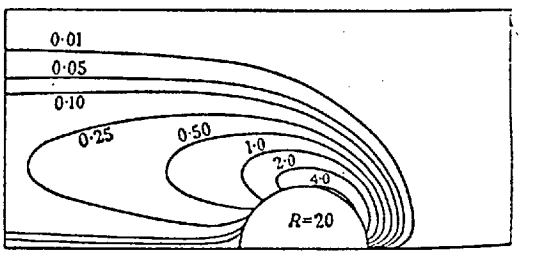

9

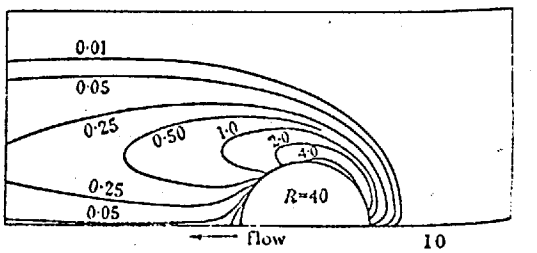

← flow 10

FIGURES 7 TO 10. Vorticity.

detected at Re = 17 (corresponding to a cloud drop of $R \sim 130\mu$). Shafrir (1962) repeated these computations and differentiated to obtain values of U_r and U_θ .

The same author (Shafrir, 1964) has recently made an interesting investigation into the differences between the various analyses described above. He recomputed the velocity fields (Ur and U$_\theta$ fields) using the formulae of Stokes, Oseen, Pearcey and McHugh, and Proudman and Pearcey. A computor was then programmed to plot directly the Stokes U fields and to plot the differences between these and those of each of the other authors. These provided a clear visual representation of the differences between each author's results for drops of Re = 0.1, 0.5 and 1.0. The diagrams confirm many of the remarks made earlier about the various approximations; Shafrir restricts himself to pointing out that Proudman and Pearson's correction (to Stokes U field) progresses closer and closer to the sphere, but Oseen's correction changes only slightly with the increasing Reynolds number. He also points out that Pearcey and Hill's correction should closely follow Oseen's, but that in practice the one is a mirror image of the other.

As a further demonstration of the differences between

these various approximations, Shafrir compared his own and Hocking's linear collision efficiency diagrams with those computed using the U fields of the other authors. Again, because they are computed by a single author using the same procedure and criterion for collision, and because they are all presented in the same way, these are most instructive and show clearly the differences between the various approximations. However, Shafrir did not publish any specific conclusions arising from these comparisons.

B. Collision Efficiency Computations

The first collision efficiency diagram was published in 1948 by Langmuir, who assumed the flow around a collector drop to be given by either the Stokes solution (for small drops) or the potential flow solution (for large drops). Previously Langmuir and Blodgett (1945) had used a differential analyser to compute the trajectories of small particles in the flow field round a sphere falling at terminal velocity in air, and had obtained expressions for the collision efficiency as a function of a dimensionless parameter

$$K = \frac{2\rho}{9\eta} \cdot \frac{r^2}{R} \cdot (V - v)$$

where ρ = density of water, η = viscosity of air, and

the collector and droplet have radii R and r and fall at terminal velocities V and v respectively.

In the case of potential, or aerodynamic flow (where the fluid is assumed to have no viscosity) Langmuir and Blodgett found that

$$E_A = 0 \qquad \text{for} \qquad K < 0.833$$

$$\text{and} \quad E_A = \frac{K^2}{\left(K + \frac{1}{2}\right)^2} \qquad \text{for} \qquad K > 0.2$$

and, for Stokes flow (where viscous forces predominate)

$$E_v = \left[1 + \left(\tfrac{3}{4} \ln 2K\right) \Big/ (K - 1.214)\right]^{-2}$$

except for $K < 1.214$, where $E_v = 0$.

In the 1948 paper, these two values are combined into an interpolated expression

$$E_{Langmuir} = \left[E_v + \frac{E_A \cdot R_e}{60}\right] \Big/ \left[1 + \frac{R_e}{60}\right]$$

which makes the collision efficiency curve for R = 250μ lie midway between the aerodynamic and Stokes limits.

Langmuir's theory incorporates an assumption which limits it to small values of r/R. In computing the droplet trajectories he assumed that they were points with mass and drag coefficient appropriate to the chosen droplet radius, but with negligible volume. This assumption introduces two important faults into the theory. Firstly, collision is now defined as occurring when the droplet centre touches the collector surface, whereas it should

occur when the centre passes within a droplet radius of the collector surface. Ludlam (1951) made a rough correction by adding the droplet radius r to Langmuir's grazing impact parameter, to obtain

$$E_{Ludlam} = \left(\sqrt{E_{Lang.}} + r/R\right)^2$$

Das (1950) and Fonda and Hearne (1957) repeated Langmuir's computations using the correct collision criterion, i.e. that the envelope of the trajectory of the colliding droplet's surface must touch the collector surface. Mason (unpublished) extended Fonda and Hearne's computations to values of E_v beyond the critical value of K (K = 1.214). In his book, Mason (1957) compares the values of E_o given by these authors and gives a table of "best values" based on Fonda and Hearne's and his own computations (see Fig. 2.5).

The second fault introduced by Langmuir's assumption that the droplet size is negligible is less tractable and rather more serious. Being of negligible size the droplets were assumed to cause no disturbance to the airflow round the collector. While this is a reasonable approximation when the collector is very much larger than the droplet, it clearly fails when they are of comparable size. Recognizing this limitation, Mason limited his table of collision efficiencies to values of $r/R \leqslant 0.25$; Hocking

Fig 2.5 COLLISION EFFICIENCY DIAGRAM

[after Mason 1957]

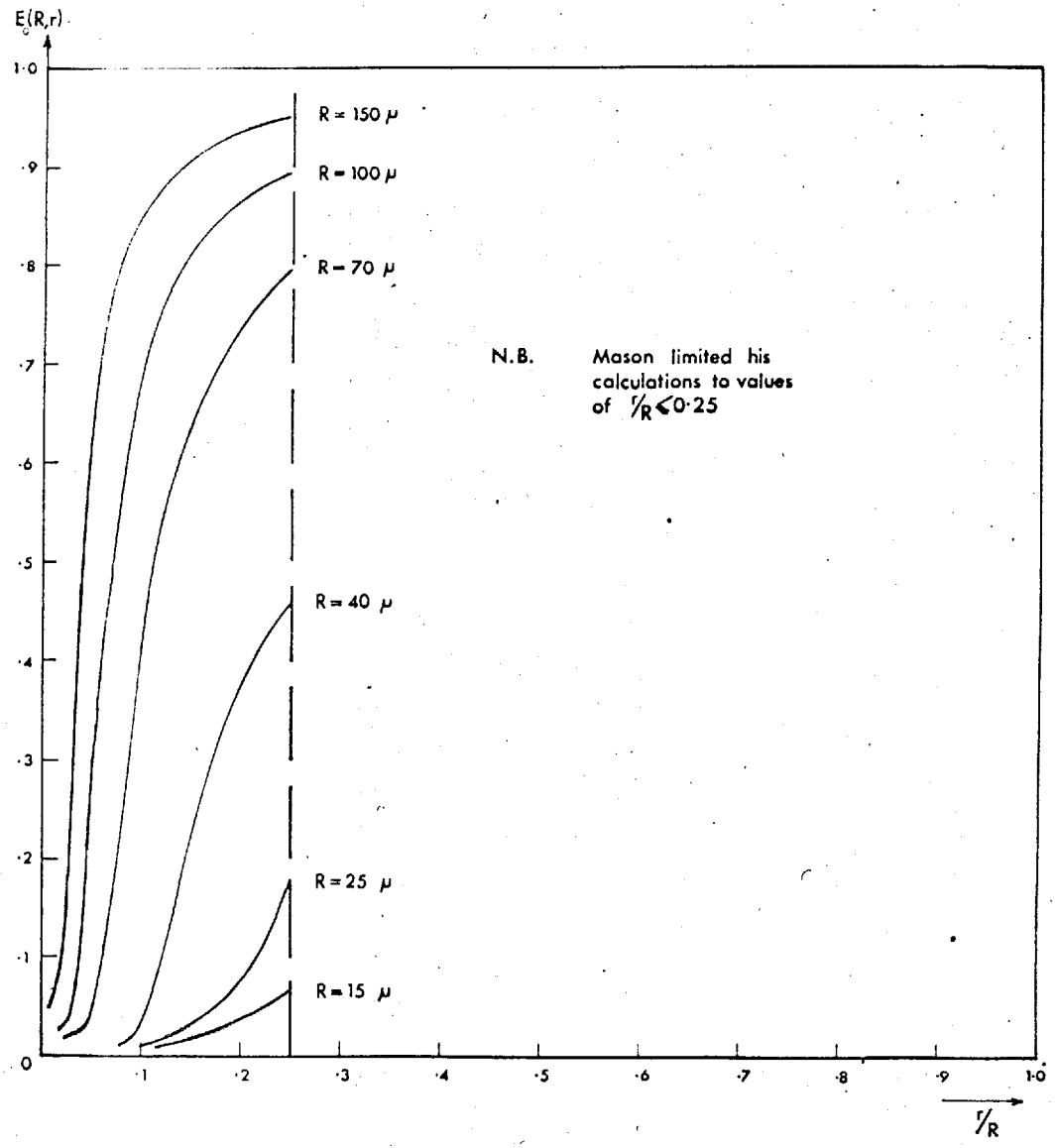

(1958) suggests that the results are suspect beyond $r/R = 0.1$

Pearcey and Hill (1956) sought to overcome this objection by superimposing the individual flow fields of the two drops. The combined field so obtained satisfied the boundary condition of zero flow at infinity, but gave a non-zero flow of fluid through the surface of each drop. However, this error was considered to be unimportant as the duration of close approach, when the error is largest, is only a small fraction of the total interaction time. The authors used the same formula for the drag force as had Langmuir, but assumed the flow round the individual drops to be that calculated by Pearcey and McHugh (1955) using Oseen's approximation. The limitations to Oseen's solution have already been discussed and it is not surprising that the collision efficiency diagram of Pearcey and Hill (see Fig. 26) differs strikingly from Mason's (Fig. 2.5). The collision efficiencies for collectors of $R > 13\mu$ rise beyond unity as $r/R \rightarrow 1$ and larger collectors have collision efficiencies up to 100 and even larger. The authors explained that these large collision efficiencies result from the attractive force supplied by the wake of the lower droplet.

Later workers (e.g. Hocking, 1958; Shafrir, 1964)

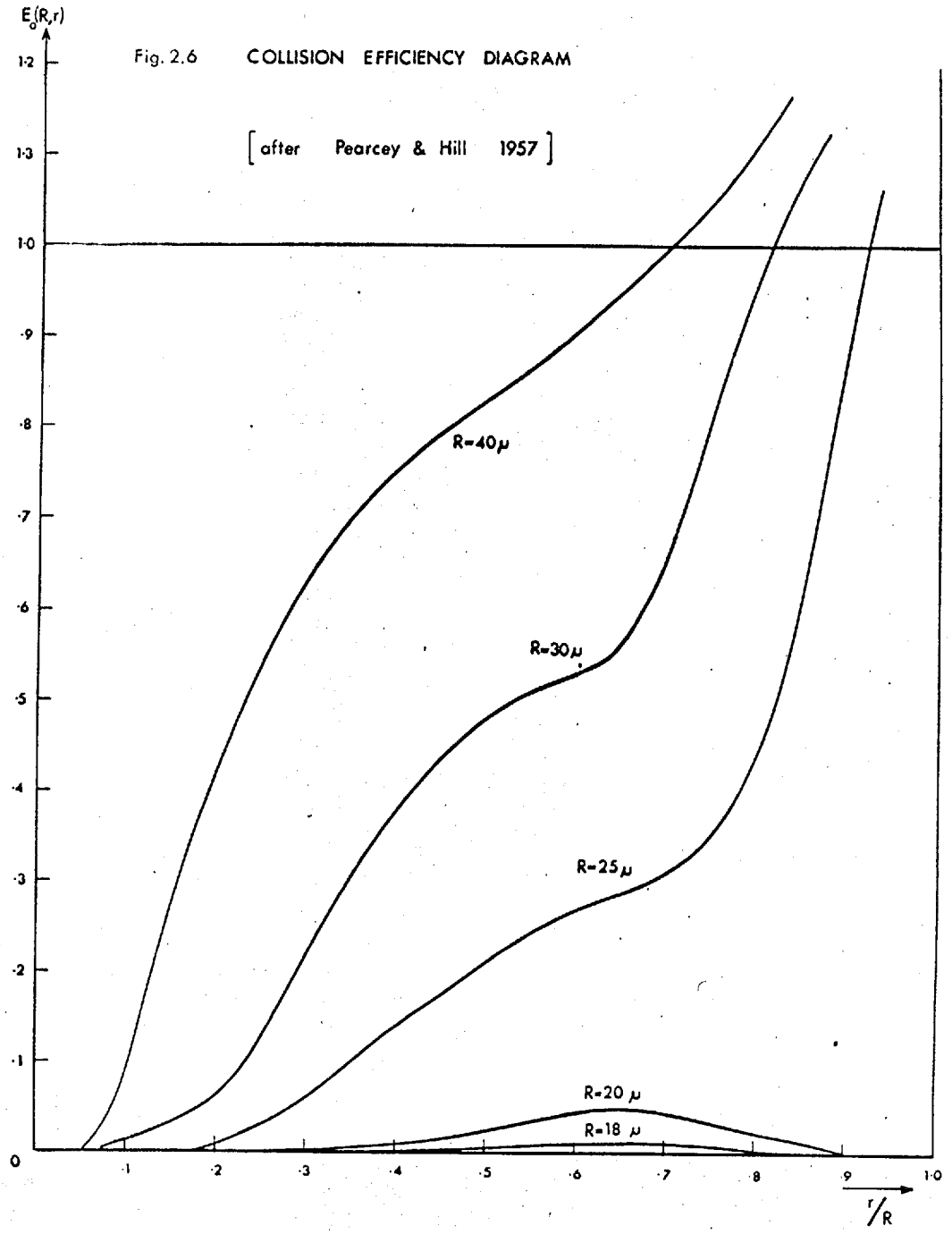

Fig. 2.6 COLLISION EFFICIENCY DIAGRAM

[after Pearcey & Hill 1957]

have suggested that the large collision efficiencies are in fact incorrect and that they arise from errors in the combined flow field when the drops are in close proximity. As has already been remarked, both the Oseen approximation and the method used by Pearcey and Hill to combine the two flow fields will be least accurate when the drops are close together. Furthermore, the high collision efficiencies are obtained for droplets of comparable size which, having very similar terminal velocities, remain in close proximity for a considerable period of time.

Although their theory is now discredited, Pearcey and Hill's paper remains one of the most comprehensive (qualitative) surveys of the collision of two water drops in air. They alone emphasise the potency of the wake as an agency for capture. Besides considering the enhancement of E_0 when the lower drop (the "droplet") has an attractive wake, they also discuss the possibility of "indirect" capture which, they conclude, may occur when the droplet misses the lower surface of the collector and passes round it only to be trapped in the collector's wake and brought into collision with the latter's upper surface (see Fig. 2.7). The authors predict that indirect collision may occur for similar drops in the range $1 < Re < 10$ for certain impact

Fig. 2.7 INDIRECT COLLISIONS. from Pearcey and Hill.

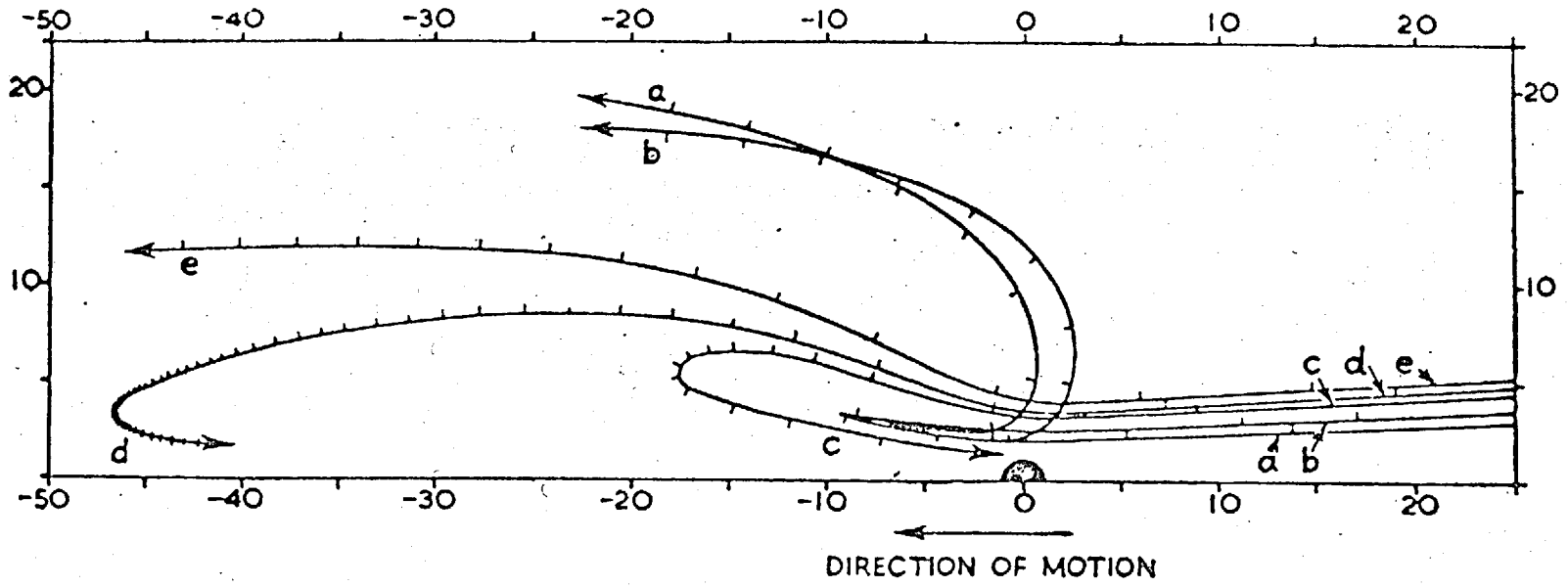

parameters. However, as this effect is only found in rare instances it is unlikely seriously to alter the collision efficiency diagram.

Hocking (1958) was the first worker to allow fully for the mutual interference of two drops. For the case of Stokes flow he analysed numerically the complete boundary condition problem for the flow of air round two spheres. This was achieved by superimposing the flows of two spheres moving along and perpendicular to their line of centres (permissible since the Stokes equations are linear). Trajectories were followed from an initial drop separation of fifty radii and the grazing impact parameter found by trial and error.

Hocking's collision efficiency diagram is shown in Fig. 2.8. The most important result of his work is that drops with radius less than or equal to 18μ do not collide with smaller drops of any size. This sets a crucial limit on the start of the coalescence mechanism. Collectors with $R > 18\mu$ have values of E_o which increase with R, each curve having a maximum value at $r/R \sim 0.5$ and dropping to a cut-off on either side of this. The calculations were terminated at $R = 30\mu$ beyond which value the Stokes solution is not valid. The author also limits his collision efficiency

Fig. 2.8 COLLISION EFFICIENCY DIAGRAM

[after Hocking 1958]

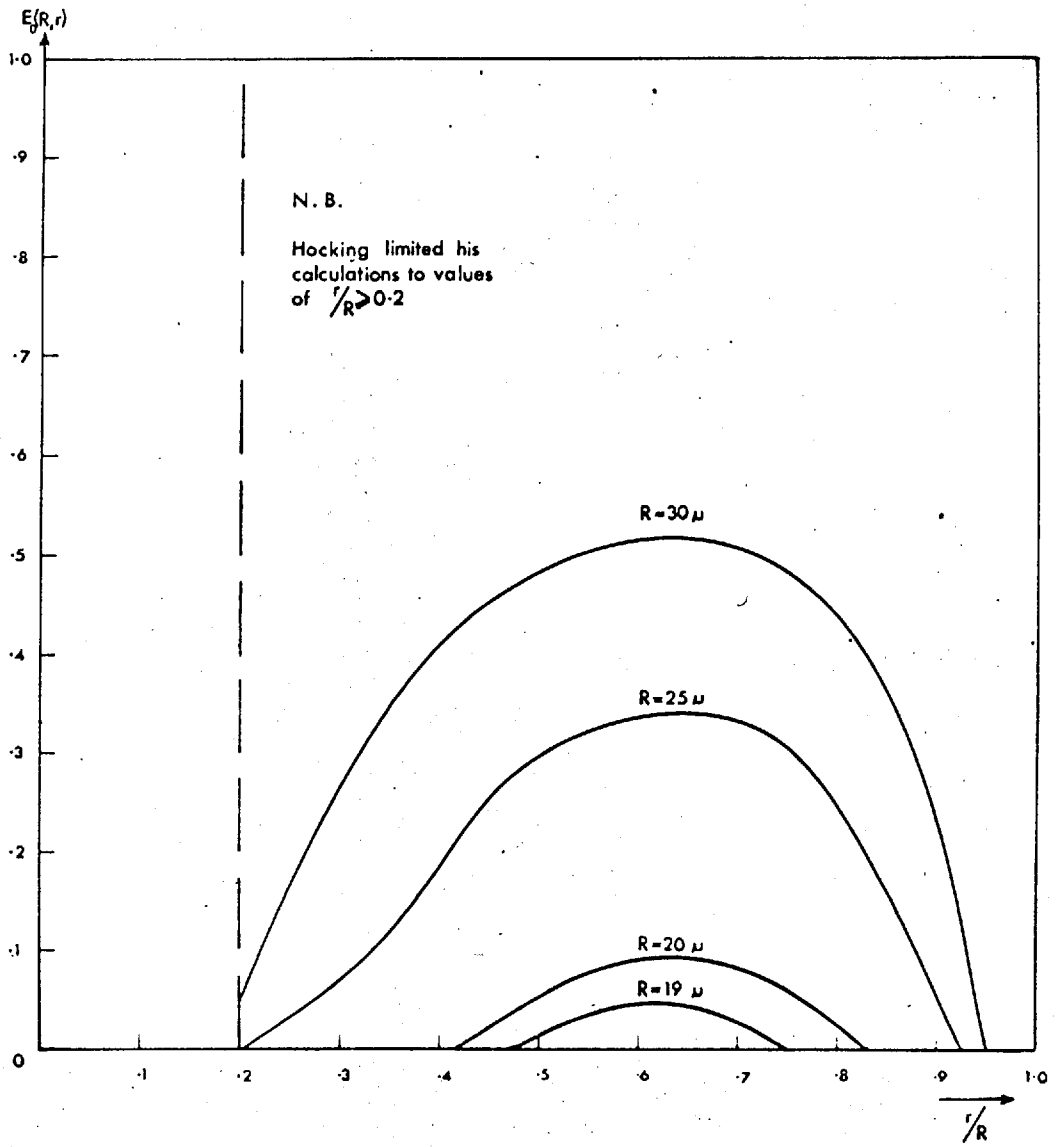

curves to $r/R > 0.2$; at smaller values of r/R his theory is inaccurate, but approximate calculations showed that for $R = 25\mu$ and 30μ the curves flatten off to a roughly constant value of $E_o = 0.004$. Hocking points out, however, that the values quoted by Mason should be reliable for such small r/R. There seems to be little doubt that Hocking's theory gives accurate values for collision efficiency and it has become customary to use his results as a standard for testing the accuracy of each new theory at $R < 30\mu$.

In 1960 Mason (unpublished) modified his collision efficiency diagram to include Hocking's new data. He used an IBM 709 computer to interpolate between Hocking's $R = 30\mu$ curve and Langmuir's aerodynamic limit. However, this new diagram (Fig. 2.9) was soon superseded by new calculations by Shafrir and Neiburger (1962, 1963) who used Jenson's (1959) method for determining the flow round each drop, assumed to be independent of the other. The authors proceeded to calculate the drag force on each drop due to the isolated flow pattern of the other. The drop trajectories were then computed in the usual way using an electronic computor. The resulting collision efficiency diagram is reproduced in Fig. 2.10.

This technique bears some similarity to that used

Fig. 2.9 COLLISION EFFICIENCY DIAGRAM

[after Mason 1960]

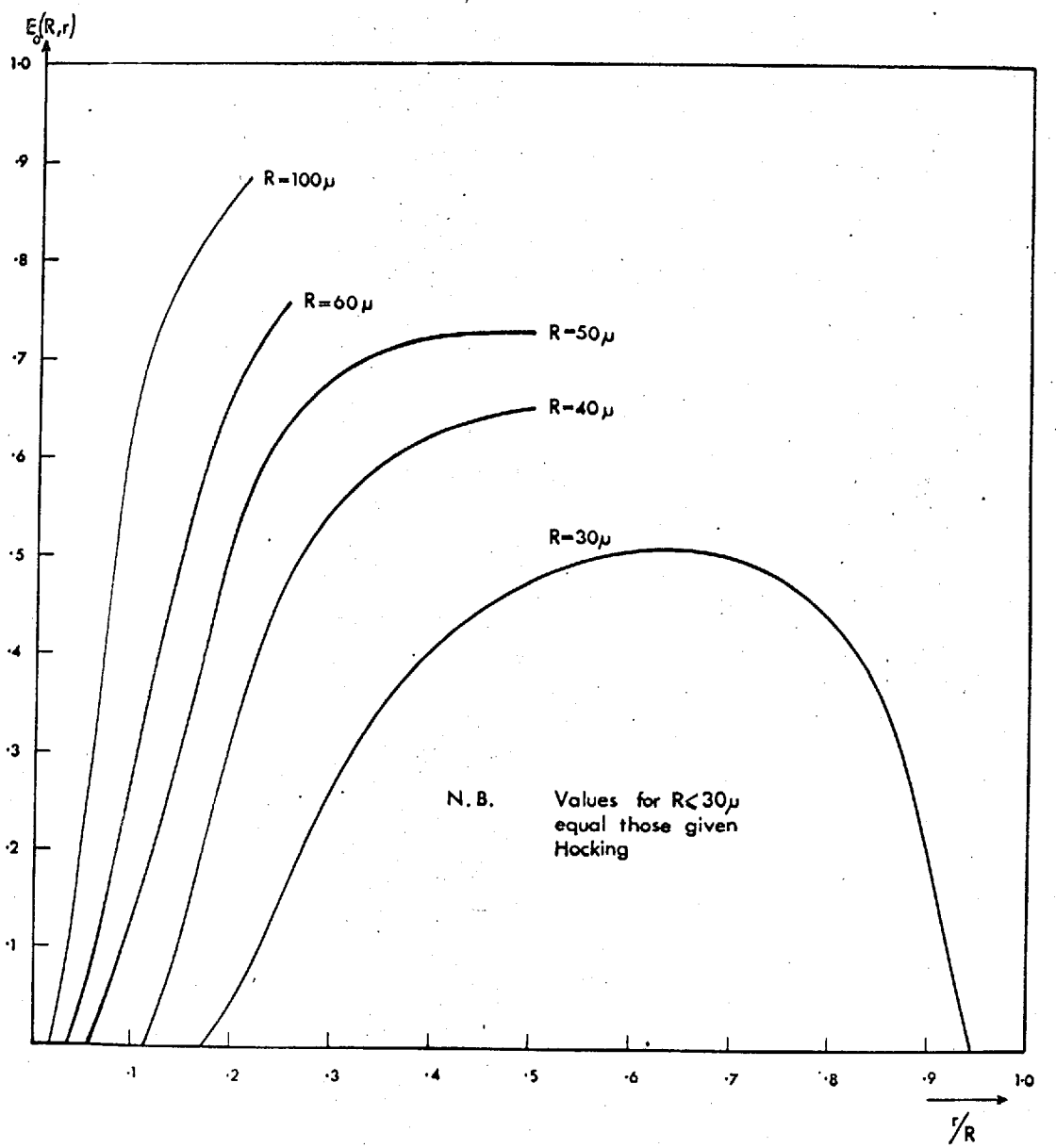

Fig. 2.10 COLLISION EFFICIENCY DIAGRAM

[after Shafrir & Neiburger 1963]

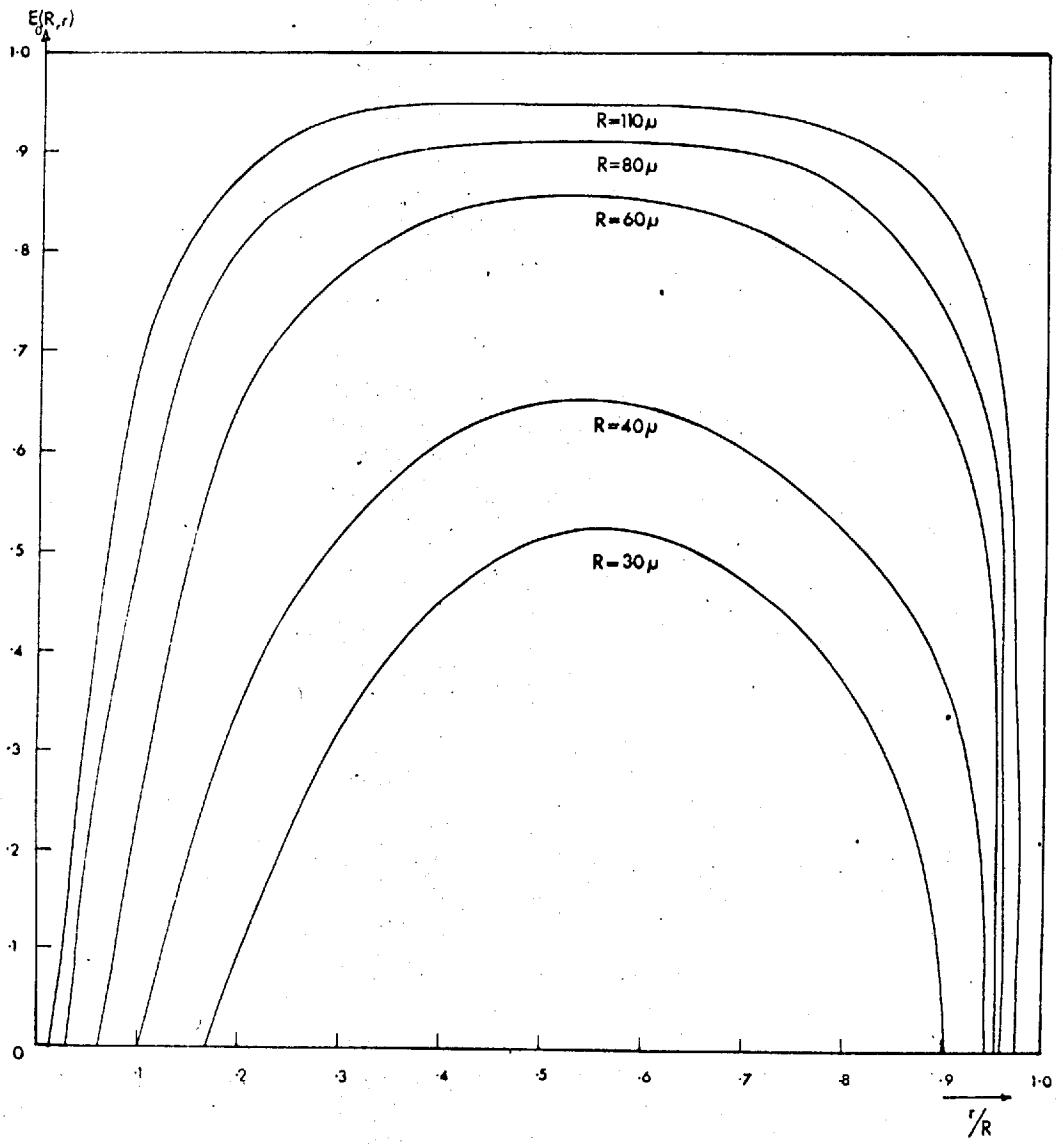

by Pearcey and Hill (1956), which suffered from two major faults, namely the incorrect extension of Oseen's solution to large Reynolds numbers and secondly, a failure to satisfy the boundary condition of no flow through the drop surfaces, especially when they were close together. Shafrir and Neiburger avoid the first objection by using Jenson's flow field, which appears to be satisfactory for $Re < 40$, but the second objection may also be levelled against their analysis. Thus Shafrir and Neiburger's theory may be unreliable when the colliding drops are of similar size. In fact the two theories give opposite results; Pearcey and Hill predict very large E_c as $r/R \to 1$, while Shafrir and Neiburger predict $E_c \to 0$. The difference results from differences in the flow diagram given by the Jenson and Oseen solutions. Pearcey and Hill actually stated that their theory would be expected to exaggerate the effect of the wake, and experimental evidence will be produced later (Chapter 4) to show that Shafrir and Neiburger's values are too small.

2.2 EXPERIMENTAL INVESTIGATIONS

The prime task of experimental investigation is to compile a complete collection efficiency diagram for comparison with the various collision efficiency diagrams

obtained theoretically. Differences beyond experimental or computational error may be explained in one of two ways. They arise either from errors in the theoretical analysis (and it has been shown in the preceding section that different authors provide conflicting values for E_o), or from a coalescence efficiency of less than unity. A variety of evidence is now available to support the theory that coalescence efficiency is nearly always, in practice, unity (see summary by Jayaratne, 1964). This being so, collection efficiency and collision efficiency should be identical and experimental values for the former may be used as tests of the latter.

A. Indirect methods

Hitschfeld and Gunn (1951) investigated the growth of large drops (R = 1.59 mm) falling through a heterogeneous cloud of small drops ($2 < r < 20\mu$) formed continuously by cooling a steam jet. Five hundred drops were passed down a three-metre column of cloud and their gain in weight measured. An average collection efficiency calculated for the 1.59 mm collectors and the cloud used in the experiment was compared with Langmuir's collision efficiency values. The authors obtained very close agreement for

Table 2.1 Experimental collection efficiencies

(Hitschfeld and Gunn)

cloud type	1	2	3
range of droplet radii	2 → 22 μ	2 → 68 μ	2 → 100 μ
E_o (Langmuir)	0.15 ± 0.045	0.51 ± 0.04	0.60 ± 0.04
E (measured)	0.14 ± 0.02	0.50 ± 0.1	0.62 ± 0.08

four different cloud spectra, thus confirming the validity of Langmuir's calculation for large collectors colliding with very much smaller droplets ($r/R < 0.1$). Their results are summarized in Table 2.1.

Kinzer and Cobb (1956, 1958) devised an interesting variation on this technique. The droplet cloud was sucked up through an 8 mm diameter glass tube, arranged vertically. One of the largest of the cloud drops was kept at rest in the tube opposite a microscope by adjusting the updraught to balance its fall speed. Every minute or so the selected drop captured a smaller cloud droplet and the updraught was adjusted to compensate for the drop's increased fall speed. A record of the updraught gave the rate of change of fall speed and hence the rate of growth of the observed drop. Two clouds were used. The first consisted of drops with $4 < r < 11\mu$ and the second consisted of drops with $4 < r < 13\mu$. From the growth rate and the liquid water content of the cloud the authors derived the collection efficiency* for the drop at various stages of its growth.

---

* In general it is only useful to consider an average collection efficiency $E(R \rightarrow R + \Delta R, r \rightarrow r + \Delta r)$ when ΔR and Δr are small compared with $(R-r)$. This condition is satisfied in Hitschfeld and Gunn's experiment and in

/continued at foot of next page.

The graph of variation of E with collector radius R for the second cloud is reproduced in Fig. 2.11, together with the corresponding collision efficiency curve based on Langmuir's theory. Within the range R = 25μ - 400μ the experimental and theoretical curves are in tolerable agreement, but below R = 25μ the collection efficiency rises rapidly to near unity at R = 7μ (the peak of the cloud distribution), and for R > 400μ the experimental curve drops to reach E = 0.15 at R = 1.5mm.

The authors state that this fall in E at large values of R, quoted in their first paper (1956), was subsequently found to be caused by evaporation of the cloud at the higher wind speeds. When this was eliminated their values followed closely the theoretical curve.

The rise in E for R < 25μ is the subject of a new

Kinzer and Cobb's first (1956) experiment in which the collectors were raindrops. However, in the present case, where at the start R is within the cloud range $r \rightarrow r + \Delta r$, the concept of an average collection efficiency for a known collector in a given cloud, while formally correct, provides little physical insight into drop collisions beyond showing that they do, or do not, occur.

Fig. 2.11 EXPERIMENTAL COLLECTION EFFICIENCY CURVE

[from Kinzer & Cobb 1958]

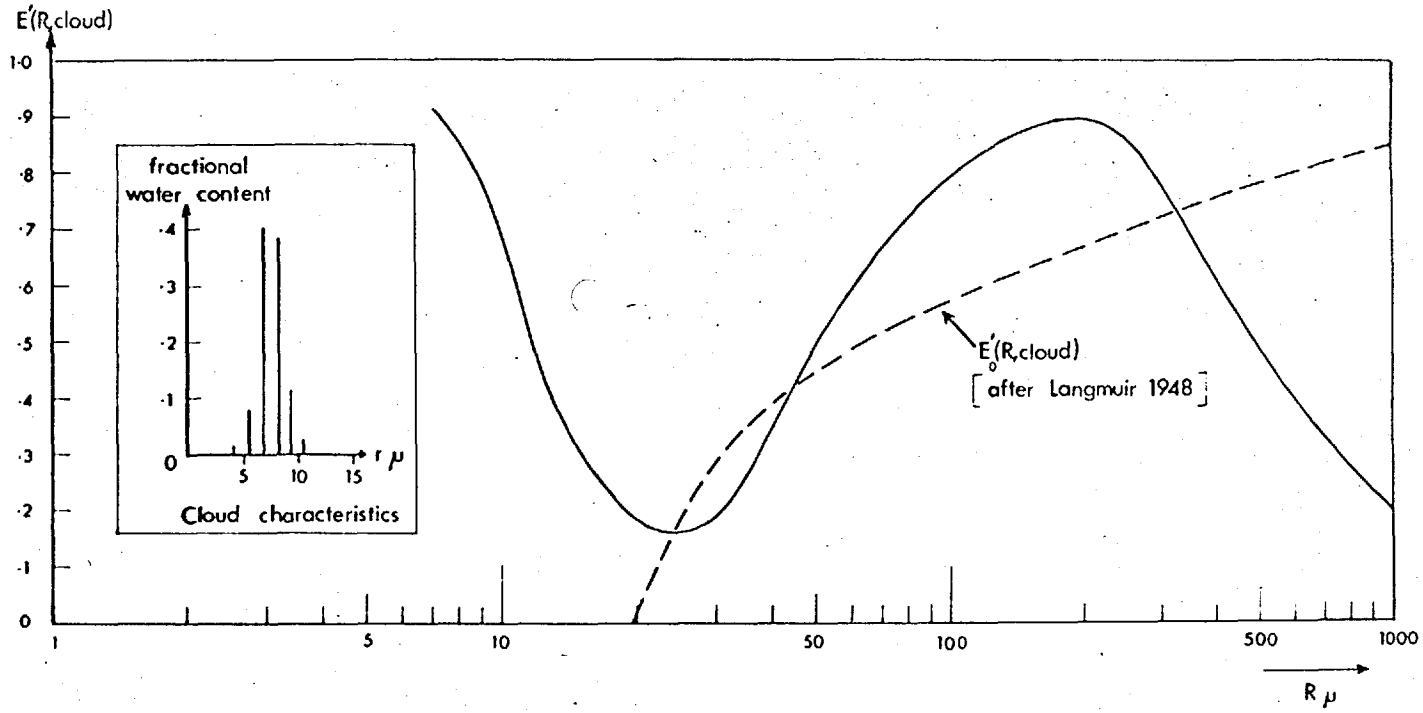

theory presented by the authors. They suggest that the Stokesian flow round a falling drop may be represented by an "eddy" which moves with the drop. Each eddy is supposed to extend out until it meets one from another drop. As the drops are falling at different speeds this "eddy field" is in continuous change so the authors treat it as a random mixing process capable of promoting turbulent diffusion. The selected drop is considered to start growing by chance. In so doing it will act as a sink of liquid water causing a gradient of liquid water content around itself. Treating the cloud as a continuum with the same liquid water content, the authors calculate the growth rate expected in the postulated eddy field. They claim that this gives a collection efficiency curve which closely matches their experimental one.

In the concluding discussion the authors admit that their analysis is "intuitive and necessarily crude". It is possible to criticize it on a variety of counts. The most important objection is that the theory does not consider actual collisions between individual drops. Even if one accepts the postulate that cloud drops will be introduced into the vicinity of the collector by a process of turbulent diffusion, the flow patterns round

the two drops will still decide the outcome of the final collision. Hocking has analysed the collision of drops smaller than 18μ radius and has shown that contact does not occur. Hocking's theory would be invalid if the droplet approached the collector at some velocity other than their difference in terminal velocities, or if there were some external influence deforming the flow patterns during the collision. Neither of these factors is suggested in the author's analysis, where it is implied that there is no disturbance of the flow round the individual drops due to the eddy field.

The strength of the liquid water sink caused by the growing collector is very weak indeed. Figures quoted by authors show than an average of one capture was made every 150 seconds. The droplet concentration was 1,500 cm^{-3} so in 150 secs about 200,000 cloud droplets would pass a 15μ collector, i.e. the liquid water gradient results from a droplet deficit of 1 in 200,000. By treating the environment as an aqueous continuum the authors obtained a finite transport of liquid water along this very small gradient of liquid water. When this corresponds to such a small fraction of the cloud droplets it is essential to consider the motion of the individual drops. For example,

a simple computation shows that the gradient of liquid water content causes only a minute addition to the approach velocity of the one droplet out of 200,000 that is captured.

It is not difficult to find a more reasonable explanation of the observed rise in E for $R < 25\mu$. The velocity profile in the narrow tube will be parabolic in cross-section at these low speeds. The velocity shear across the drops will tend to concentrate them at the centre of the tube and if in fact there were a small non-zero collection efficiency the increased concentration would give a corresponding increase in the growth rate. However, a more important factor is the disturbance that the velocity profile will cause to the flow pattern round a pair of drops in collision. The cloud droplet will be forced in towards the collector. This horizontal force will have greatest effect when the drops are of comparable size so that they remain together for a relatively long time, but a considerable difference in radii could be tolerated given a reasonable velocity shear. As the collector grows larger than the largest cloud drop the effect will decrease, although this decrease will be slightly off-set by the rise in the air velocity through the tube.

It would be interesting to repeat this ingenious

experiment with a larger diameter tube, thereby avoiding the major objections to it. If necessary a reduced droplet concentration could be used, for the authors predict that the mechanism will still hold at a tenth of the concentration used by them. The proposed theory should also be independent of the tunnel size. Indeed, the same mechanism would be present in conditions of free fall, where it would considerably accelerate onset of the coalescence mechanism.

Picknett (1960) devised a technique for determining E for a very narrow range* of droplet sizes while still using a heterogeneous cloud. He sprayed salt solution into a one-metre vertical glass column (internal diameter 13 cm) within which the air was maintained at 84% R.H. The salt droplets rapidly attained an equilibrium radius in the column, establishing a stable cloud. The size spectrum of the cloud was determined by allowing the droplet to settle on to a hygrophobic slide, which was subsequently placed into a box maintained at 84% R.H. There the traces of salt left by the settled cloud droplets grew to an equilibrium hemisphere and were measured under an optical microscope. The droplet spectrum derived in this way

---

*See footnote on page 65

extended to 9μ radius with a peak at 1μ .

The experimental procedure was as follows. The cloud was established in the top metre of a four metre vertical glass tube. Pure water drops, all of identical size, were then injected into the top of the cloud from a spinning top generator. On their way through the cloud some of these captured a single cloud droplet. The collectors were allowed to settle onto a slide which was half hydrophobic and half coated with a layer of magnesium oxide. This collector slide was removed from the apparatus before the cloud fell through the lower 3m settling tube and on to the slide.

The collector slide was examined under the microscope. Impressions left by the collectors in the magnesium oxide gave their size and concentration; salt hemispheres grown in the humidity box corresponded to captured cloud droplets. The size distribution of the collected droplets was measured and, together with the collector concentration, used to compute the collection efficiency for the chosen collector size and droplets within each of fifteen ($\Delta r = \frac{1}{2}\mu$) size ranges.

Picknett plotted these values to give curves of $E : {}^{r}/_{R}$ for $R = 30\mu$ and 40μ (see Fig. 2.12) which agree

Fig. 2.12 EXPERIMENTAL COLLECTION EFFICIENCY CURVES

[from Picknett 1960]

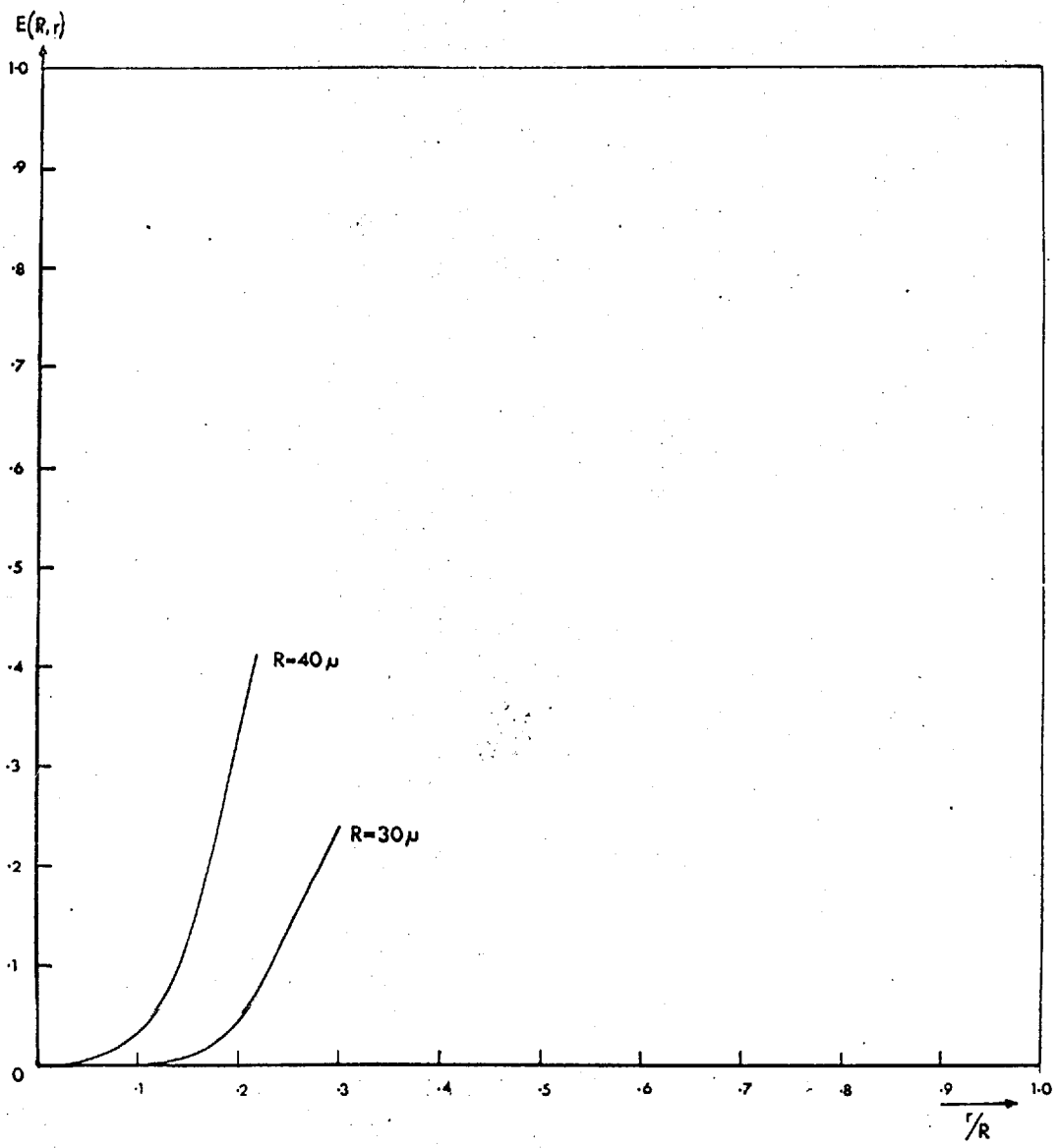

with the collision efficiency curves of Hocking and of Shafrir and Neiburger. The one significant difference occurs at low values of r/R. Here Picknett found a tail with finite (but small) values of E extending back beyond the theoretical cut-off. It will be remembered that although Hocking terminated his collision efficiency curves at $r/R = 0.2$, approximate calculations did predict a tail of the kind found by Picknett.

The experiment to be described in Chapter 3 is based upon Picknett's technique.

B. Direct observations of drop collisions

The C.S.I.R.O. cloud physics group at Sydney, Australia, has developed a technique which enables them directly to observe water drops in air. Two experiments have been described. In the first, Telford, Thorndike and Bowen (1955) and Telford and Thorndike (1956) used the updraught in a vertical wind tunnel to support a cloud of nearly identical drops from a spinning disk generator. The drops were photographed with a specially designed camera, in which the film moved horizontally at a constant speed. They were illuminated by an arc lamp which pulsed at 100 c.p.s. in response to the A.C. supply. Photographic

exposures of up to a quarter of a second gave streaks with a slope proportional to the speed of the drop. The wind speed in the tunnel was adjusted to equal the mean fall speed of the drops, so that slower moving drops gave streaks with a positive slope and vice versa. Occasionally two drops coalesced to give a double-mass drop which accelerated down against the updraught. A photograph of one such collision is included in the 1956 paper.

The authors derived from the general accretion equation (equation 1.1) a formula for the collection efficiency of these events

$$E = \frac{2NVc}{\pi R^2 . n . v H .} \qquad 2.1$$

where n and N are the counts of the original and double drops in the photographs, V is the coalesced drop fall speed, R the original drop radius, c the volume containing the photographed drops and H the distance between drop injection and photography. The average approach velocity, v , was determined separately from a series of $\frac{1}{10}$th. second exposures. The relative velocity between each drop and the nearest one below it was measured and plotted on a histogram. The factor v is then the averaged relative velocity of those pairs of drops that were approaching one another, separating

drops being ignored.

The authors used equation 2.1 to calculate that nearly identical 65μ radius drops have a collection efficiency

$$E' = 12.6 \qquad (E = 3.2)$$

This implies that the grazing impact parameter (assuming a coalescence efficiency of unity)

$$b_g = \sqrt{E'}R \qquad R = 3.5R$$

which would necessitate a considerable "sucking in" of the upper drop in the wake of the lower one. This value is surprisingly large for 65μ drops which have $Re < 6$ and provoked criticism from Dessens (1955) and Sartor (1956), both of whom suggested that the wind tunnel profile had not been flat. In reply Telford and Thorndike (1956) provided a graph showing the remarkable linearity of their velocity profile. They also included further results for drops of 50 to 100μ radius, all of which had collection efficiencies of $E \simeq 3.2$.

Close inspection of the photograph in the 1956 paper fails to reveal a large horizontal sucking in of the upper drop, but this may be masked by the poor resolution or by the displacement superimposed by the film transport. If a few exposures had been made with the film stationary the large

impact parameters would have been easily detected. In the absence of this evidence there must remain some doubt as to the validity of the high collection efficiencies claimed by the authors. If their result is correct, then in provides strong evidence in support of the theory of Pearcey and Hill. However, it has not been confirmed elsewhere and is in direct contradiction to experiments to be described in Chapter four.

Telford and Thorndike (1961) later used the same photographic technique to investigate nearly equal drops falling freely through tranquil air. The drops were produced by a spinning top generator which gave a spread of sizes of about $\pm$ 6%. Electrical charges on the drops were reduced by applying a potential of 0.75V to the spinning top and then passing them through a highly ionized "discharge section" at the top of the settling column (5 cm x 1.5 cm in cross-section). Measurements with a horizontal electric field showed that each drop carried less than 300 electronic charges.

The authors investigated the behaviour of two drop-sizes, used independently. The smaller drops, $R = 16.25\mu \pm 1.25\mu$, were never observed to coalesce, although on 80 occasions two drops were observed to remain very close

together for about 2 cm fall before separating and continuing as individual drops. During their close association the drop pair accelerated downwards as the result of a reduction in their total aerodynamic drag and drifted sideways. This behaviour is very similar to that observed in model experiments described in the next section.

The absence of coalescence provides experimental evidence for Hocking's prediction that $E_o = 0$ for the range of drops used in this investigation, even for the extreme case of $R = 17.5\mu$ & $r/R = 0.88$. The authors show that Pearcey and Hill's value for the collision efficiency ($E_o = 1.5$, for $R = 16.5\mu$ & $0.88 < r/R < 1$) is at least an order of magnitude too large.

For the larger drops ($R = 22.5\mu \pm 6\%$) the authors detected a single coalescence after exposing one hundred feet of film. While they made no estimate of the collection efficiency corresponding to this event frequency, it must be very small indeed. Hocking's theory predicts $E_o = 0$ except for the extreme experimental case of $R = 23\mu$ and $r/R = 0.88$, where E_o has a very small finite value. Again, there is good agreement between experiment and Hocking's theory.

The experiment reported in Chapter 4 is a logical extension of this work by Telford and Thorndike.

C. Model experiments

One of the most useful techniques available to the aerodynamicist is the construction of a scale model of the system under study. In the case of coalescence studies the object of using model experiments is to increase the size of the particles so that their production may more easily be controlled and their behaviour may be followed without recourse to elaborate optical techniques. The factors necessary for the construction of a reliable model have been discussed by Sartor (1954) and by Schotland and Kaplin (1956). They may be reduced to two necessary conditions.

Firstly, the spheres used in the model must have the same Reynold's numbers as the prototype water drops in air. Thus the size of the sphere may be scaled up only if the viscosity of the medium is correspondingly adjusted, following the formula

$$Re = \frac{2\rho v R}{\eta} \qquad 2.2$$

where v and R are the velocity and radius of the sphere, and ρ and η are the density and dynamic viscosity of the medium in which it is immersed.

Reynolds number similarity at terminal velocity ensures that the flow pattern round an isolated sphere

falling through a tranquil medium will be precisely similar for airborne water drops as for solid spheres in a liquid, or for any other system. However, when the steady state is disturbed by introducing a second sphere the combined flow pattern round them will only be similar in all systems if a further condition is obeyed. This second condition becomes very pertinent when replacing a gaseous medium by a liquid one. The density ratio of water droplets and the air in which they are immersed is approximately a thousand , but in model experiments using a liquid medium the density ratio is generally lower than ten . The consequence of this hundred-fold decrease in the relative medium density will be to change the response of the spheres to the interaction of their flow patterns. The proportional change produced in the medium's inertia in the case of a liquid will be very much larger than in the case of a gas. Thus as the medium's acceleration is different in each case the trajectories and collision efficiencies will differ also.

This objective may be overcome by limiting the experiments to spheres with Reynolds numbers so small that the fluid inertia is a negligible factor and the spheres follow a creeping motion. This is essentially an extension of the criterion used by Stokes for his solution of the

(viscous) flow round an isolated sphere, i.e. $Re \ll 1$. In both cases the inertia term in the complete Navier-Stokes equation may be neglected at very small Reynolds numbers. During the interaction of two spheres the boundary conditions are varying with time, so the time derivative of the inertia term becomes important unless $Re \ll 1$, when it also is negligible compared with the viscosity term.

To summarize, model experiments may be used to obtain an accurate quantitative picture of collisions between cloud drops with $R < 30\mu$ *. The spheres used in the model correspond to cloud drops with the same Reynolds numbers.

Sartor (1954) studied pure water drops falling through mineral oil ($\eta = 3$ poise, density ratio $\simeq 1.2$). Droplet trajectories, reconstructed from ciné film of the models, were compared with Langmuir's computed trajectories. Two examples are quoted in his paper, for $R = 24.7\mu$, $r/R = 0.5$ (model sizes 2.5 mm and 1.25 mm) and for $R = 17.5\mu$, $r/R = 0.5$ (model sizes 2.24 mm and 1.25 mm). Sartor reported that

---

* The Reynolds number for an isolated drop of 30μ radius is 0.5. Hocking and others consider that this is the largest drop size that may safely be described by Stokesian flow.

the droplets' wake gave a horizontal attraction which "sucked in" laterally the collector when their separation was about 4R. This was followed by a decrease in the vertical approach velocity and a lateral deflection just before collision, although in neither case did the two drops coalesce. The collision efficiency for the second case was stated to be 0.650 compared with Langmuir's E_c - 0.203* and Hocking's E_c - 0.1.

The failure of the drops to coalesce although they had collided became the major subject of Sartor's investigation. He tried a variety of different liquids, both for the drops and for the medium, without success, but eventually made the drops coalesce by giving them large electric charges. In fact, of course, the failure of the uncharged drops to coalesce was a direct consequence of the modelling technique. The increased drainage time of the liquid medium (compared with air) trapped between the impacting drops exceeded the time that they remain in contact, so coalescence efficiency was zero. The subject of coalescence between liquid drops in a liquid medium has received detailed study by S.G. Mason (e.g. Mason, 1961).

Schotland and Kaplin (1956, 1957) extended Sartor's investigation of drop trajectories with a much improved

---

* Sartor's interpolated value.

technique. They photographed steel ball bearings falling through an aqueous sugar solution (η = 20 poise , density ratio = 5.6) with two cameras set at right angles. The full three dimensional trajectories of each drop were reconstructed from photographs taken against a dark background using reflected stroboscopic illumination. A single multiple-image exposure on each camera carried a complete record of each experiment.

By carefully varying the initial horizontal separation of two spheres, released in sequence, the authors were able to find the grazing impact parameters and hence deduce collision efficiencies for each pair of drops. Their collision efficiency curves for collectors with modelled radii, R = 11, 14, 17 and 21μ are reproduced in Fig. 2.13. A graph showing the collection efficiency of pairs of identical drops as a function of drop radius is reproduced in Fig. 2.14.

Schotland stated that equal spheres collided if the initial vertical separation* was less than 24R and that the upper drop accelerated continuously towards the collector, the average approach velocity being about one tenth of their

---

*See comment on "wake length" in Woods and Mason, 1965.

Fig. 2.13 MODEL EXPERIMENTS Schotland 1957

FOR UNEQUAL SPHERES

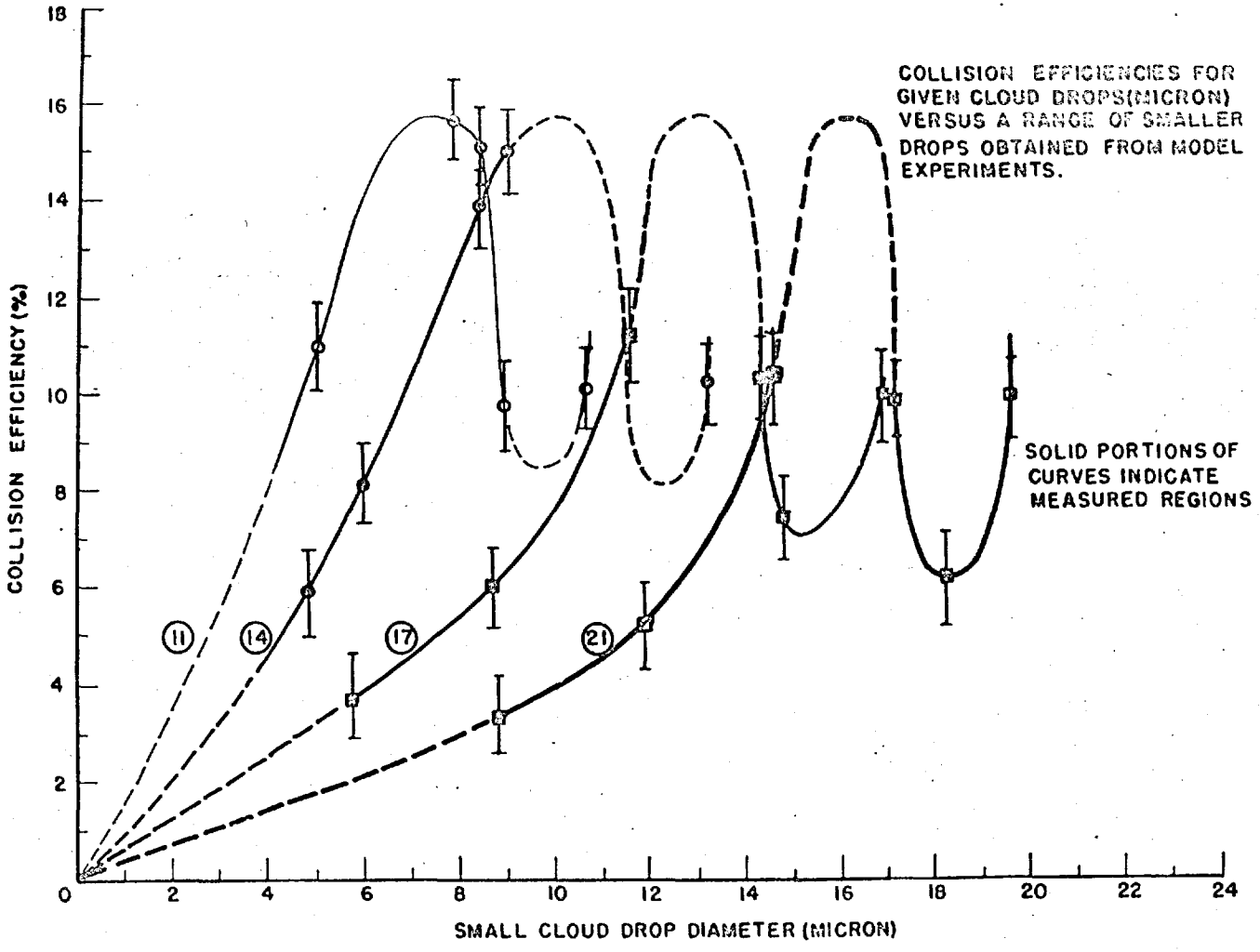

FIG. 2.14 MODEL EXPERIMENTS by Schotland 1956

FOR EQUAL SPHERES

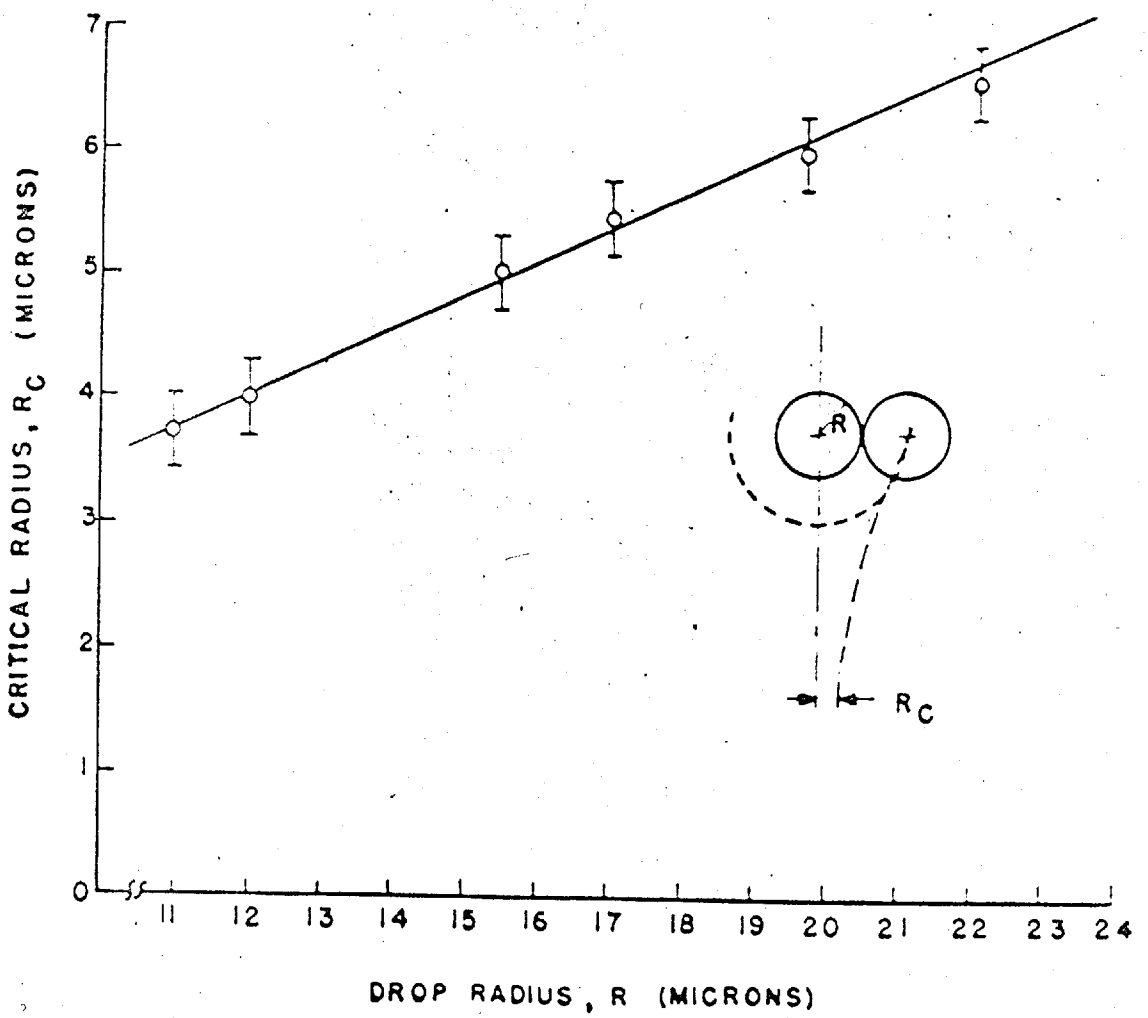

Plot of critical collision radius as function of drop radius.

terminal velocity. (This confirms the identical observation of Telford and Thorndike (1961) for equal water drops in air.) When unequal drops collided, however, there was a steady deceleration of the upper drop. The lateral "sucking in" found by Sartor was not reported by Schotland, although close examination of the trajectories for $R = 17.3\mu$ and $r/R = 0.5$ colliding with an impact parameter $b = 2.6\mu$ does appear to reveal some slight lateral displacement of the kind described by Sartor.

2.3 PERTURBATIONS TO GRAVITATIONAL COALESCENCE

Bowen (1950) and Ludlam (1951) independently predicted that the coalescence mechanism would make negligible contribution to the development of a cloud droplet spectrum unless the condensation process supplied drops with radii greater than 20μ . None of the theoretical or experimental results quoted so far in this chapter alters this fundamental limitation. Hocking (1958) in fact emphasised the situation by predicting that no collision would occur unless drops of at least 18μ radius were present. The similarity between these two results is fortuitous. Hocking's limit is due to the disappearance of the collision efficiency when $R < 18\mu$, whereas the Bowen-Ludlam limit results essentially

from the very low terminal velocity of drops with $R < 20\mu$ (their calculations were based on Langmuir's collision efficiency data which gives sizeable values for $R < 20\mu$).

The growth of such large drops by condensation may not be possible in many conditions owing to lack of the required giant hygroscopic nuclei or through insufficient vigour in the ascending thermal. It is pertinent, therefore, to investigate whether some extra factor might succeed in extending the coalescence mechanism to smaller drop sizes ($R < 20\mu$) for which gravitational settling is an insufficient agency. Two possible factors immediately present themselves, namely electrification and turbulence, both of which have been omitted from the theories described so far.

The investigations to be described in this section have sought to deduce the effect of these two factors on cloud droplet collisions. The eventual objective of such work is to find out whether they are capable of assisting gravitational coalescence in the early stages of cloud development.

A. Electrification

In considering cloud drop electrification it is necessary to differentiate between net charges carried by

individual drops and their polarization under electric fields in the cloud. Gunn (1952) quotes an average value of 2×10^{-8} e.s.u. for the charges on cloud drops and fields of 10 V/cm, both in small growing cumulus. In larger warm cumuli the fields will be still larger and, if reports of warm lightning are substantiated, they may rise to breakdown potential.

Several workers have estimated the forces between electrified cloud droplets, but the only complete values are those computed by Davis (1962), who gives formulae and tables of data for calculating the force between equal or unequal drops carrying net charges and/or in an electric field of arbitrary orientation.

It would be possible to combine the electrical forces of Davis with the hydrodynamic forces of Hocking or, perhaps, Shafrir, to calculate collision efficiencies for electfified drops. This introduces four new variables into the definition of collection efficiency, which now becomes a function of the charges carried by each drop (Q and q) and their radii (R and r) and the magnitude (F) and orientation (θ) of the electric field.

Thus,

$$E_o = E_o (R, r, Q, q, F, \theta)$$

The computation for a single collection efficiency diagram for a given set of values of Q, q, F and θ would be enormous, and the compilation of a comprehensive set of data covering all the likely situations would be a lengthy task on even the most advanced computor.

As yet, no such comprehensive calculations have been attempted, although the general trend in the balance between electrical and hydrodynamic forces has been investigated by Sartor and Davis (1960). They show that a vertical electric field of the order found in growing cumulus would cause a significant increase in collision efficiency. A collector of 19μ radius which cannot collide with a 15μ droplet in the absence of electrification (Hocking, 1958), does so with a collision efficiency of at least 0.03 when a vertical field of 40 volts/cm is applied.

Using less rigorous theory, Linblad and Semonin (1963) have computed the effects of a vertical electric field for a variety of collector and droplet sizes. They combined Proudman and Pearson's solution to the flow round a sphere with the simple dipole:dipole force between the spheres. Their results show that fields of less than 200 volts/cm scarcely effect the collision efficiency of 30μ radius collectors, and larger sizes even less so. It is a pity

that the authors do not quote values for smaller collectors, which are particularly important in the early stages of cloud growth. If the trend of their results continues, then 15μ collectors might have non zero collision efficiencies in fields of only a few tens of volts/cm. Their theory, which has been criticized by Sartor (1963), would also be more reliable for these small drop sizes.

So far the effect of electrical forces on drop trajectories has been considered. Davis's results show that when the collector and droplet approach one another very closely the force of attraction will be very strong. This will accelerate the rate at which air is expelled from the gap between the drops and so assist coalescence. However, when the drops are very close together, it is necessary also to consider the electric field between them. This may achieve very large values at small separations and leads to distortion of the adjacent drop surfaces. Linblad, Plumlee and Semonin (1964) have detected long unstable filaments drawn out from the surfaces by the intense local field. Sartor (1964) claims to have detected radio emission from a spark which crosses from one drop to the other, presumably from one of the liquid

filaments. Both the micro distortion and the accompanying electric discharge will have the important effect of rupturing the air film and forming a continuous liquid neck between the drops, thereby ensuring coalescences before all the air is driven out from the gap. Jayaratne (1964) found that fields of the order of 100 volts/cm or charges of 10^{-4} e.s.u. were sufficient to ensure the coalescence of a drop with a plane water surface when they would otherwise separate without coalescing. Historically it is worth noting that in 1829 Rayleigh suggested that electrification may play an important part in ensuring the coalescence of two colliding cloud drops.

As yet, there has been no quantitative experimental corroboration of the electrification theories of Davis and of Linblad and Semonin. Telford, Thorndike and Bowen (1955) found an increase in the coalescence rate of nearly equal 65μ radius drops when they were charged randomly by induction using an A.C. field. When the drops were all charged to the same polarity by using a D.C. field all coalescence was prevented. Their graph of variation of coalescence rate with drop charges is reproduced in Fig.2.15.

The interpretation of such correlations between coalescence rate and electrification is confused by experimental difficulties in differentiating between the

Fig. 2.15 EFFECT OF ELECTRIFRICATION ON THE COALESCENCE RATE FOR 65μ RADIUS DROPS Telford et al. 1955

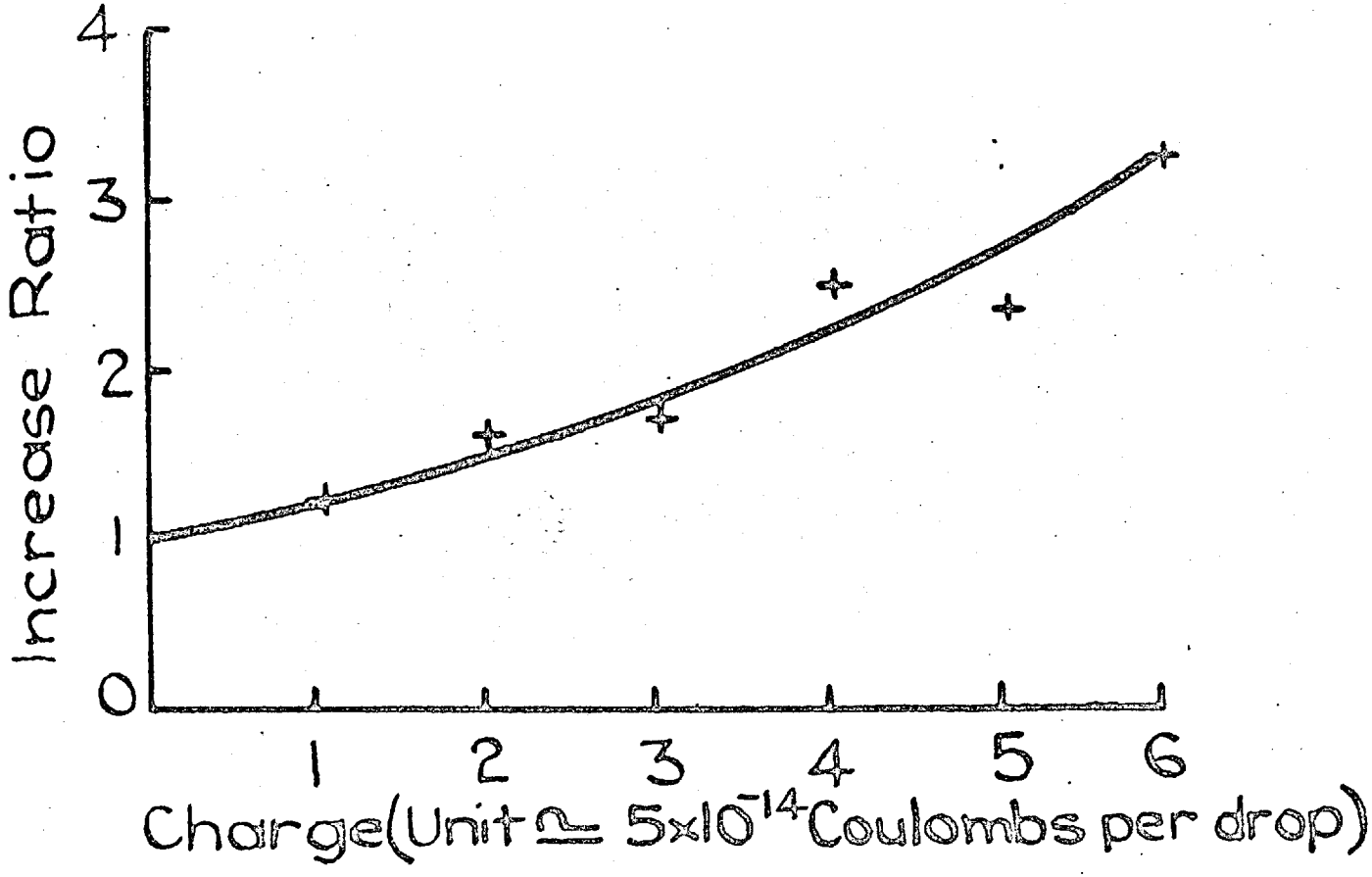

relative effect of electrification upon drop trajectories on the one hand and upon their coalescence on the other. It is conceivable that weak electrification, incapable of measurably raising the collision efficiency, may be sufficient to promote coalescence of drops colliding with $b > b_g$ by sparking across the gap. This would be equivalent to having no change in the collision efficiency, but a coalescence efficiency (as described in Section 1.3B), of greater than unity. Alternatively it may always be necessary for electrical forces to attract drops into collision (i.e. $b < b_g$) before a spark may cross the gap to cause coalescence.

The latter proposal is supported by the results of Telford and Thorndike's second experiment (1961). They found that in the absence of electrification 17μ radius drops falling through undisturbed air often approached one another and remained in close association for a fall of 2 cm. Application of a horizontal electric field of 150 volts/cm (sufficient to cause coalescence in the case of Jayaratne's impacting drops) failed to cause any coalescences. However, when the field was raised to 1 Kv /cm many of the drop pairs coalesced and the coalescence rate was further increased by raising the field to 3 Kv /cm. This result

indicates that sufficient electrical force must be developed between the nearly equal drops in order to pull together before microdistortion may bridge the gap and cause coalescence.

Sartor (1954) found that electrification was necessary to ensure the coalescence of dissimilar sized water drops falling through mineral oil. Without electrification the drops collided but did not coalesce. A vertical electric field of 50 volts/cm was sufficient to make some drops coalesce and higher fields raised the coalescence rate. On the face of it this appears to be readily explained by a rise in the coalescence efficiency as the result of microdistortion. However, Sartor proceeded to divide the events into two groups, those drops that coalesced when the collector was above the droplet, and vice versa. He suggested that in both cases a spark joined the drops at the instant of impact (when the collector was above). This was sufficient to ensure coalescence of drops in the first group, but failed for the remainder. In the second group the droplet continued round to the collector's rear surface, where it is attracted inwards by the resultant net opposite charge on the drops caused by the earlier spark. This, together with the polarization force, was sufficient to

bring the drops close enough for a spark, microdistortion and coalescence to follow. In some cases, the drops did not coalesce at all, but separated with opposite net charges, showing that an electrical discharge has passed between them, but that the forces acting thereafter were insufficient to cause coalescence.

It is doubtful whether this situation could exist in the case of airborne water drops. The adjacent water surfaces would distort very much more than in Sartor's model and coalescence would follow immediately. This view is supported by the fact that dissimilar cloud drops have generally been found to coalesce without application of a field (i.e. $\epsilon = 1$).

B. Turbulence

All natural clouds, but particularly those formed by strong local convection (cumulus), are in a state of continual turbulent motion. The scale of the turbulent eddies ranges downwards in a steady progression from the individual "thermal" or bubble of ascending air. As yet there are direct measurements of only the large-scale motion, so the amplitude of eddies of smaller than a metre across must be estimated theoretically on the basis of these

measurements. Computations (e.g. Taylor, 1952) suggest that there may be vigorous eddies as small as a few millimetres across. While the large scale motions cannot provide sufficient acceleration or velocity shear to affect the coalescence of two cloud drops, the very small microturbulence may do so. It is therefore necessary to extend the investigation of drop collisions to those occurring in an atmosphere whose velocity distribution is some complicated function of position and time.

East and Marshall (1954) have considered the vertical component of the turbulent accelerations. Cloud drops in a parcel of air that accelerates downward behave as if their weights were temporarily increased, their terminal velocities increase accordingly and dissimilar drops approach one another with a higher relative velocity. East and Marshall showed that the resulting increase in collision efficiency will be greatest for air motions with a time constant of about ten milliseconds. However, their calculations for the increase in E, were based upon Langmuir's theory which is unsatisfactory for small drops ($R < 100\mu$). Their theory also fails to account for the effect of spatial variations in the air motion.

Saffman and Turner (1956) investigated theoretically

the effect of turbulence upon a monodisperse cloud of small drops ($R \simeq 20\mu$). Truly identical drops of this size do not encounter one another in tranquil air as they have the same fall speed and there is no wake attraction (see Chapter 4). However, the shear motions in turbulent air drag drops into collision. Saffman and Turner analysed this mechanism for homogeneous isotropic turbulence. Assuming that $E = 1$, they were able to derive an expression for the coalescence rate as a function of ϵ the rate of dissipation of turbulent kinetic energy and ν, the kinematic viscosity of air.

The authors extended their treatment to consider the combined effects of gravity and turbulent velocity shear and acceleration upon collisions between the double mass drops resulting from the previous mechanism and those of the original cloud ($r/R = 0.8$). Again they derived equations for the coalescence rate in terms of ϵ and ν when $E = 1$. They concluded that in a moderate cumulus with $\epsilon \sim 1500$, the coalescence would be nearly double that due to gravity alone in the initial stages immediately after a few double mass drops become available, but that, as the drop size spectrum broadens, turbulent accretion plays a smaller part.

There are two major objections to the analysis of

Saffman and Turner. Firstly, they considered a cloud that is not at all typical of natural cumulus clouds, which from the start contain a far wider spectrum of drop sizes (see typical spectrum in Fig. 1.1). In natural clouds, drops of different sizes are continually encountering one another, but all except a small fraction fail to coalesce because their collision efficiencies are small or zero. This leads to the second objection. Saffman and Turner base their claim that E = 1 in conditions of velocity shear upon the model experiments of Manley and Mason (1952, 1955), whose results are not applicable to the case of small water drops in air.

By far the most important part that microturbulence may play in the early development of a natural cloud is by raising the collision efficiency of small drops formed by condensation. In particular it is necessary to investigate the effect of turbulence upon collisions involving drops near the Hocking limit for collector size, R = 18μ . The approach of East and Marshall was much more pertinent to the problem of natural clouds, but their detailed analysis is not satisfactory. By limiting themselves to vertical accelerations they may have considerably underestimated the potential of microturbulence. The effect of horizontal

accelerations is considered in Chapter 4.

CHAPTER 3

COLLECTION EFFICIENCIES FOR DROPS OF DISSIMILAR SIZES

3.1 OUTLINE OF THE EXPERIMENT

Several thousand identical collector drops of effectively pure* water from a vibrating needle apparatus were allowed to fall through a one-metre-deep cloud of salt solution droplets maintained at equilibrium sizes between 0-15μ radius in a controlled environment of 84% relative humidity. A small fraction of the collectors collided with and captured droplets on their way through the cloud and each of these arrived at the foot of a three metre settling tube with a mass of salt equivalent to the mass of the captured cloud droplet. The concentration of the droplets was adjusted to reduce to a negligible proportion the number of collectors making multiple captures.

By analysing the salt content of each collector it was possible to deduce the number that had captured cloud droplets in each size range. The droplet size distri-

---

*Contamination by radio-orthophosphate solution was very weak and did not effect the collector's equilibrium vapour pressure.

bution in the cloud was analysed in the same way and the collector efficiency for each size range was then calculated using the formula derived below.

The experiment is essentially the same as one undertaken by Picknett whilst working in the same laboratory. The present technique improves upon his in a variety of aspects. A narrower range of collector sizes in each experiment was obtained by using a vibrating needle apparatus in place of Picknett's spinning top generator. More precise timing afforded by use of a radioactive tracer in the collector drops permitted the use of a broader range of cloud droplet sizes. The experiment also covered a wider range of collector sizes than did Picknett.

3.2 THEORY

The basic equations required for this experiment may be derived from the general coalescence equations given in Section 1.3

$$\frac{dN(R,r)}{dt}.dR.dr = N(R).N(r).E(R,r).\pi.(R-r)^{2}.(V-v).dR.dr \qquad (1.1)$$

The rate at which a specified collector of radius R captures droplets in the finite range $r \pm \frac{\Delta r}{2}$ is obtained

by integrating (1.1)

$$\int_{\Delta r} \frac{dN(r)}{dt}.dr = \int_{\Delta r} N(r).E(R,r).\ \pi.(R+r)^2.\ (V-v).dr \qquad (3.1)$$

In the present experiment the droplet concentration, $N(r)dr$, is calculated for a cloud depth H. The collector takes a time $T = H\ (V-v)$ to pass through the cloud droplets in the chosen range from top to bottom. The average number $\int_{\Delta r} N_c(r)dr$ of droplets in the range captured during the collector's passage through the cloud is obtained by integrating equation (3.1) with respect to time.

$$\int_{\Delta r} N_c(r)\ dr = \int_0^T . \int_{\Delta r} N(r).E(R,r)\ .\ \pi(R+r)^2.(V-v).dr.dt$$

$$= \int_{\Delta r} H.N(r).E(R,r).\pi.(R+r)^2\ .dt \qquad . . (3.2)$$

The range of droplet sizes in the experiment was one micron. The factor $E(R,r).(R+r)^2$ is effectively constant over this small range, so equation (3.2) reduces to

$$\int_{\Delta r} N_c\ (r)dr = E(R,r).\ \pi(R + r)^2\ .\ H \int_{\Delta r} N(r).dr \qquad . . (3.3)$$

It is necessary in the experiment to ensure that the probability of a collector capturing two or more droplets during its passage through the cloud is very much smaller than the probability of it capturing a single droplet. The full integral of equation (3.2) over all values of r

found in the cloud may be used in the Poisson formula to obtain the probabilities of one, two, three etc. captures.

If $A = \int_r H.N(r).E(R,r).\pi.(R+r)^2 .dr$

then,

p_0, the probability of a collector making no capture

$= \exp(-A)$

p_1, the probability of a collector making one capture

$= A \exp(-A)$

p_2, the probability of a collector making two captures

$= \frac{A^2}{2!} \exp(-A)$

etc.

The condition that there shall be virtually no multiple captures becomes

$$p_1 \gg p_2 + p_3 + \ldots \text{ etc.}$$

In practice A is chosen to be much smaller than unity. As $\frac{p_n}{p_{n-1}} = \frac{A}{n}$ then $p_0 \gg p_1 \gg p_2 \gg p_3 \gg p_4$ etc. and the condition reduces to $p_1 \gg p_2$. It is clear that this condition requires $A \ll 1$, which has been satisfied.

Now, using Poisson's formula for a single range of drop sizes, the probability that a collector will capture no droplet is obtained from equation (3.3).

$$p_0' = \exp\left[- \int_{\Delta r} H.N(r)dr \quad x\ E(R,r)\ \pi (R+r)^2 \right]$$

As $\sum_{i>2} p_i'$ is negligible, then $p_1' = 1 - p_0'$ and the probability of a single capture is given by

$$p_1' = 1 - \exp\left[-\int_{\Delta r} H.N.(r).dr \quad x \quad E(R+r) \quad \pi (R+r)^2 \right]$$

The range of sizes ΔR of the large number of collectors used in a given experiment is very narrow ($\Delta R \leq 1\mu$), so the factor $E(R,r).(R+r)^2$ is constant over ΔR. All the collectors being comparable, the fraction $\int_{\Delta r} F(r)dr$ of them that capture a single droplet within the range $r \pm \Delta r/2$ is equal to p_1 above. If the number of droplets in this range captured by the N collectors is $\int_{\Delta r} N'(r)dr$, then

$$\int_{\Delta r} F(r)dr = \int_{\Delta r} \frac{N'(r)dr}{N} = 1 - \exp\left[-\int_{\Delta r} H.N(r)dr.E(R,r)\pi(R+r)^2 \right]$$

Rearranging, the formula for E(R,r) is obtained.

$$E(R,r) = \frac{- \ln \left[1 - \frac{\int_{\Delta r} N'(r)\, dr}{N} \right]}{\pi (R+r)^2 . \int_{\Delta r} H.N(r)\, dr.} \qquad (3.4)$$

where

N = no. of collectors

$\int_{\Delta r} N'(r)dr$ = no. of droplets in the range $r \pm \frac{\Delta r}{2}$ captured by the collectors.

R = collector radius

r = droplet radius

$\int_{0}^{\infty} H.N(r)dr$ = no. of droplets/cm^2 cross-section in the cloud.

Each of these factors is obtained directly from the experiment.

3.3 THE EXPERIMENT

A. Apparatus

The complete apparatus is shown in Fig. 3.1 (photograph) and Fig. 3.2 (diagram). The one-metre long vertical glass tube A, internal diameter 8 cm, is the centre of the apparatus and will be called the cloud column, C. Above the cloud column is a draught resisting perspex box containing the vibrating needle apparatus, V, and for generating the collector drops. Below the cloud column is a pivoted frame which permits the location under the cloud column of either a Collison atomizer, A, for producing the cloud of droplets, or a further three-metre section of 8 cm. glass tube, S, lagged with foam plastic. At the foot of this lower tube, called the settling column, is a perspex "slide box", B, containing racks for the slides used in analysing the collectors and the cloud droplets. A Geiger-Müller radiation detector G attached to the side

Fig. 3.1

The experimental apparatus

V - vibrating needle apparatus

C - cloud column

A - Collison atomizer

S - settling column

B - slide box

R - radiation meter

G - Geiger-Müller head

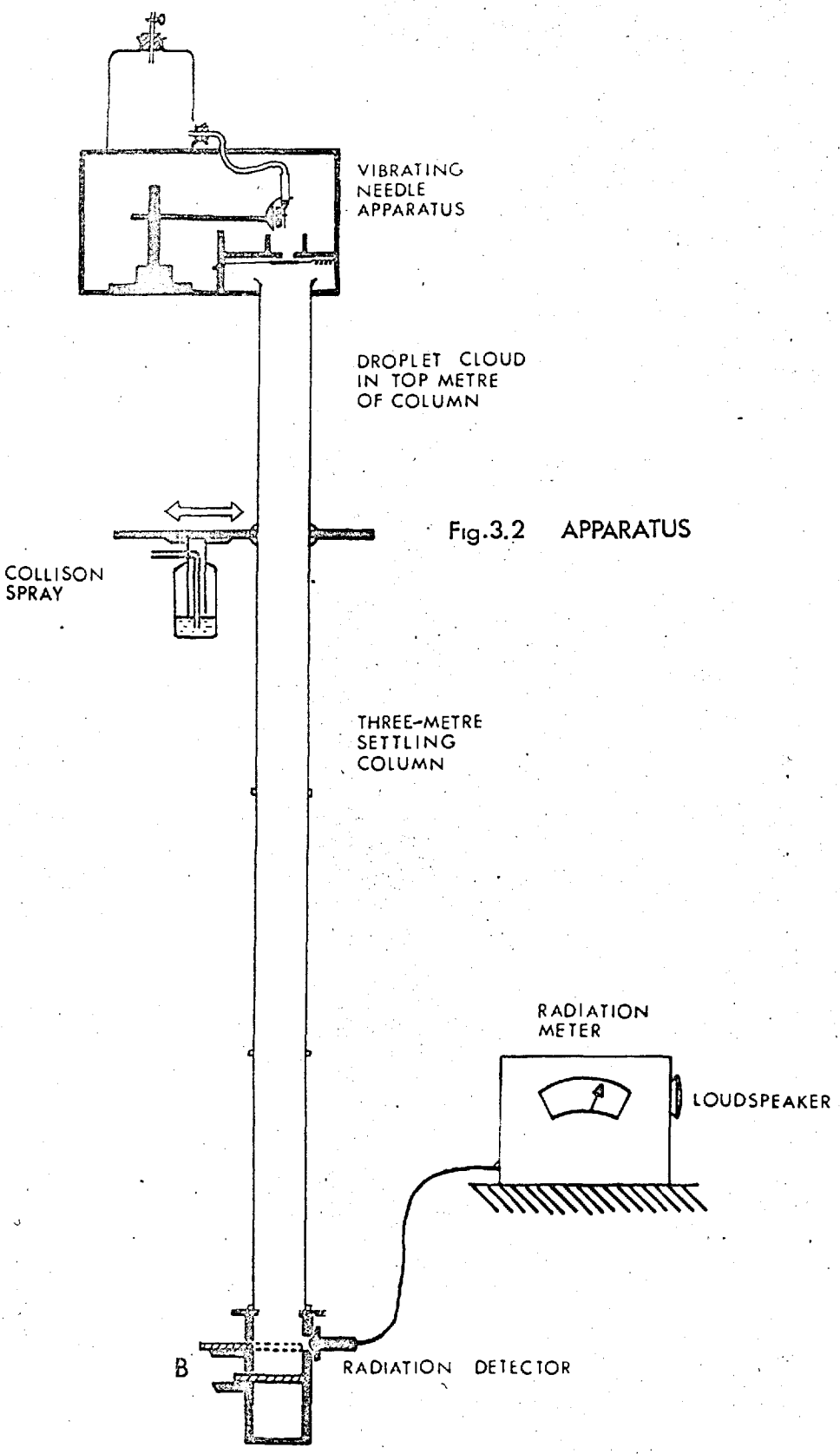

Fig.3.2 APPARATUS

of this "slide box", feeds into a radiation monitor, R, giving aural and visual indication of the radiation detection rate.

The Cloud Droplets

An atomizer (Collison, 1935) designed for testing gas masks was modified to give a broader droplet spectrum by opening out the injection hole to a diameter of 0.025 inch. The jar was filled to the bottom of the baffle with an aqueous solution of sodium chloride (concentration 270g/litre). This was dispersed by injecting compressed air at 10 p.s.i.

Droplets from the spray were injected into the cloud column, which was opened at the top, for sixty seconds. The inside walls of the glass tube had previously been washed with the brine solution (270 g/litre) to raise the internal relative humidity to 84%. The top of the cloud column was closed after the cloud had been injected. The droplets were then allowed 60 seconds to grow to their equilibrium radii in the ambient humidity.

The equilibrium droplet size spectrum was measured by allowing the entire cloud to settle on to a hydrophobic surface prepared by coating a 2 inch square glass cover

FIG. 3.3 TYPICAL EXPERIMENTAL CLOUD DROPLET SPECTRUM.

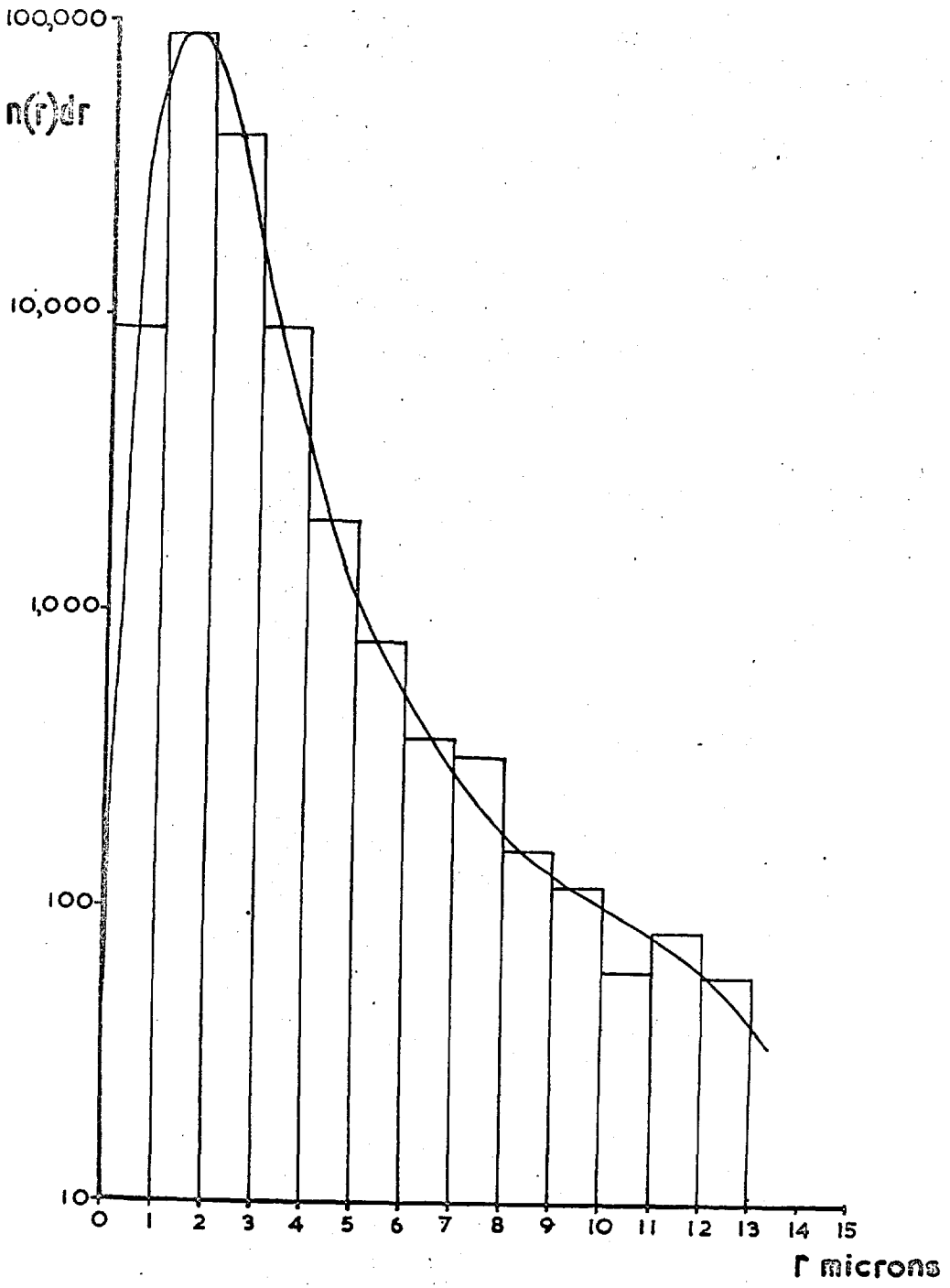

slide with a thin even layer of Apiezon M grease. Each of the cloud droplets evaporated leaving a small salt crystal in its place on the hydrophobic slide. The slide was then inserted into an enclosed microscope stage containing a trough of saturated potassium bromide solution. By vigorous stirring with a small electrically driven fan it was possible to maintain the air inside the enclosure at 84% R.H. In this humid air the salt crystals on the slide absorbed water vapour and grew to hemispheres with the same volume as the original cloud droplets. The radius of each of the hemispheres within forty, randomly scattered fields of view of the microscope (x 20 objective) was measured using a calibrated micrometer eyepiece. The hystogram for $H.\int_{\Delta r} N(r)dr : r$ shown in Fig. 3.3 was constructed from these measurements. Tests were made to ensure that the cloud was randomly distributed across the area of the slide.

Although, with care, the droplet spectrum was reasonably reproducible, a separate cloud analysis was carried out for each experiment.

The Collector Drops

The vibrating needle apparatus was used to inject

about 8000 collector drops of very nearly identical size into the cloud during a ten second period. The instrument was developed jointly with O.W. Jayaratne from a prototype by Professor B.J. Mason and has been described in a joint paper (Mason, Jayaratne and Woods, 1963) bound into the back of this volume. The present experiment required one special modification to the instrument. Because of radiation hazards the liquid supply was limited to 3 ml per loading, so it was stored in the barrel of a hypodermic syringe fitted directly into the needle (Figs. 1 and 2 of the paper). The liquid was forced through the needle by compressed air from a 2 litre reservoir pumped up by hand to a pressure of about 0.3 Kg/cm^2. This emptied the liquid reservoir in about 5 minutes.

Using a 30-gauge (140μ i.d.) hypodermic needle it was possible to obtain a main stream of drops ranging in radius from 80 to 200μ depending upon the flow rate of the liquid and the frequency and amplitude of the signal driving the microphone. A second stream consisting of satellite drops from the liquid jet break-up (see Fig. 3.4) and ranging in size from 10μ to 60μ could also be obtained by careful control of the operating parameters (flow rate, signal frequency, etc.). In the early stages of work on this

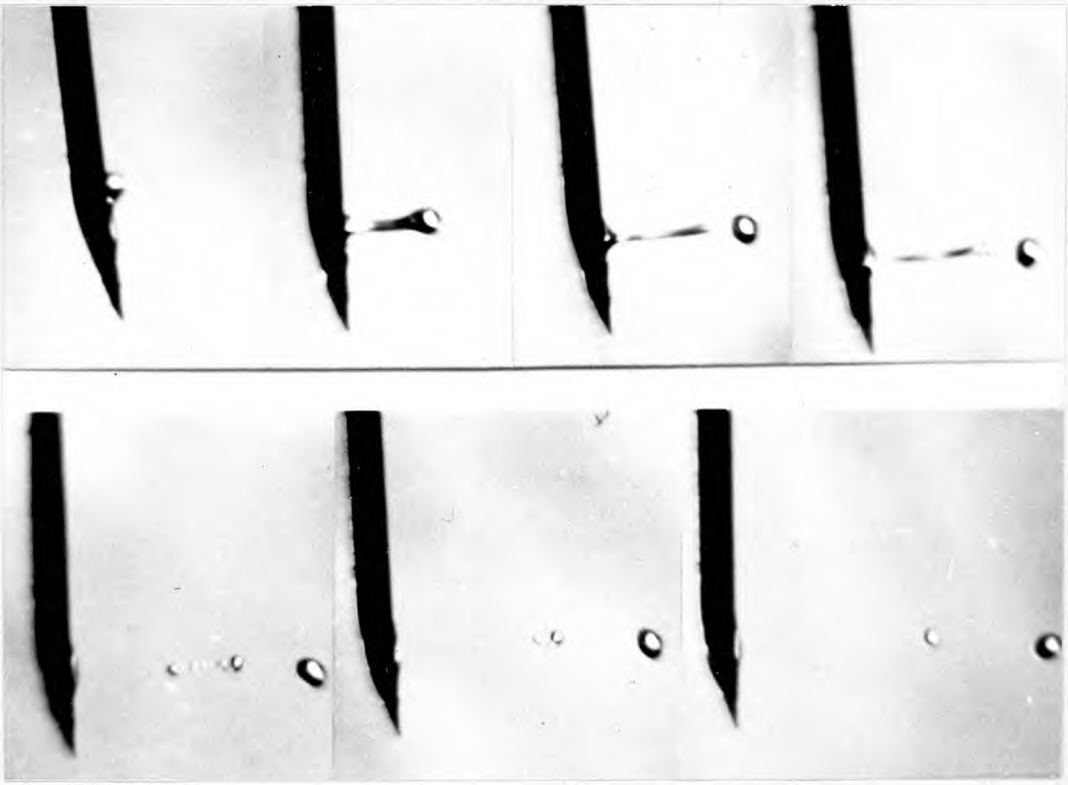

Fig. 3.4 The formation of a satellite drop (above), and (below) a stream of satellite drops ejected horizontally from the vibrating needle.

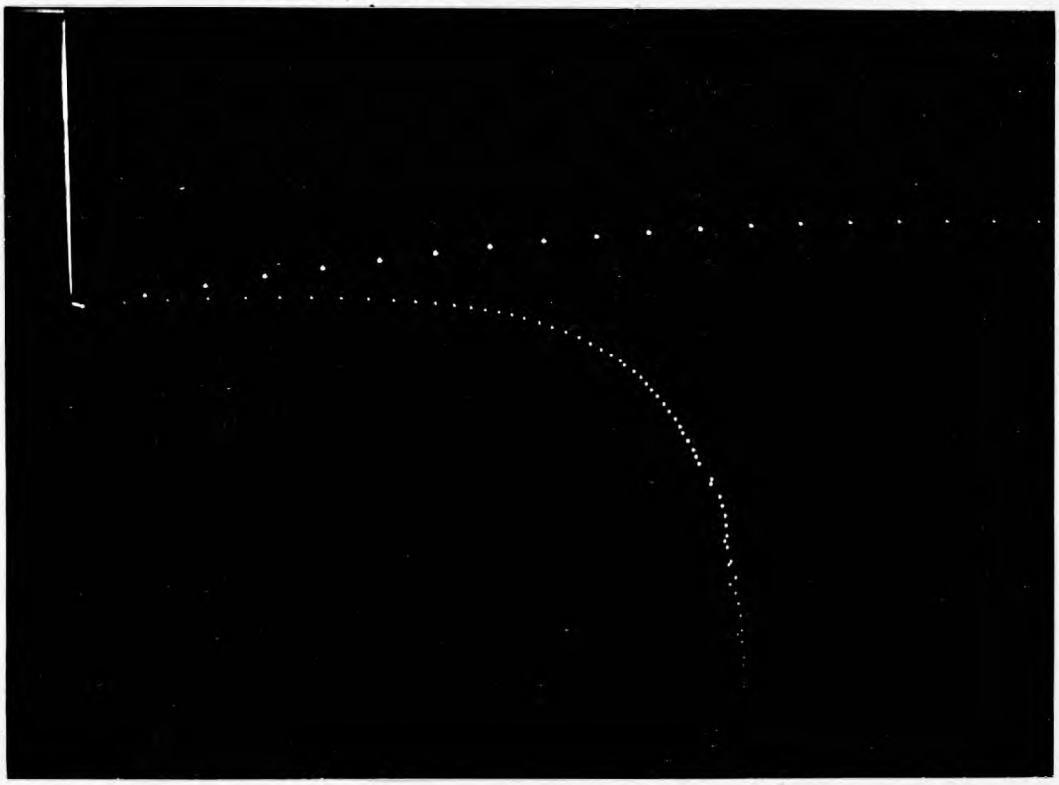

experiment, the needle tip was reduced to half the internal diameter as described in the paper, but later, when greater skill in controlling the very fine satellite drops had been attained, the modified tip was dispensed with. While the apparatus provides a considerable test of the operator's skill, it is possible with practice to produce satellite drops so small that they drift around as an aerosol. These minute drops, which are probably smaller than 10μ radius, could not be used in the experiment, however. The smallest drops that formed a stable stream capable of being injected into the apparatus were about 15μ radius.

In all cases the collector drops entered the apparatus vertically at their terminal velocity. This was achieved by arranging the needle so that the drops were ejected horizontally and locating it about five centimetres above and the same distance to one side of the hole through which the drops entered the cloud column. During their curved fall from the needle tip to this hole the drops lost their initial horizontal momentum and accelerated nearly to their terminal fall speed.

Drop Size Determination

The average size of drops in a single stream was

determined to within $\pm 1\mu$ by weighing a known number of them. To prevent evaporation the stream was directed into a half centimetre layer of light oil in a glass petri dish for between 1 and 5 minutes, depending upon the drop size. The dish was weighed before and after collection on a Metler balance accurate to 1 milligram. The drop production rate equalled the frequency of the driving signal except at very reduced liquid flow rates, where it was half or even a third of the driving frequency. A stroboscopic lamp was used to distinguish between these cases.

The drop sizes obtained by this weighing technique compared well with direct microscope measurement of individual drops collected in oil or by microscope measurement of the craters left by individual drops landing at terminal velocity on a thin layer of magnesium oxide. This last technique (due to May, 1950) was used as the standard method for the determination of drop sizes. A 2 inch square glass cover slide was coated with an even layer of magnesium oxide by holding it about 5 cm above burning magnesium ribbon. A 30 cm length of ribbon produced enough smoke to give the slide an opaque white coating. Drops settling on to this oxide layer left a crater which

had a radius 1.16 times the radius of the drops. This calibration by May (1950) gave values which agreed well with those from the weighing method.

Examination of the magnesium oxide also showed clearly that drops within a given stream all had very similar sizes. It was not possible to detect any differences by this technique or by measuring drops collected under oil. It seems likely that the drops were in fact considerably more uniform that the resolution of the oxide layer technique ($\pm \frac{1}{2}\mu$). Observations of the drop productions under stroboscopic illumination synchronized to the needle frequency showed that they were ejected with the same velocity and that they decellerated thereafter at an identical rate, so far as the eye could see. Time exposures taken under the same stroboscopic illumination gave photographic evidence that the velocities at ejection and the subsequent decellerations were probably within 1% of each other. The photographs were quite sharp. Thus the drops had the same drag coefficient and hence the same radius, to within about 1% of each other.

Collector Drop Solution

The collector drops were formed from a radioactive

solution which emitted soft β-rays. The liquid concentrate obtained from the Radiochemical Centre, Amersham, where it is known as PBS1 was an aqueous solution of sodium orthophosphate containing P_{32} which decays with a half-life of 14.2 days to S_{32} by emitting 1.7 MeV β-rays. The concentrate was diluted with distilled water to the minimum concentration consistent with detection of the drops. Control of this dilution compensated for the solution's loss of radioactive strength during the days after its delivery from Amersham. However, each batch was usually finished within two weeks of delivery. A concentration of 1 milliCurie/ml gave about 20 disintegrations per second from a drop of 50μ radius.

The radiation served two purposes. Primarily, it provided a means of determining the precise moment at which the collector drops arrived at the foot of the settling column. An end-window detector was fitted into the slide box so that radiation from collector drops which had settled on to the upper slide penetrated the detector's thin mica window. The signals from the detector were fed into a radiation meter (Harwell type 1650 A) which gave a dial reading of the counting rate in disintegrations per second and also a loudspeaker "click" for each β-ray detected.

The radioactive solution also helped to neutralize electric charges on the collector drops; they were ejected from the vibrating needle with an average of about 10^3 electronic charges. This degree of electrification is unlikely to have affected the capture of cloud droplets (Gunn and Hitschfeld, 1951) and could be reduced by applying a potential of about 1 volt to the needle. However, this was not considered necessary as the β-rays emitted by the drop solution created a cloud of ions in the vibrating needle housing which reduced the charges by an order of magnitude. Calculations showed that the housing contained an equilibrium concentration of about 10^7 ion pairs/*c.c.*, and that on average a collector would capture about 10^8 of these before entering the cloud column. These estimates were confirmed by tests with a vibrating reed electrometer.

Timing

Identification of the collector drops by a radioisotope provided the precision timing necessary to satisfy the basic condition for the experiment, namely that all the salt particles on the collector slide should arrive there only as the result of being captured by the collectors. It was imperative that no cloud droplet fell on to the collector slide without first being captured. So in designing the

experiment it was necessary to determine how long the cloud droplets took to fall down the settling column. Calculations based upon the terminal velocity of the droplets gave an estimate of 100 seconds for the fall time of the largest droplets ($r = 15\mu$), however, in practice they usually arrived after about 60 seconds. The difference between the observed fall time and the calculated one arose from the bulk fall of the dense droplet cloud as a whole.

The fall time (over 4 m.) of the smallest collectors was calculated to be about 40 seconds, although they also fell slightly faster in bulk. There was therefore only a very brief period, about 10 seconds, between the arrival of the last collector on the slide and the start of contamination by the largest cloud droplets. The radiation meter usually signalled the arrival of the collectors with sufficient precision for the collector slide to be covered before contamination started. However, several experiments had to be abandoned because of faulty timing. Luckily it was possible to check for contamination when the collector slide was being analysed. The collected droplets were concentrated in a small area in the centre of the slide, while any falling down directly landed evenly over the slide.

B. Procedure

The inside walls of the glass tubes were thoroughly washed with the salt solution and the apparatus was sealed for ten minutes for the air to reach 84% R.H. Meanwhile two greased slides and two magnesium oxide slides were prepared. One grease slide (the collector slide) was placed in the lower tray of the slide carrier and was covered by one of the oxide slides in the upper tray.

The Collison atomizer was then swung into position under the cloud column and operated for sixty seconds. During the next minute, while the cloud was settling and reaching equilibrium, the vibrating needle was adjusted to give a stream of drops of the required size. These were sampled using the second oxide slide held directly over the cloud column.

The oxide slide was removed from the slide carrier and the settling column was swung into position under the cloud column, precisely sixty seconds after the cloud had been injected. Immediately afterwards the trap door was opened for ten seconds, allowing a pulse of collector drops to pass into the top of the cloud. The radiation meter was then watched closely for a rise in the counting rate which announced the arrival of the collector drops on the collector

slide. Ten seconds later the collector slide was covered by re-inserting the oxide slide into the upper position in the carrier. The collector slide was removed to the microscope humidity stage for analysis later. The collector drops were usually visible to the naked eye, so that their central distribution could readily be checked.

After a further thirty seconds the oxide slide was removed and checked for impressions (its unpitted surface confirmed that all the collectors had arrived on the collector slide). Finally the second greased slide was inserted into the upper tray and left there overnight to collect all of the slow-falling cloud droplets. It was subsequently transferred to the microscope humidity stage for analysis.

Measurement of every saline hemisphere on the collector slide gave a hystogram for the number of collected droplets in each size range. Collected droplet hystograms for $R = 33.5$, 48.5 and 55μ are shown in Fig. 3.5.

The number of collectors used in a given experiment was estimated from the injection time, usually ten seconds, and the rate at which the drops were being produced, usually about 800 per second.

The collection efficiencies for each size range of

Fig. 3.5 COLLECTED DROPLET SPECTRA.

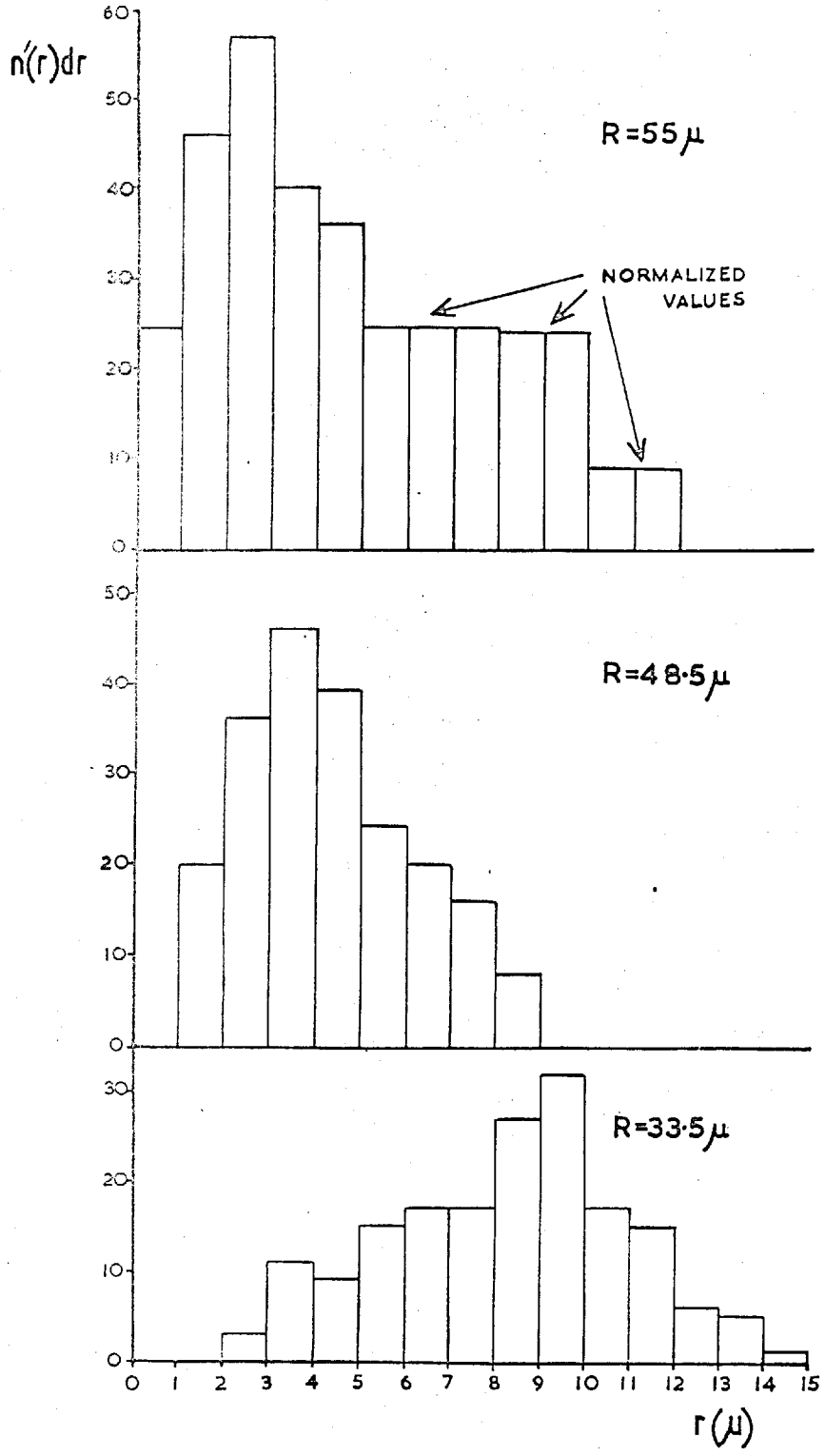

of droplet radius were calculated using the data in equation 3.4.

C. Subsidiary experiment -

Collection efficiencies for collector drops with radius $R < 20\mu$

Hocking (1958) predicted that drops of radius less than 18μ cannot collide in still air with smaller drops of any size. In an attempt to test this prediction the experiment was modified to permit the use of collectors with $R < 20\mu$. In particular it was found necessary to raise the relative humidity in the apparatus from the 84% used previously to near saturation. The reason for this change and the consequences of making it require separate discussion.

Relative humidity

Measurements were made of the evaporation loss suffered by collector drops during their four-metre fall at 84% R.H. and also at 98% R.H. The latter humidity was obtained by washing the inside of the tubes with tap water at room temperature. Table 3.1 summarizes the results of this investigation. It is clear that the higher humidity

is necessary for experiments using collectors of radius less than 20μ . However, such a high humidity is

Table 3.1

Collector radius (microns)			Fall time (seconds)
Top	Bottom		
	84% R.H.	98% R.H.	
30	29	30	40
20	-	19.5	80
15	-	14	140
10	-	-	-

difficult accurately to maintain. Measurement also produces difficulty, because it depends upon circulation of the air past the wet and dry thermocouples, whereas during the experiment the air in the tubes must be static if the cloud is not to be carried rapidly down the settling column. This objection is of course equally valid at 84% R.H. but at that lower humidity a small deviation does not produce any large change in the equilibrium droplet radius,

Fig. 3.6 EQUILIBRIUM RADIUS FOR A DROPLET CONTAINING 10^{-13} g NaCl

[from Mason 1957]

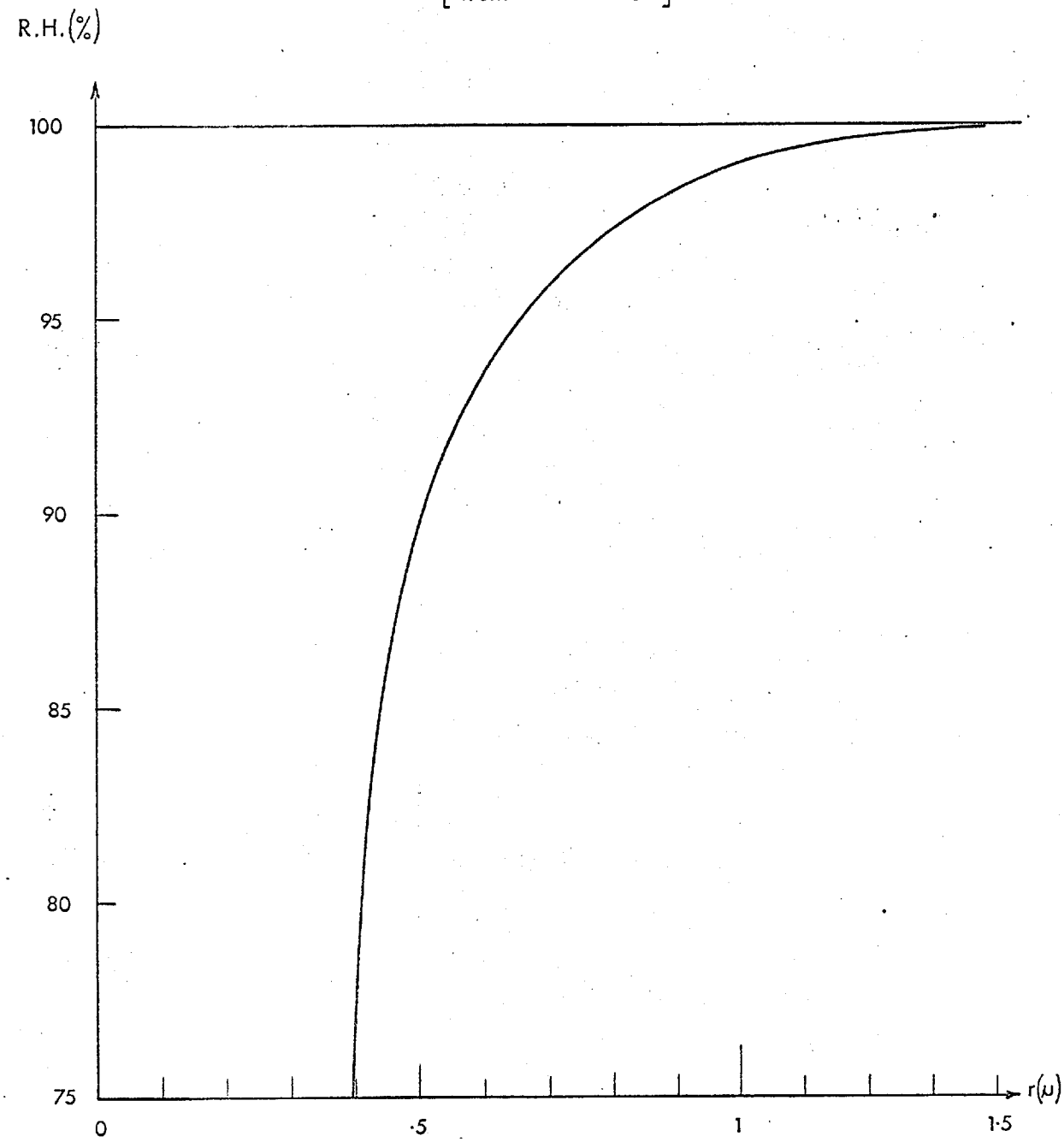

while at 98% R.H. the equilibrium droplet size varies rapidly with small changes of humidity. Fig. 3.6. shows the change of equilibrium radius with humidity for a droplet containing 10^{-13} g of sodium chloride.

In consequence it was necessary to accept the fact that the droplet cloud would not accurately be defined at the high humidity. In practice the cloud was formed by atomizing an aqueous solution of 50 g/litre of NaCl. It was calculated that this reduced concentration would give an equilibrium droplet size spectrum at 98%R.H. which closely matched that shown in Fig. 3.3 with a maximum droplet radius of 14μ . This was confirmed by collecting the cloud on a greased slide and inspecting it under the microscope as before. (In this case tap water was used in the humidity box instead of a saturated solution of KBr).

Procedure

With the exception of those modifications described above, the experiment proceeded exactly as described in Section B. The collector drops were made of very highly concentrated radioactive solution (up to 2 mC/ml) in order to obtain a clear indication of their arrival on the collector slide. Timing was even more crucial in this

experiment because of the very similar fall speeds of the collectors and the largest cloud droplets.

The collector slide was examined for collected droplets as before, but in the one case when these appeared no attempt was made to derive the corresponding collection efficiencies.

3.4 RESULTS

Collection efficiency curves for R = 33.5, 37.5, 48.5 and 55 μ are shown in Fig. 3.7. The experimental errors drawn on these curves represent the sum of the standard deviations of the cloud and collected droplet hystograms. Smoothed values of E(R,r) for selected values of r/R are listed in Table 3.2.

Experimental errors

Evaluation of the collection efficiency involves four measured quantities. Random fluctuations in the cloud may be described by standard deviations which are shown on the collection efficiency curves in Fig. 3.7. Errors in the other two quantities, N($\pm$ 5%) and R($\pm$ 1) are the same for all values of r and, therefore, have the effect of introducing a constant uncertainty in each of the smoothed curves of Fig. 3.7. To this must be added a further error

Fig. 3.7 EXPERIMENTAL COLLECTION EFFICIENCIES.

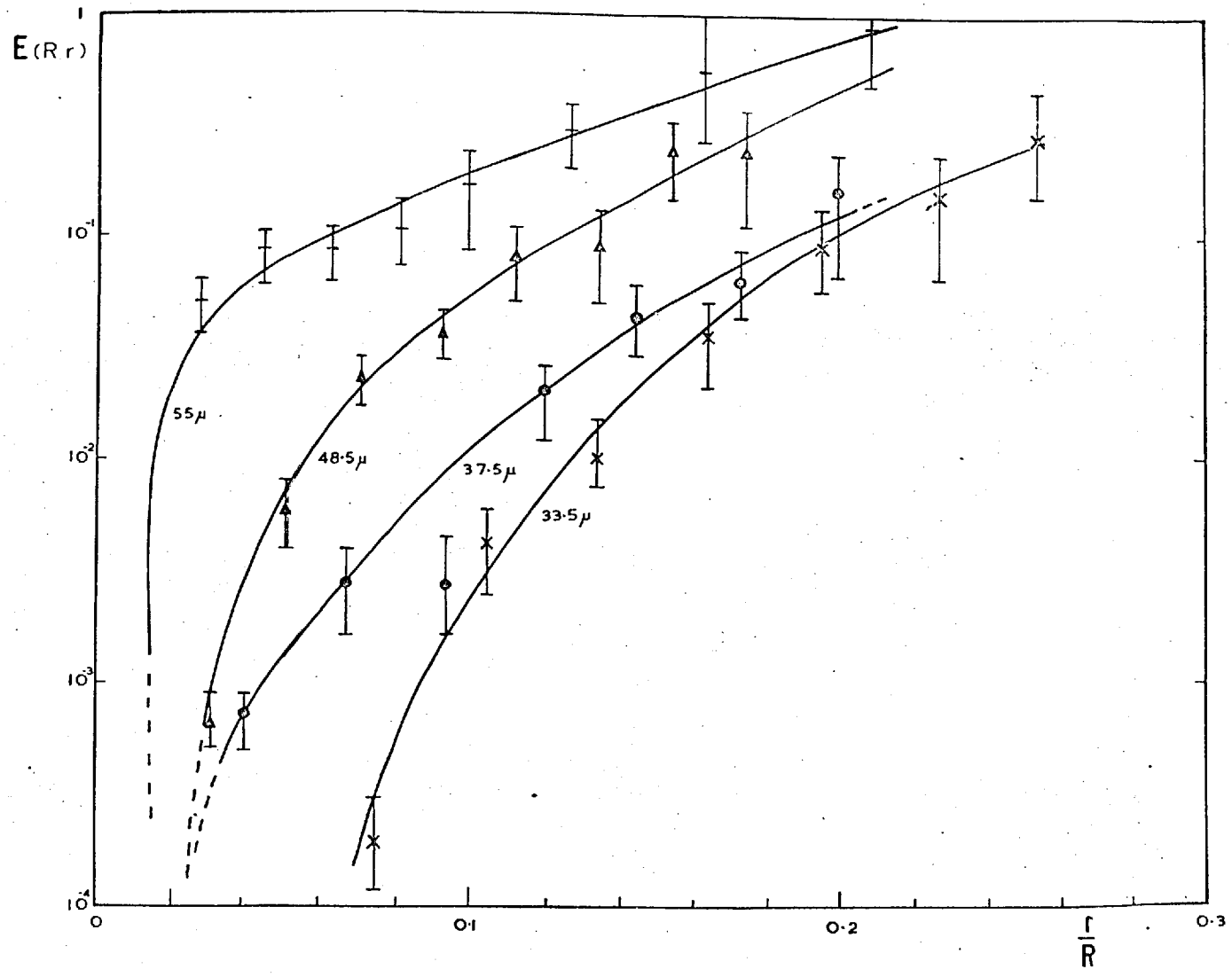

TABLE 3.2

Smoothed experimental values of

Collection Efficiency

r/R	R = 33.5μ	37.5μ	48.5μ	55μ
0.02	-	-	-	.02
0.04	-	.0003	.003	.07
0.06	-	.001	.01	.09
0.08	.001	.005	.03	.13
0.10	.003	.01	.05	.18
0.12	.008	.02	.09	.25
0.14	.02	.04	.14	.34
0.16	.03	.06	.21	.45
0.18	.06	.08	.34	.60
0.20	.10	.12	.48	.70

which results from the small fraction of collector drops that pass down overlapping paths and so do not pass through a representative volume of cloud. Tests showed that such overlapping was very rare and the maximum probable error is estimated to have been ± 3%. The combined effect of these last three types of error will be to give the same "scaling factor" of up to ± 10% to all the experimental collection efficiencies on a given curve in Fig. 3.7.

Subsidiary experiment

The results of five experiments are summarized in Table 3.3. In four of these no droplet was captured, which implies that the actual collection efficiency was almost certainly smaller than that corresponding to the capture of a single droplet (column 4). In the fifth experiment, seven salt droplets with $10\mu < r < 14\mu$ were found on the collector slide, but these may well have been deposited directly from the cloud. This is particularly likely because of the extra delay required in the experiment to allow the longer pulse of drops to arrive after the radiation meter count started to rise.

A further experiment with collector drops of $R = 30\mu$, produced the range of collected droplets expected after the

TABLE 3.3

Tabulated Results for the

Subsidiary Experiment

Collector radius R(μ)	No. of Collectors	Fraction of Collectors that captured a droplet	Collection Efficiency corresponding to a single capture	Theoretical Collision Efficiency (Hocking)
17.0	8000	0	0.03	0.0
17.5	8000	0	0.03	0.0
18.5	6000	0	0.07	0.015
19.0	15000	0.0045	0.08*	0.03
19.5	7000	0	0.02	0.04

*In this case, with R = 19μ , 7 droplets were captured, and the corresponding collection efficiency is 0.08.

previous results, but these were not analysed in detail to give a collection efficiency curve because of the errors inherent in using such a high humidity.

3.5 COMPARISON OF EXPERIMENTAL AND THEORETICAL RESULTS

In Fig. 3.8 are drawn the experimental E curves ($R = 33.5\mu$, 37.5μ, 48.5μ and 55μ) together with the experimental curves of Picknett ($R = 30\mu$ and 40μ) and the theoretical E curves of Hocking ($R = 25\mu$ and 30μ), Shafrir and Neiburger ($R = 40\mu$ and 60μ) and Mason ($R = 60\mu$ and 100μ). The experimental and theoretical curves exhibit the same general trend and at large values of r/R the magnitudes of E and E_o agree within the errors of experiment. However, a significant difference occurs at small values of r/R. The experiments give non-zero collection efficiency values for droplets significantly smaller than the cut-off values predicted by theory. This "tail" is particularly clear on the linear collection efficiency diagram, Fig. 3.9. As the peak of the cloud droplet spectrum lies at $r = 2\mu$ the experiment is particularly reliable for small drop ratios, so the discrepancy cannot be rejected as experimental error. There are two alternative explanations. Either the experiment introduces some factor which enhances the chance

Fig. 3.8 COMPARISON WITH THEORETICAL COLLISION EFFICIENCIES.

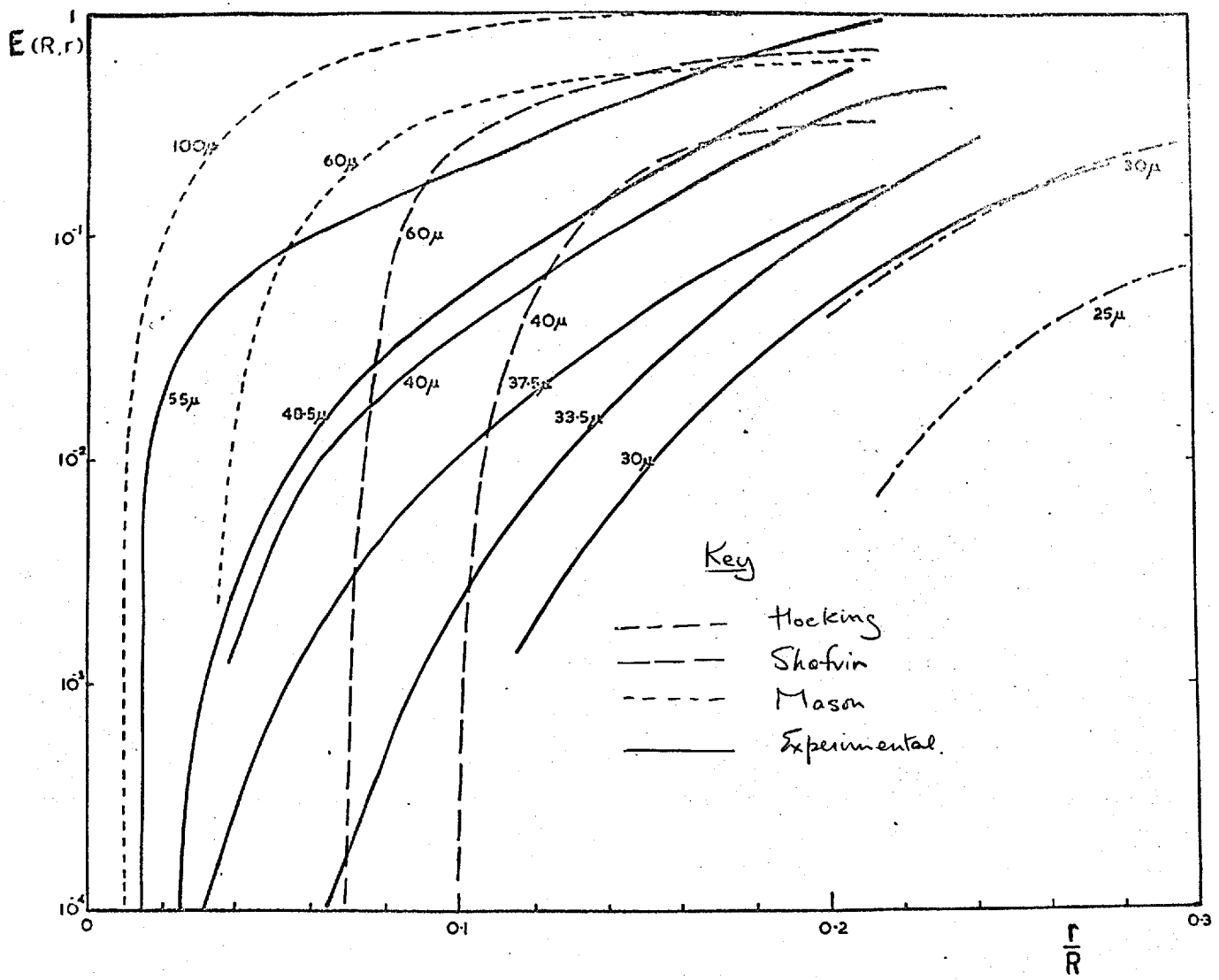

Fig. 3.9 COLLECTION EFFICIENCY DIAGRAM

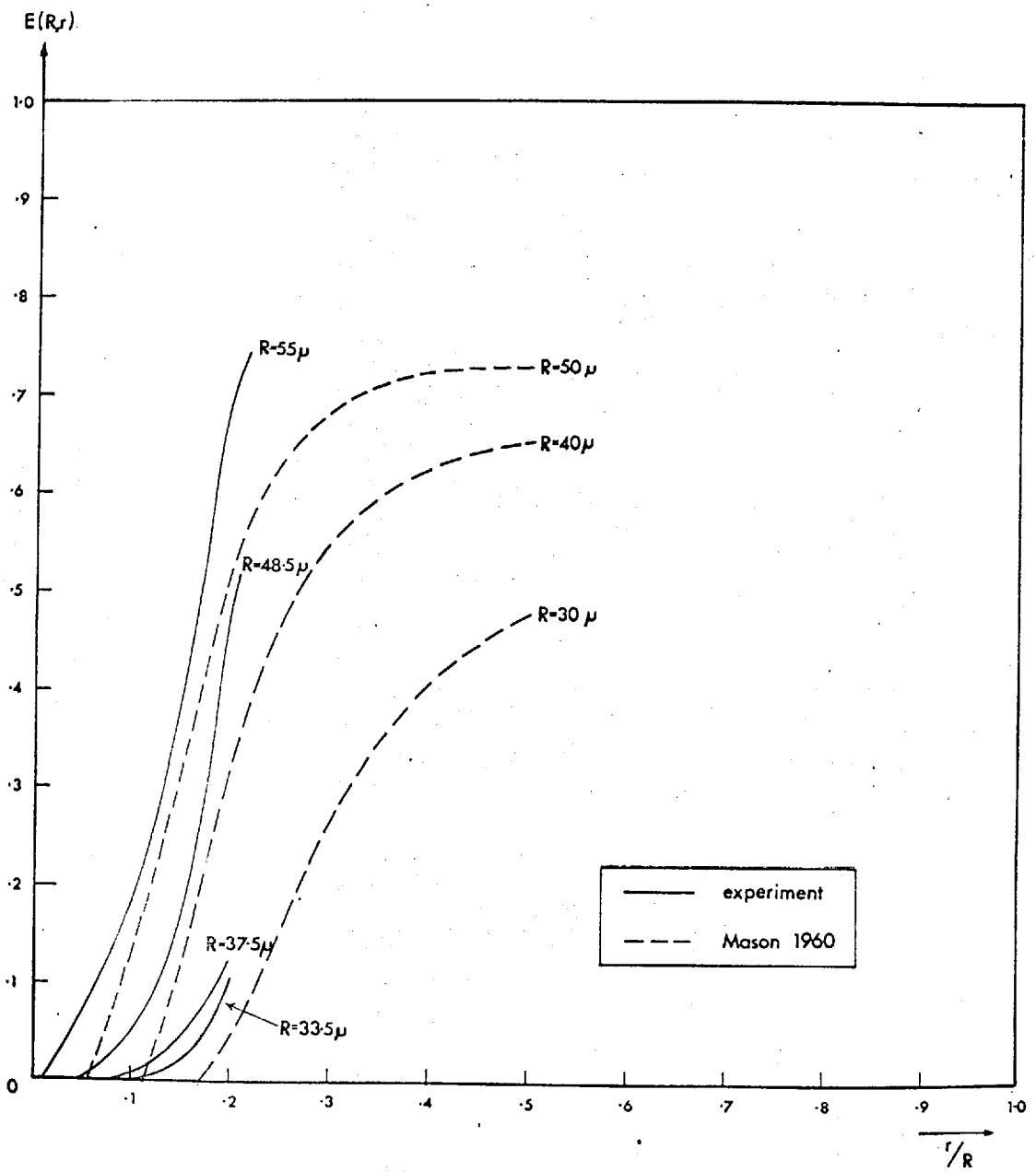

for capture of the smallest droplets or else the theoretical E_o curves are incorrect.

The two experimental factors most likely to perturb gravity coalescence are electrification and turbulence. Both were factors in the experiment but it is unlikely that they played a significant part in effecting capture. The collector drops carried charges of up to about 10^{-4} e.s.u. and the cloud droplets about 10^{-9} e.s.u. However, using Davis' formula it is possible to show that the forces produced by these charges are negligible compared with the hydrodynamic collision forces.

It is less easy to show convincingly that the degree of turbulence in the cloud could not affect the collisions. When the cloud was injected it swirled around quite rapidly inside the glass tube, but this motion was largely damped out during the sixty second delay before injection of the collectors. An early experiment for $R = 57\mu$ was carried out without the full sixty seconds delay. The Collection Efficiency curve for this experiment is compared in Fig. 3.10a with the curve for $R = 55\mu$ obtained by the standard method. The growth of the "tail" is quite striking. A similar experiment for $R = 30\mu$ presents an even more remarkable tail when compared with the standard curve for $R = 33.5\mu$

Fig. 3.10a COLLECTION EFFICIENCY CURVES

The effect of reducing the delay between cloud injection and collector injection

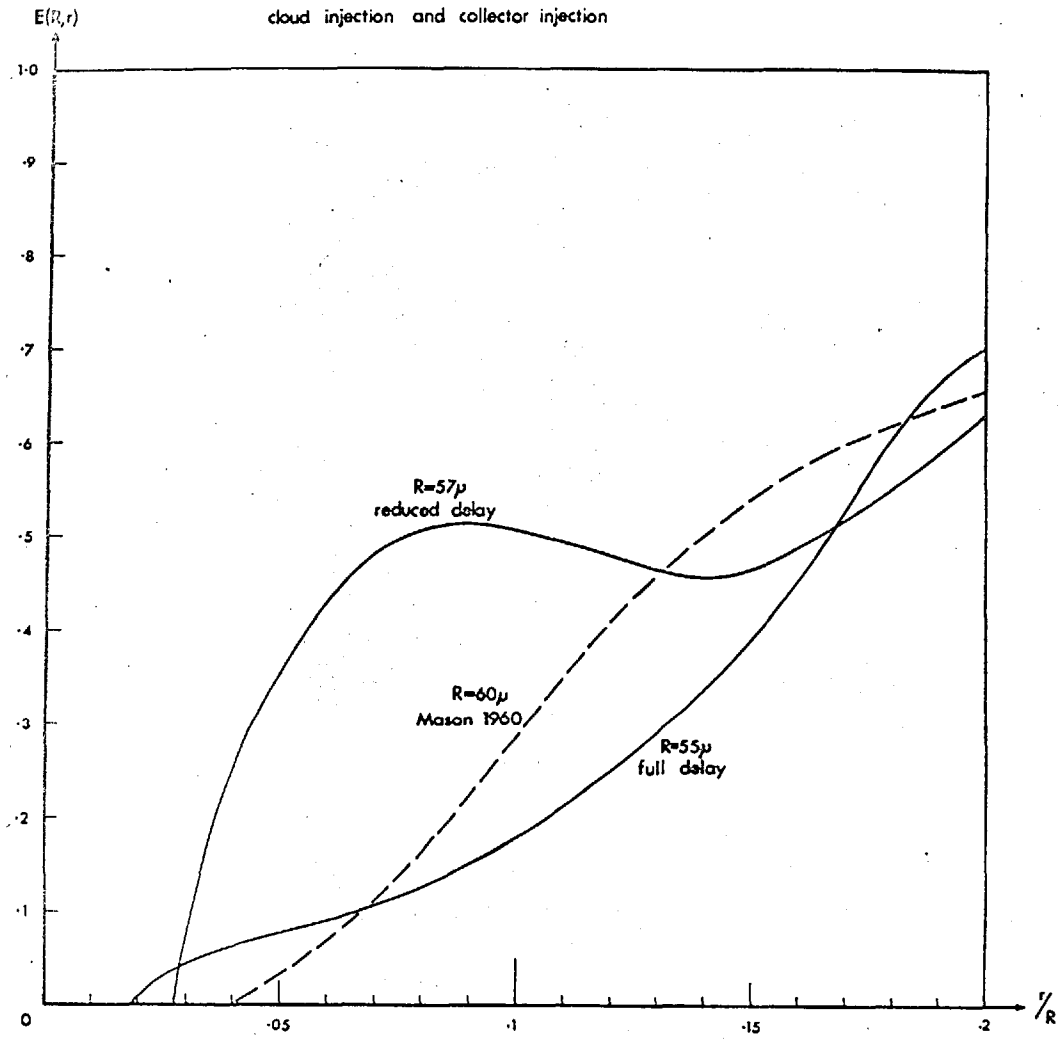

Fig. 3.10b COLLECTION EFFICIENCY CURVES

The effect of reducing the delay between cloud injection and collector injection

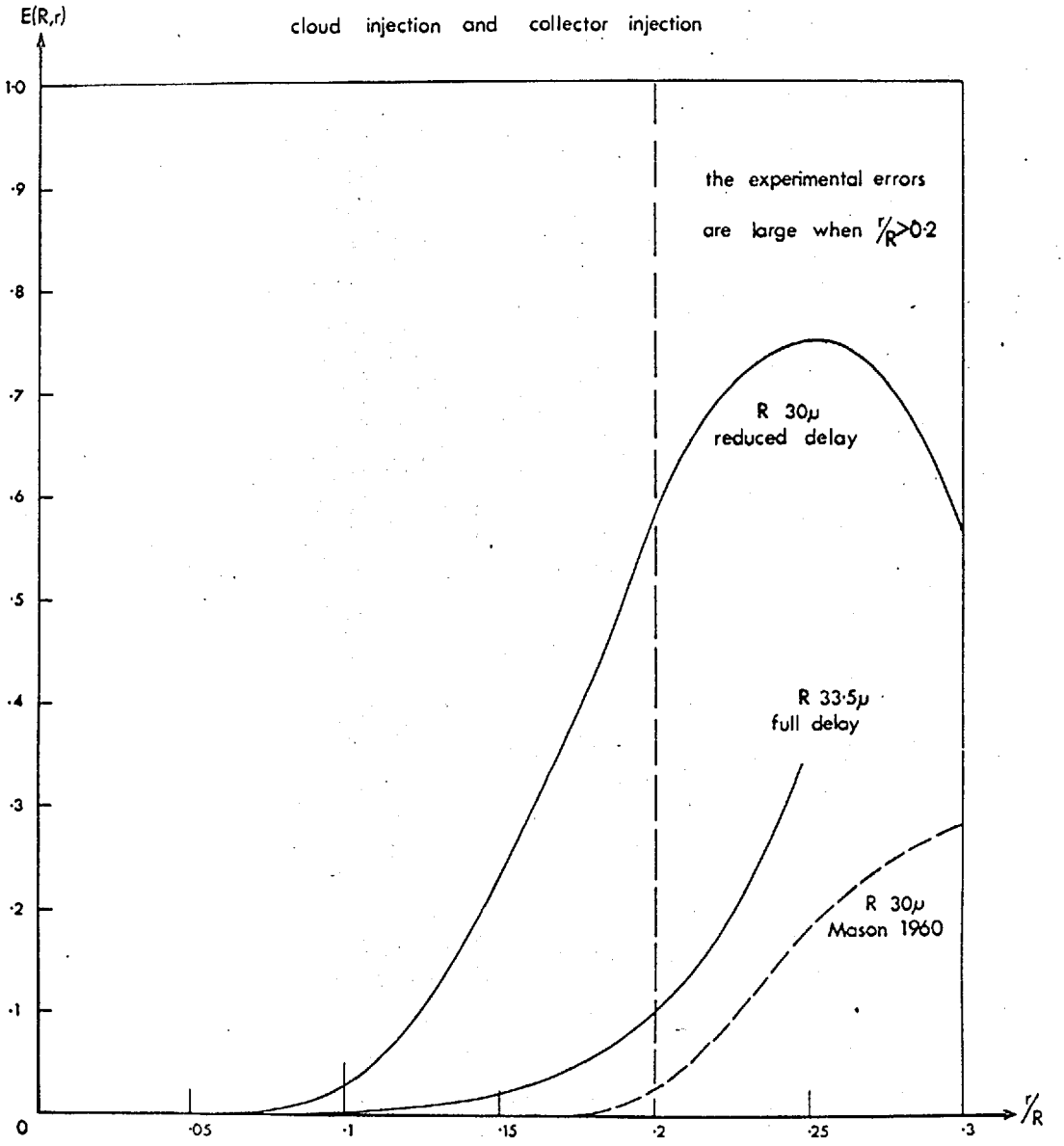

(Fig. 3.10b). The expansion of the tail may result from the more turbulent state of the cloud or from the fact that the cloud droplets had not reached equilibrium radii before the collectors were injected, or both. Attempts were made to distinguish between these two factors by artificially stirring the cloud (and so raising its turbulence) after leaving it for the full sixty seconds delay. Unfortunately this caused the cloud droplets to fall more rapidly down the settling column and to contaminate the collector slide. The experiment was therefore abandoned in favour of the more direct investigation to be described in Chapter 4. However, tests were made to confirm that the sixty second delay was sufficient for the cloud to reach equilibrium. Experiments with larger delays gave collection efficiency curves with the same tail at low droplet ratios.

Whether the tail is due to a residual long-lived turbulence in the cloud or whether it represents a genuine aspect of gravity coalescence could not be determined with this experiment. It is reasonable to postulate that in fact the theoretical curves are at fault in not showing a similar tail for E_{ℓ}. Hocking considered that his theory was unreliable for drop ratios $r_{\ell}/R < 0.2$, but stated that his calculations for $R = 30\mu$ gave a collision efficiency

curve with a tail of $E_o \sim 10^{-3}$ down to low values of r/R. Shafrir and Neiburger predicted a sharp cut-off for all E_o curves, but as their theory is less reliable than Hocking's it is possible that more accurate calculations might give non-zero E_o values beyond the quoted cut-off values of r/R. Shafrir has pointed out that, whatever theory is used, the precise value of r/R at which E_o disappears may vary considerably depending upon the smallest droplet size judged first to give a "grazing trajectory". This is well illustrated by Shafrir's (1964) recalculation of the E_o curve for $R = 30\mu$ following Hocking's theory precisely. Where Hocking gave the cut-off ratio as $r/R = 0.45$, Shafrir gives 0.35.

The subsidiary experiment provides strong support for Hocking's prediction that collision efficiency is zero for collectors smaller than 18μ radius. The experimental result is in direct conflict with that of Kinzer and Cobb, who found large values of collection efficiency for $R < 18\mu$. Their range of droplet sizes is comparable with that used in the present experiments, but the tube diameter in the present experiment was 8 cm compared with 8 mm in Kinzer and Cobb's. The other major difference lies in the latters' use of an

updraught to support the collectors.

The theory developed by Kinzer and Cobb does not depend upon the tube diameter or upon the presence of an updraught. It should therefore apply equally in the present experiment. It is reasonable, therefore, in view of the present results, to assume that Kinzer and Cobb's theory is incorrect and that their experimental result arises from the use of an updraught in a narrow bore tube.

CHAPTER 4

COLLECTION EFFICIENCIES FOR DROPS OF SIMILAR SIZES

4.1 OUTLINE OF THE EXPERIMENT

A stream of identical drops from a vibrating needle was allowed to fall vertically at terminal velocity* in a closed box. A small section of the stream was illuminated obliquely from behind by a parallel beam of light from a tungsten lamp and by a focussed beam from a point source stroboscopic lamp. Photographic time exposures of this illuminated section showed vertical streaks, corresponding to the highlights of the falling drops, accompanied by a regular series of points formed by the stroboscopic light. The streaks gave the drop trajectories to which the strobe highlights added time markers.

Many of the photographs included collisions between two drops. These were indicated by an oscillatory highlight, formed in the coalesced drop immediately after the disappear-

---

* As described later, this often exceeded the terminal velocity for isolated drops of the same size.

ance of the highlights of the two colliding drops. It was possible to calculate the velocities and accelerations of the drops from the spacing of the stroboscope time markers; the size of the drops from the frequency of oscillation of the coalesced drop; and the impact parameter of each collision from the orientation and separation of the drops, using a new analysis. The state of the environment in which these collisions took place was deduced from the behaviour of the streaks and by separate tests.

The experiment is similar to that of Telford and Thorndike (1961). However, by employing an optical system of greater magnification, it provides more intimate detail of the drop motions during the few milliseconds immediately before coalescence.

4.2 THE EXPERIMENT

A. Apparatus

The apparatus is illustrated in figures 4.1 and 4.2. Distilled water for the vibrating needle apparatus, V, was siphoned through a narrow-bore polythene tube from a reservoir, R, suspended one metre above the needle, giving a steady pressure of 0.1 Kg/cm^2 . The vibrating needle was situated about 10 cm above and to one side of the optic

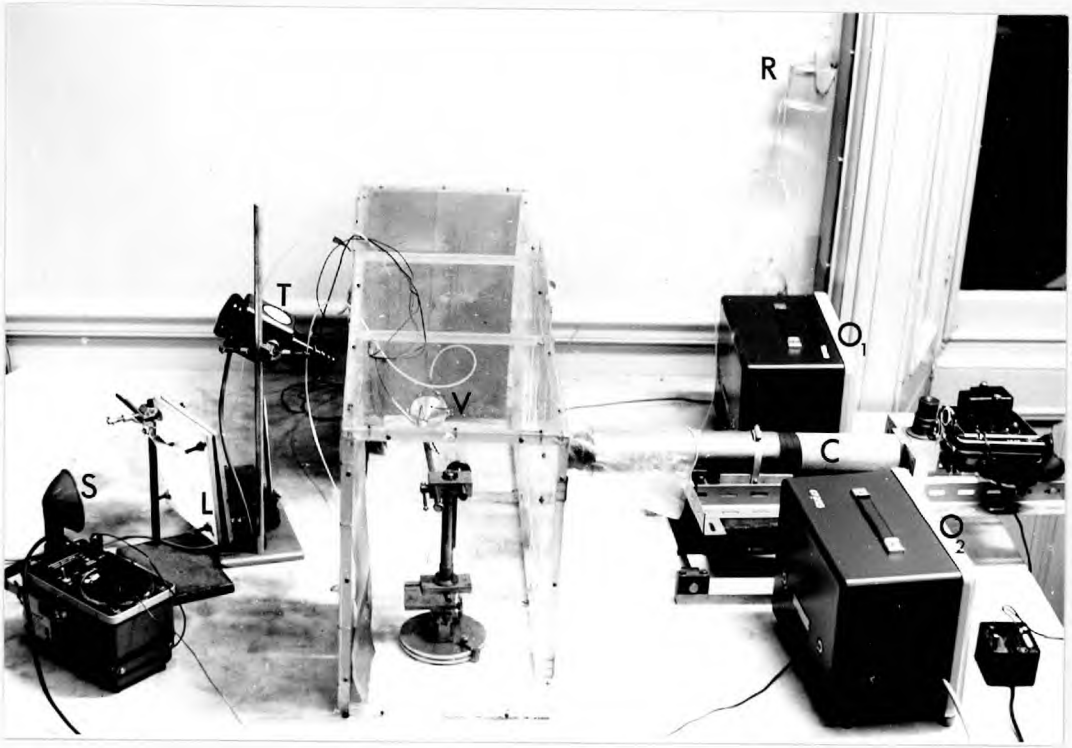

Fig. 4.1 The experimental apparatus

(Some of the brass foil lining the perspex box has been removed to show the vibrating needle.)

L - lens

S - stroboscopic lamp

T - tungsten lamp

C - camera

O - vibrating needle oscillator

O - strobe oscillator

V - vibrating needle apparatus

R - reservoir

Fig. 4.2 THE APPARATUS: vertical and horizontal section

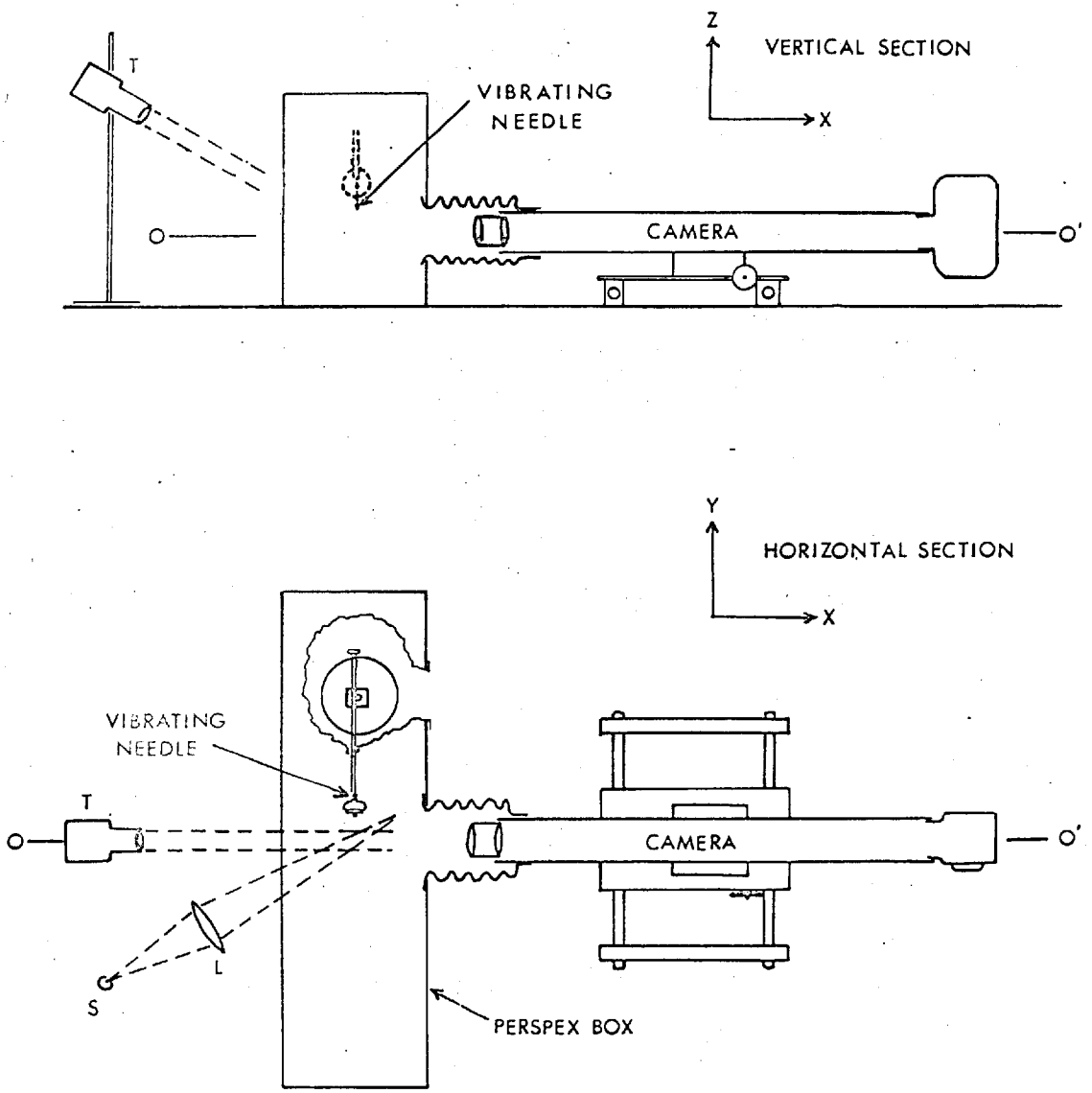

axis, OO′ , so that a stream of satellite drops, ejected horizontally from the needle, turned and passed vertically through the optic axis at terminal velocity, as shown in Fig. 3.4 (p.112).

Two lamps illuminated a one cm. square zone where the drops passed through the optic axis. A tungsten lamp, T, was focussed to give a parallel beam of light at 30° to the optic axis in the vertical plane through it, and a stroboscopic lamp, S, was directed at 30° to the optic axis in the horizontal plane through it. Fig. 4.3 shows this illumination acting on a water drop. The tungsten lamp gives a highlight at a distance K below the centre of the drop. As the drop falls under gravity this appears as a vertical streak. The stroboscopic illumination gives an interrupted highlight at a distance K to one side of the drop centre. For the falling drop this appears as a series of dots alongside the streak. The effective duration of each flash of the stroboscope was 0.5 μ sec. Before filming commenced the intensity of the tungsten lamp was adjusted until the intensities of the streak and the strobe highlights were similar.

The camera, C, comprised a Dallmeyer lens of 8 inches focal length and having a maximum aperture of f/4.5, joined

Fig. 4.3 ILLUMINATION OF THE DROPS.

T — tungsten lamp S — stroboscopic lamp

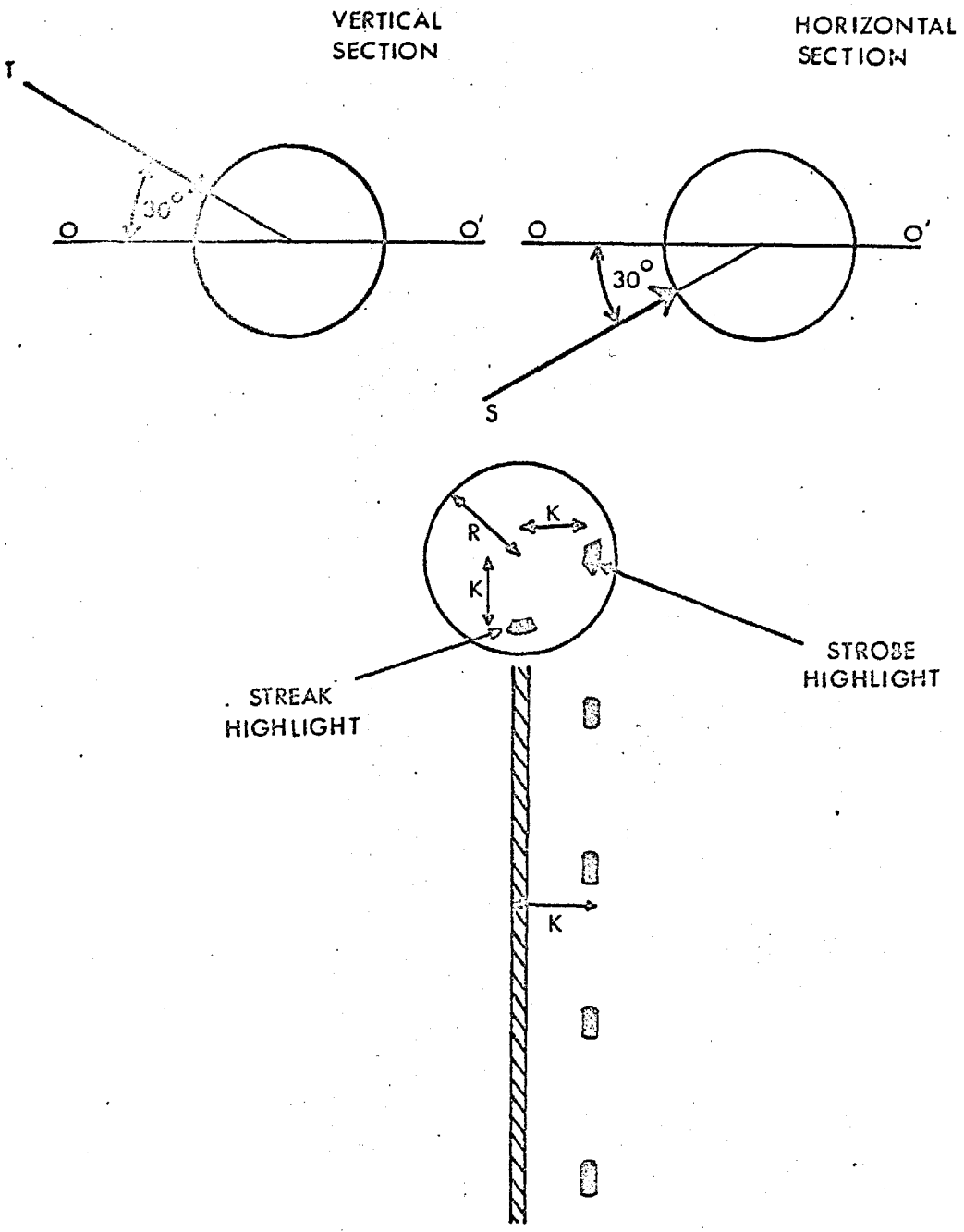

by a 120 cm. extension tube to one of two reflex camera bodies. The more useful was an electrically-driven Bolex H 16R cine camera which permitted the rapid exposure of up to 4,000 pictures on 16 mm film. This camera body is shown in the photograph, Fig. 4.1. The second camera, an Asahi Pentax SV using 35 mm. film, afforded a larger field of view, but required reloading after 36 exposures. The field of view of either camera could be increased by exchanging the 120 cm extension tube for one of 50 cm. length. This reduced the magnification from 6 to 2.8, the minimum consistent with accurate interpretation of the streak photographs. The camera was mounted on an assembly which permitted fine adjustments to be made for focussing and framing.

The droplet stream was shielded from draughts by a perspex box lined with earthed brass foil to exclude stray electric fields. A flexible polythene sleeve connected the camera to an aperture in the front of the perspex box and another permitted adjustments to be made to the vibrating needle mounting without opening the box.

B. Procedure

The vibrating needle apparatus was set to give a

stream of satellite drops of the required radius, as determined by the magnesium oxide method described in Chapter 3; the droplet stream was moved to the illuminated area; the camera was aligned and focussed; and, finally, the lamps were adjusted to give highlights of comparable intensity.

A number of photographs were then taken in rapid succession. The focus was checked before each exposure made on the 35 mm camera, or before each sequence of 100 exposures on the 16 mm camera. The drops were sampled on a magnesium oxide slide before and after each film was exposed. In general it was possible to maintain a stable satellite drop stream for up to 30 minutes without the drop radius varying by more than one micron. Changes in the drop size of even less than 1μ were clearly marked by a large change in their trajectory. The original trajectory and drop size were readily restored by fine adjustment to the amplitude control on the vibrating needle oscillator.

The film was processed in ID2 contrast developer and analysed as described in the following section.

4.3 ANALYSIS OF THE STREAK PHOTOGRAPHS

The water drops were scattered randomly within the

the cross-section of the stream (Fig. 3.4). To obtain the position in space of the trajectory of a single drop would require a synchronized stereoscopic pair of streak photographs, each carefully aligned against a fixed frame of reference. Schotland and Kaplin (1956) used this technique to follow steel spheres colliding in a viscous fluid. Telford et al (1955 and 1961) took single streak photographs of water drops colliding in air but being more concerned with drop velicities, they did not consider the spatial co-ordinates of colliding drops. It will be shown below that, provided the drop sizes are known, a single streak photograph provides sufficient information to calculate the impact parameter of a collision and the actual motion of the drops in space during the fifteen milliseconds prior to collision.

Impact parameter

A basic premise of the argument that follows is that the highlights of the individual drops disappear at the instant they start to coalesce. Before proceeding it is necessary to justify this assumption. The time required for the growth of the liquid neck between two coalescing drops, from the initial thin filament up to the instant

when all concavity between the drops disappears, has not been measured directly for water drops of the sizes found in clouds. Berg, Fernish and Gaulker (1963) measured the coalescence time for 1 mm radius drops using a Dynofax camera operated at 26,000 frames per second. They obtained values of about 600 μ sec. Charles and Mason (1960) quote a formula* for the growth rate of a liquid neck in another liquid. If this is valid for the case of water drops in air it would give a coalescence time of about 20 μ secs for the growth of a liquid neck between two 50 μ radius drops. Another useful estimate of the coalescence rate in the present experiment may be obtained by comparison with the readily measurable period of natural oscillation τ of a water drop. For a 50 μ radius drop, $\tau = 85\,\mu$ seconds. The coalescence time will be rather less than half of this, say 30 μ sec. Finally, high-speed cine film, taken at 7,000 frames per second, (see Fig. 4.4) gave a coalescence time

---

* Rate of thickening of a neck of liquid between two spheres

$$\frac{dr}{dt} = \sqrt{\frac{4\sigma}{(\rho_1+\rho_2)h}}$$

where ρ_1 = air density
ρ_2 = water density
σ = surface tension
h = air film thickness
r = neck thickness

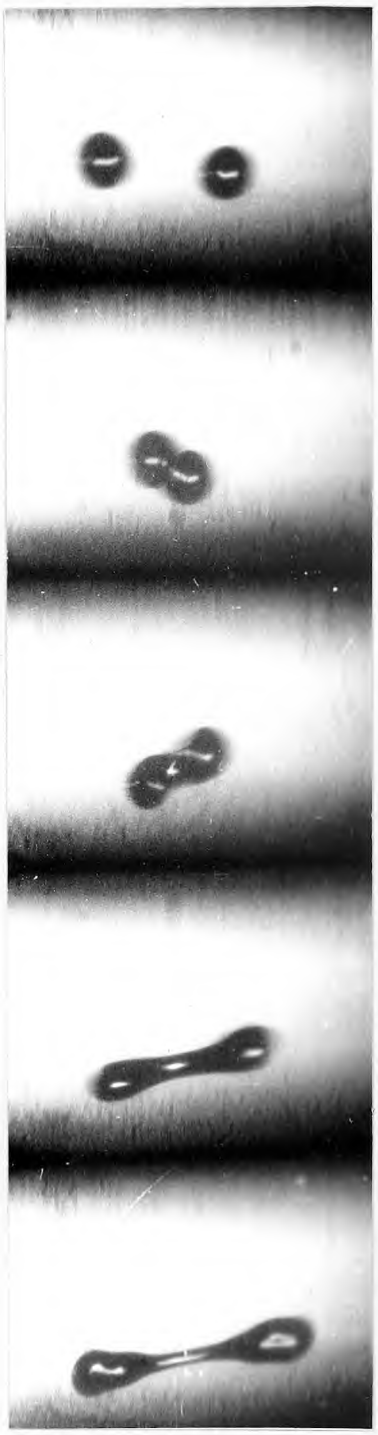

Fig. 4.4

The coalescence of two 130μ radius drops colliding head on at a relative velocity of 3 m/sec.

Photographs taken at 7000 frames/second.

Coalescence is completed in the 100μ sec. interval between the second and third frame.

of well under 100 μ seconds for 130 μ radius drops.

This short coalescence time causes the surface of the coalescing water mass to change very rapidly, giving an even faster movement to the streak highlight. The intensity of the streak on the film depends upon its speed across the emulsion; during the initial stages of coalescence the movement is too rapid for exposure of the film. So, in practice, the highlight of each colliding drop disappears at the instant a liquid connexion forms between them. Later, when the coalesced drop is established, a single oscillatory streak appears.

The impact velocity is in all cases too small to cause appreciable distortion of the original drops, so when the two highlights disappear the drop centres (O_1 and O_2) are separated by the sum of their radii ($R_1 + R_2$). Fig. 4.5 shows the arrangement of two drops at the instant of collision. The vertical separation, h, of the drop centres at the instant of impact is measured on the streak photograph. From h and the sum of the drop radii ($R_1 + R_2$) it is possible to calculate the collision parameter, c, defined as the horizontal separation of the drop centres at coalescence.

$$h^2 + c^2 = (R_1 + R_2)^2 \quad \ldots\ldots\ldots 4.1$$

Fig. 4.5 CALCULATION OF THE IMPACT PARAMETER OF A COLLISION FROM A STREAK PHOTOGRAPH.

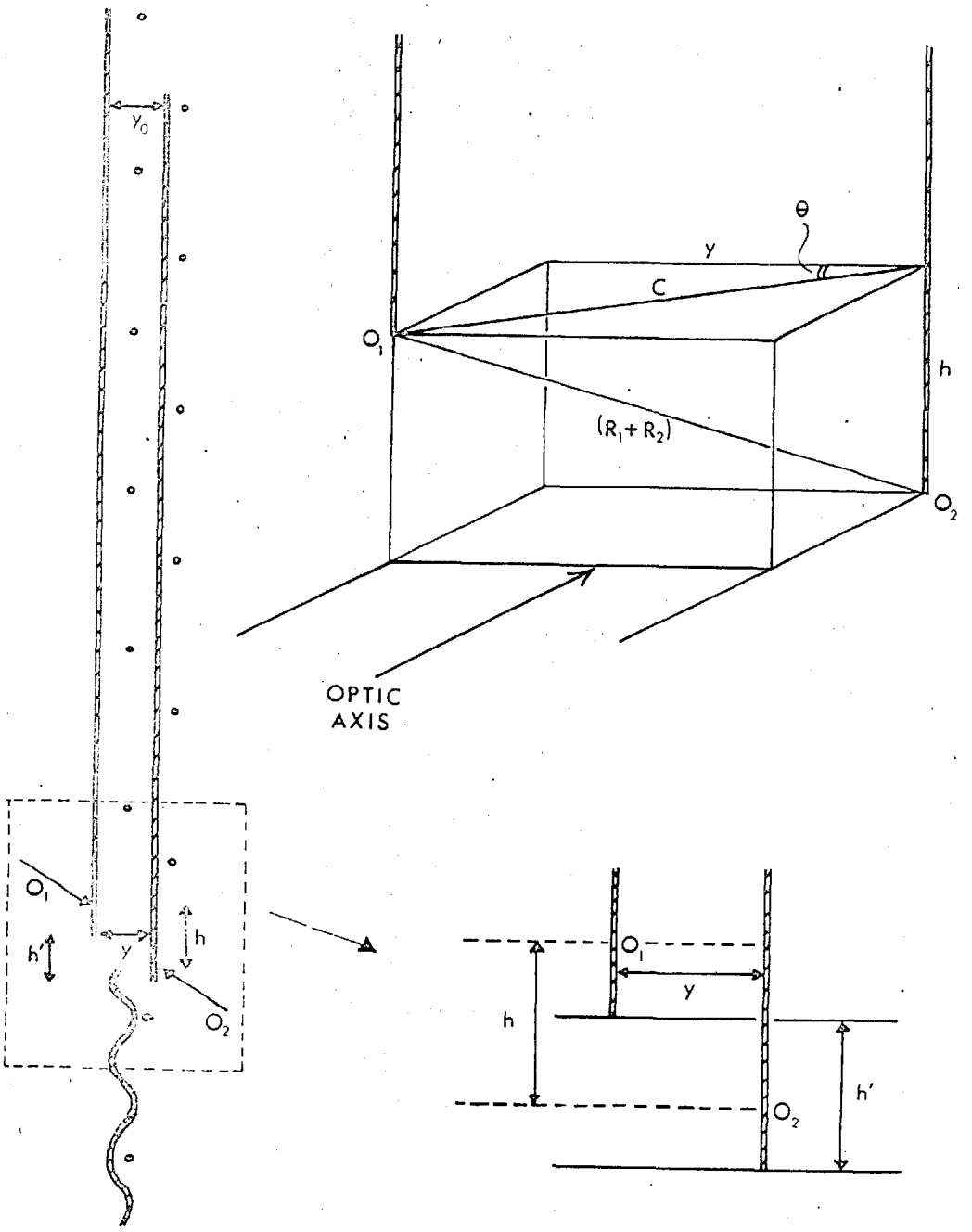

The trajectories of the centres of two drops colliding in tranquil air will be in a vertical plane which makes some angle θ with the vertical plane through the optic axis. The hydrodynamic interaction forces act only in this plane, so the drops will not deviate from it unless influenced by some external force. Thus, once the orientation θ of an undisturbed collision has been determined, the trajectories of the colliding drops may be obtained from the single streak photograph. The orientation is obtained from the streak photograph. If the separation of the streaks at the point of impact is y and the collision parameter is c, then

$$\cos\theta = {}^{y}/_{c} \qquad \ldots\ldots\ldots\ldots \quad 4.2$$

The horizontal separation, y_∞, of the streaks at some time before the collision, when the drops were falling independently, bears the same relationship to the impact parameter, b, thus

$$\cos\theta = {}^{y_\infty}/_{b} \qquad \ldots\ldots\ldots\ldots \quad 4.3$$

The experimental formula for deriving the impact parameter is obtained by combining equations 4.1, 4.2 and 4.3.

$$b = \frac{y_\infty}{y}\sqrt{(R_1 + R_2)^2 - h^2} \qquad \ldots \quad 4.4$$

If the drops are not identical, the analysis given above requires one modification. The vertical separation of the streak termination points is no longer equal to the vertical separation of the drop centres. However, it will be seen in Fig. 4.5 that a simple correction may be obtained.

$$h = h' + (k_1 - k_2)$$

where h is the measured vertical separation of the streak terminations and h is the actual vertical separation of the drop centres, at the instant of coalescence. k_1 and k_2 are the distances between the highlights and the centres of drops of radius R_1 and R_2 respectively; they equal the measured distances between the strobe highlights and the streak of each drop. An experimental determination (see Fig. 4.6) gave a value of $k \simeq \frac{3}{4}R$.

The time markers

The stroboscope highlights mark the position of each drop at millisecond intervals (see Fig. 4.3). The average velocity of each drop is obtained every millisecond by measuring the separation of these time markers. In this way it is possible to measure the vertical accelerations of pairs of interacting drops, or of a single drop in some wholesale movement of the surrounding air.

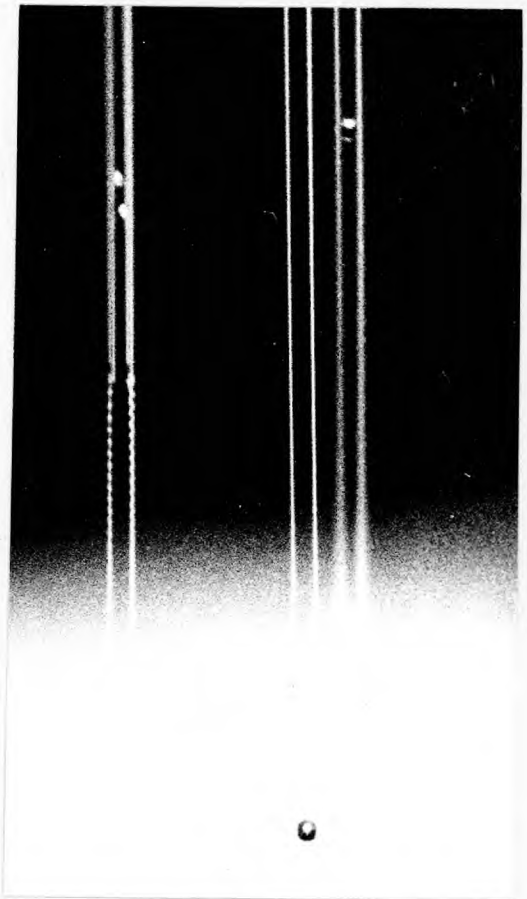

Fig. 4.6

Experimental determination of the distance, k, between the streak highlight and the drop centre.

Two parallel beams of light are directed in the horizontal plane through the optic axis and converging onto the drop stream at an angle of 30° on either side of the optic axis. Each drop is represented by a pair of streaks separated by 2k.

Halfway through the exposure, a 1μsec. flash illuminated the lower half of the field of view. At this instant, one of the drops was in line with the flash and appears in sharp silhouette. The others were higher as shown by the additional highlights between the twin streaks.

The two drops on the left of the picture coalesced soon after the flash gun was fired.

Using the time markers, it is also possible to calculate the frequency of oscillation of the coalesced drop. This damped oscillation is visible on the streak photographs for about twenty complete vibrations. The initial rather unsteady motion rapidly reduces to a constant frequency equal to the natural frequency of the coalesced drop, which may be compared with Rayleigh's (1878) formula* .

$$\tau = \pi\sqrt{\frac{\rho R_c^3}{2\sigma}}$$

where τ = natural period of oscillation

ρ = water density

σ = water surface tension

R_c = radius of coalesced drop.

In Fig. 4.7 is plotted the variation of natural period of oscillation with drop radius, calculated from Rayleigh's formula.

The coalesced drop radius deduced from its measured period of oscillation agreed well with that calculated from the original drop size (measured by magnesium oxide slide). The majority of coalesced drops resulted from the collision of two (identical) members of the original stream (radius R).

---

* Rayleigh predicts, and quotes experimental evidence for, a higher frequency at very large amplitudes. (Theory of Sound, p. 371.)

Fig. 4.7. VARIATION OF THE PERIOD OF NATURAL OSCILLATION WITH DROP RADIUS [after Rayleigh]

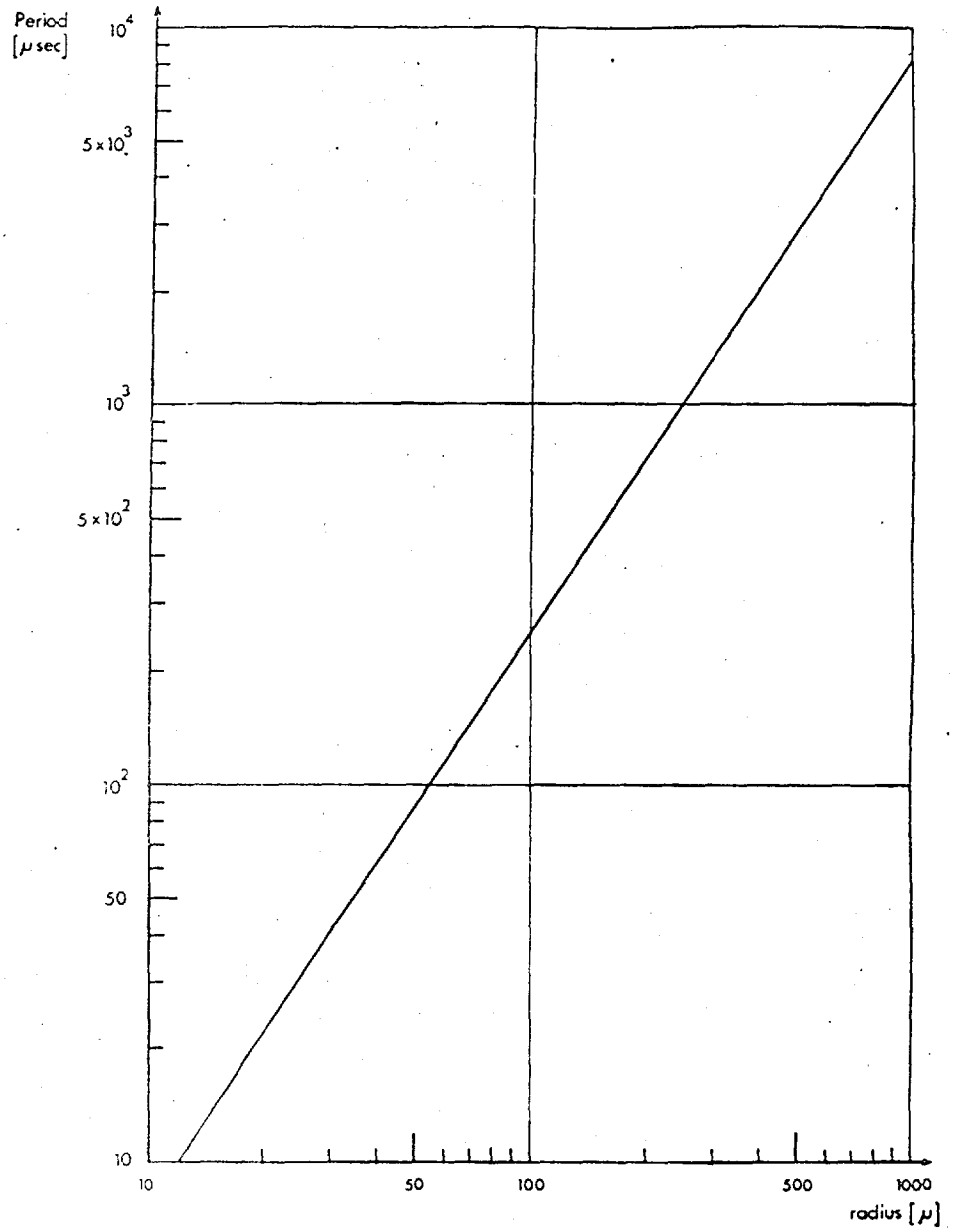

However, occasional photographs recorded the collision of a double-mass ($R_1 = \sqrt[3]{2}\,R$) drop with a single-mass drop ($R_2 = R$). These second-order and higher order collisions are readily identifiable by the lower frequency of oscillation of the resultant drop ($R_c = \sqrt[3]{3}\,R$, etc.).

4.4 RESULTS

The most striking result of the experiment is the observation that pairs of identical drops of $R > 40\mu$ collide with high collection efficiency (see Fig.4.8). Identical drops of $R < 35\mu$ were never observed to collide; many thousands of streak photographs of streams of identical drops of radii less than 35μ were examined without once detecting the oscillatory trace which marks a coalesced drop. Occasional coalescence events were recorded for drops of $35\mu < R < 40\mu$, but these were rare and in almost every case the drops approached one another at an angle rather than one behind the other, as in Fig. 4.15. It is concluded that such collisions occur only when aided by some motion of the air and they are therefore attributed to turbulent capture.

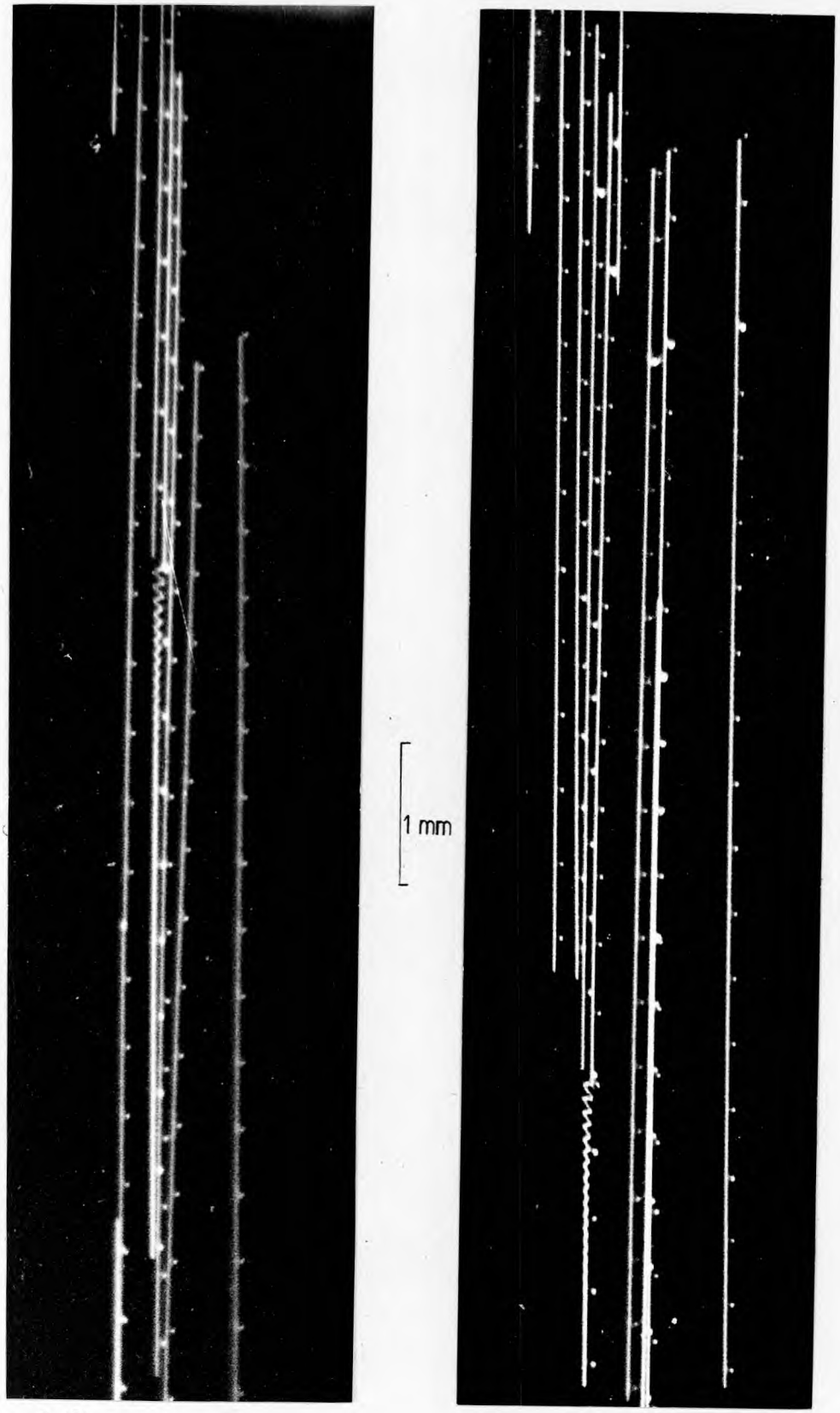

Fig. 4.8

Typical collisions between equal 62μ radius drops

THE DROP TRAJECTORIES

Horizontal motion

(a) identical drops

No horizontal attraction or repulsion was detected during the last twenty milliseconds before collisions between equal drops of radii greater than 40μ . The resolution of the streak photographs is such that a horizontal motion of greater than 5μ would be detected.

(b) unequal drops

Fig. 4.9 shows the coalescence of two equal drops to form one of double their weight, which accelerates downward until, shortly afterwards, it overtakes and captures a third drop. The first collision occurred between equal drops, so $r/R = 1$, but in the second collision the drops were of different sizes, such that $r/R = 0.8$. These unequal collisions, which appeared quite frequently in each sequence of streak photographs, were readily identifiable because of the reduced frequency of the oscillation in the resulting drop. Occasionally, unequal collisions between drops with mass ratios of 3 and even 4 were recorded. Thus in a single stream of drops it was possible to observe collisions in which $r/R = 1, 0.8, 0.69, 0.63$, etc.

A clear horizontal deflection was detected for these

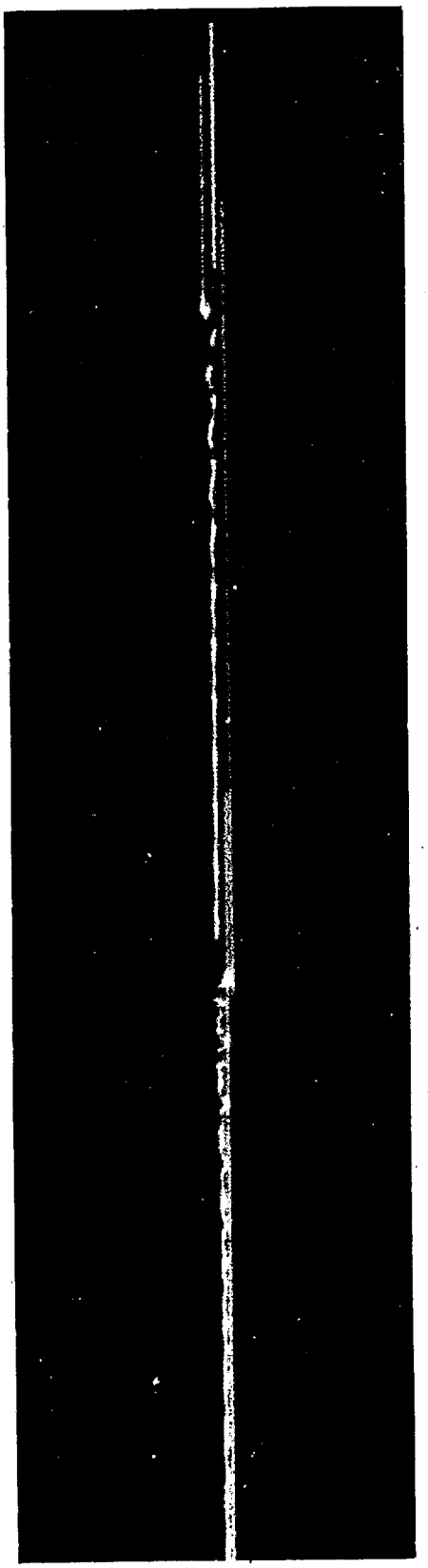

Fig. 4.9

A collision between two equal drops of 64μ radius to form a coalesced drop of 81μ radius, which then captures a third 64μ radius drop.

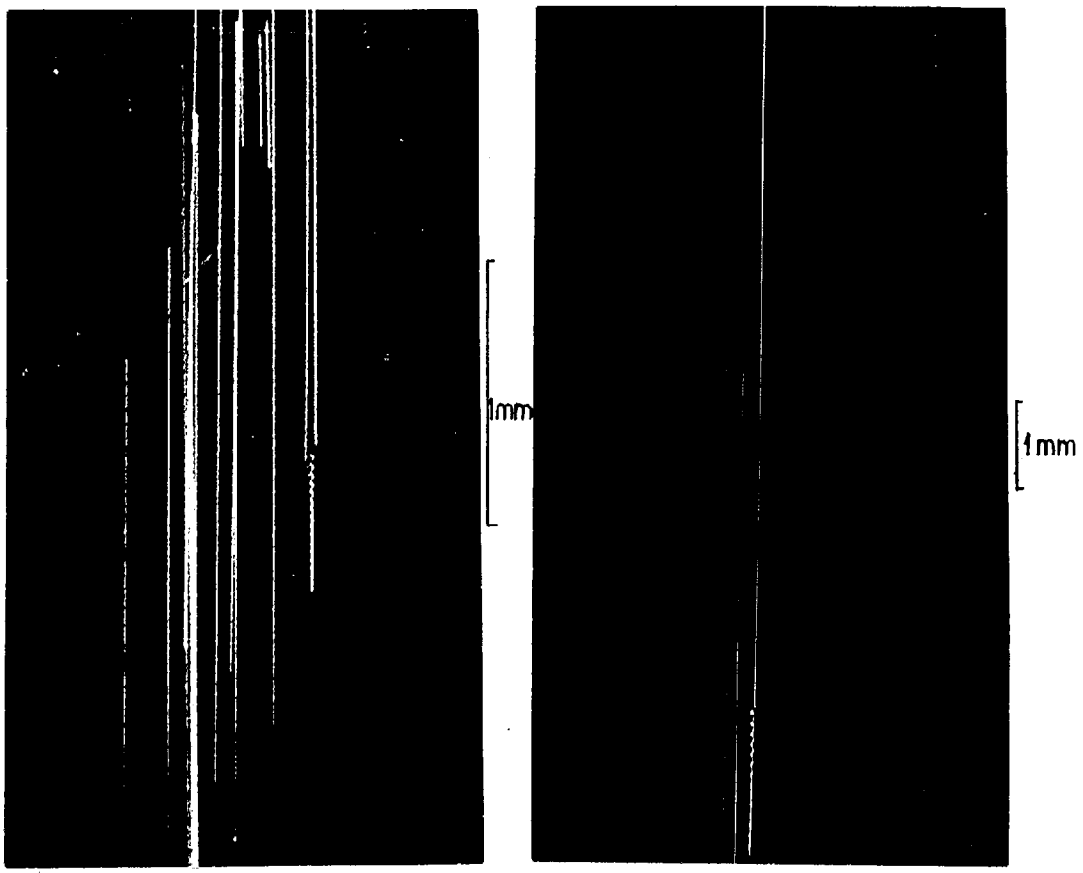

(a) R = 47μ
r ≅ 37μ

(b) R = 82μ
r = 65μ

Fig. 4.10 The collision and coalescence of a collector drop with a droplet of half its mass.

$$\frac{r}{R} = 0.8.$$

collisions between unequal drops. Two examples are shown in Fig. 4.10. In the first, the droplet has a radius of 37μ and is deflected sideways as the collector drop* overtakes it. In the second example the droplet, of radius 65μ has a well developed wake and the deflection is scarcely discernible against the turbulent perturbations to the drop trajectories.

Vertical accelerations

(a) identical drops

Changes in the fall speed of each drop were obtained from the separation of successive strobe highlights. Fig. 4.11 is a plot of the variations in fall speeds of two 62μ radius drops during the eleven milliseconds before they coalesce. Even at the start of the streaks, when the drops have a vertical separation of 15 radii, they have been interacting for sufficient time to develop a relative velocity of 10% of the terminal velocity of an isolated 62μ radius drop. However, the vertical accelerations are small until about 5 milliseconds before coalescence, when their vertical separation is approximately 5 radii. The

* In this case the collector drop was formed by a turbulent collision between two 37μ radius drops.

FIG. 4.11 FALL SPEEDS OF TWO COLLIDING DROPS WITH RADIUS 62 μ.

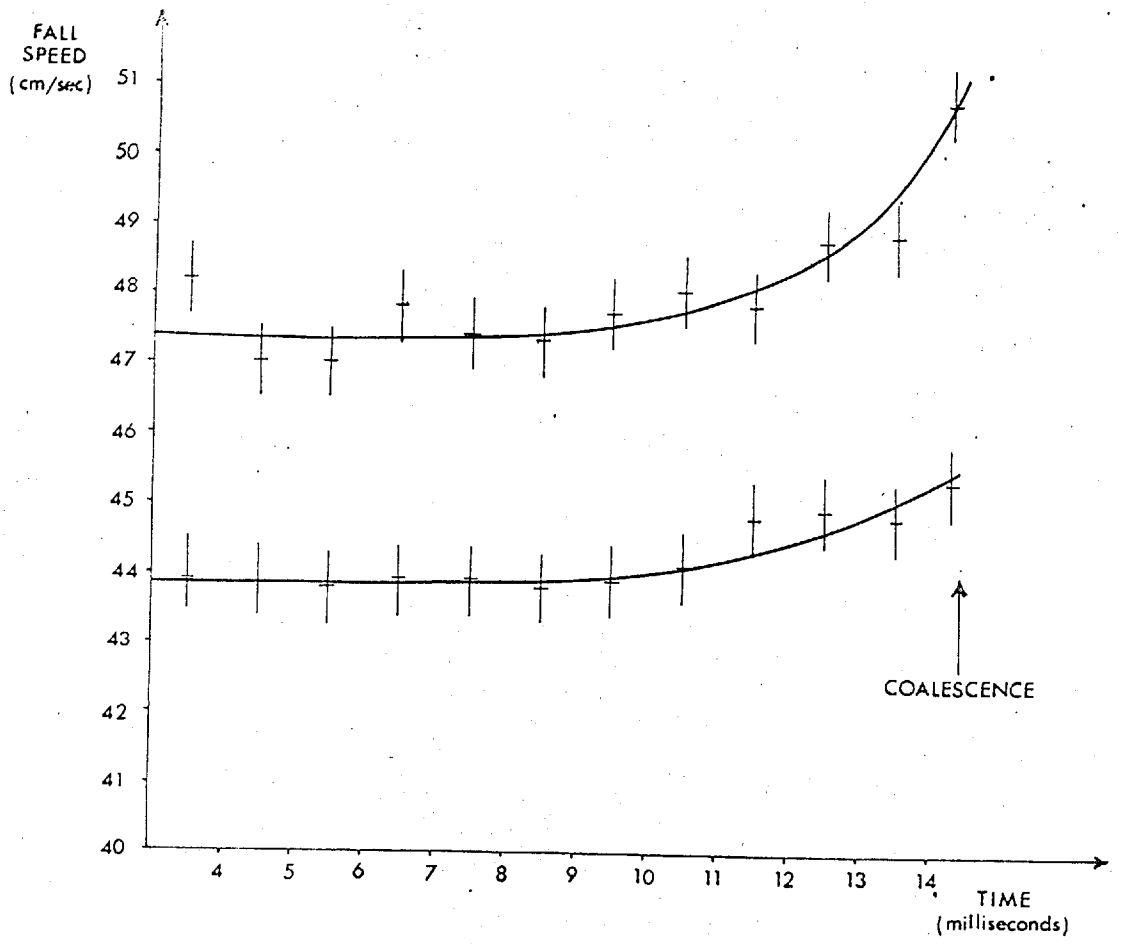

final acceleration is greater for the upper drop, so that the relative velocity is rapidly increased to almost 20% of terminal velocity when the drops collide.

(b) unequal drops

The accelerations described above are also observed in collisions between unequal drops. However, in the majority of unequal collisions, the collector drop was still accelerating towards its terminal velocity after having been formed from a collision between equal drops.

Collection efficiency

The streak photographs support the view that the coalescence efficiency is unity for equal or nearly equal water drops of radii $>35\mu$. None of the streak photographs may be interpreted as showing a collision which was not immediately followed by coalescence. Thus all collisions with impact parameter, b, smaller than the grazing impact parameter, b_g, will result in coalescence and the collection efficiency, E(R,r), which is in all respects identical to the collision efficiency, $E_c(R,r)$, is obtained from equation 1.5.

$$E(R,r) = \frac{b_g^2}{(R+r)^2} \qquad \ldots\ldots\ldots \quad (1.5)$$

In the experiment, all the streak photographs showing a collision between drops of given radii, R and r, were inspected for the largest impact parameter, b_{max}. This is obtained from equation (4.4)

$$b_{max} = \frac{y_o}{y} \left[(R + r)^2 - h^2_{min} \right]^{1/2} \quad \ldots . \quad (4.4)$$

where y_o and y are the values corresponding to h_{min}. An experimental value for the collection efficiency is obtained by combining (4.4) and (1.5).

$$E(R,r) = \frac{y_o^2}{y^2} \left[1 - \frac{h^2_{min}}{(R + r)^2} \right] \quad \ldots . \quad (4.6)$$

This experimental value will be less than the true value because it is based upon the maximum observed impact parameter, b_{max} , which is smaller than the grazing impact parameter, b_g, by some unknown quantity. However, as all impact parameters are equally likely, it is possible to estimate the probability, P_n (i), of b_{max} being within i% of b_g when the former is based upon an analysis of n collisions. For example, when n = 20, there is an 88% probability of finding b_{max} within 10% of b_g. In this case there will be an 88% probability of the experimental collection efficiency being within 20% of the true value.

The uncertainty introduced into the experimental

TABLE 4.1

EXPERIMENTAL VALUES OF COLLECTION EFFICIENCY

(a) PAIRS OF EQUAL-SIZE DROPS

$R_1 = R_2$ (μ)	E (based on lowest value of h)	No. of events
35-45	0.5	14
45-55	0.7	30
55-65	0.85	34
65-75	0.9	36
75-85	0.95	8
85-95	0.9	2

(b) PAIRS OF UNEQUAL DROPS

R_1 (μ)	R_2 (μ)	E	No. of events
113	90	0.9	7
68	47	0.9	12
60	47	0.8	8
50	30	0.5	6

Fig. 4.12 COLLECTION EFFICIENCY DIAGRAM

Tentative modification of Shafrir & Neiburger diagram to show the effect of wake capture when $r > 40\mu$

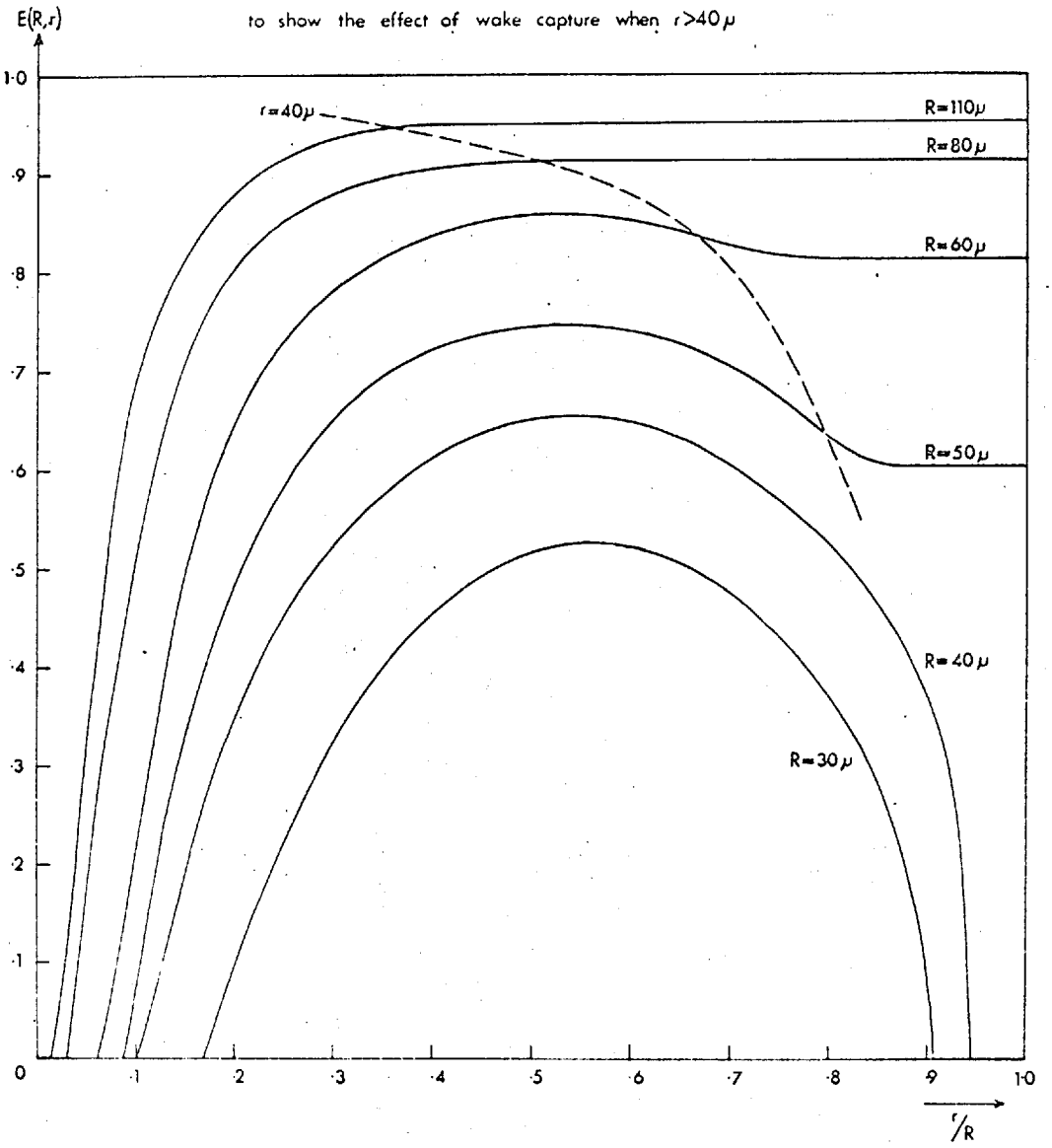

values of E(R,r) by the above factor is comparable with the random experimental error, of the order of 20%, arising from the measurement of h_{min} , y_o and y. The experimental error in measuring the drop radii was less than $\pm$ 2%.

The experimental values for collection efficiency are given in Table 4.1. Fig. 4.15 shows the effect of incorporating these results in the collection efficiency diagram proposed by Shafrir and Neiburger. No modification has been made to the theoretical curves where $r < 40\mu$.

4.5 DISCUSSION

The principle interest in studying collisions between equal drops is that they are not subjected to the constant force, equal to the difference in their weights, which acts throughout the collision of unequal drops. The force acting between equal drops arises solely from the air flow around them. Telford and Cottis (1964) have recently measured the force between two equal, solid spheres aligned in the direction of water flowing past them. This is equivalent to measuring the hydrodynamic attraction between equal cloud drops in the range $26 > R > 14\mu$ when they are separated by a few radii.

The present experiments show that the hydrodynamic

attraction between equal drops of less than 40μ is insufficient to cause them to coalesce. For larger drops this attraction, caused solely by the combined airflow around them, is sufficient to cause coalescence. The Reynolds number at which equal drops will spontaneously collide and coalesce in this way is approximately unity, the value which has traditionally been taken as the upper limit to which the Stokes theory of viscous flow may be applied to an isolated sphere without serious error. At larger Reynolds numbers the sphere develops a well defined wake, and for this reason it is convenient to give the label "wake capture" to spontaneous collisions between equal drops.

The observed trajectories followed by equal drops prior to coalescence provide a clear indication that the horizontal force between the drops is very small, probably less than one thousandth of the weight of one of the drops. The vertical force between the drops increases markedly as they approach within a few radii, when it is of the order of the weight of one of the drops.

Two previous experiments on nearly equal water drops in air have been described in Chapter 2. The present

results are in direct conflict with those of Telford et al (1955), who concluded that the high coalescence rate measured in their wind tunnel experiment indicated a high collection efficiency, E = 3.14, for drops in the range $65\mu \pm 3\mu$ radius. This, the authors claimed, results from lateral attraction caused by the wake of the lower drop, which is in agreement with the theoretical predictions of Pearcey and Hill (1956). The grazing impact parameter equivalent to E = 3.14 is $b_g = 3.6R$.

In the present experiment, no evidence was found for grazing impact parameters greater than 2R. Nor was evidence found for horizontal attraction between equal drops during the last few milliseconds before they coalesce. Although the streak photographs do not show the trajectories of the drops during the early stages of the interaction, it is unlikely that horizontal attraction would be strongest at long range when the vertical attraction is weakest. It is reasonable, therefore, to seek some other explanation of Telford's result.

Telford stated in a reply to Dessens (1956) that the turbulence in their closed circuit wind tunnel increased until, after fifteen minutes operation, it became "experimentally objectionable". It seems likely that

the turbulence in the airstream was promoting collisions between the drops even before the fifteen minute limit. If 70% of the observed collisions resulted from turbulent capture rather than wake capture, then the inferred collection efficiency of the remainder would be approximately unity, in agreement with the present experiment.

The later experiment of Telford and Thorndike (1960), in which small water drops of diameter 35μ and 45μ fell through tranquil air, considerably reduced the chance of turbulent capture. The results are consistent with the present work.

4.6 THE EFFECT OF TURBULENCE

A. Air motions within the drop stream

Close inspection of the streak photographs shows that the drops in the centre of the tightly-packed stream fall faster than those at the edges. This gradation of the drop velocities is caused by the velocity shear in the steady downward airstream which accompanies the drops. The velocity profile of the airstream is obtained by taking the difference between the calculated terminal velocity of each drop and its measured fall speed. A typical plot is shown in Fig. 4.13. In this case the maximum velocity shear would produce a velocity difference

Fig. 4.13 TYPICAL VELOCITY PROFILE FOR A STREAM OF 36μ RADIUS DROPS

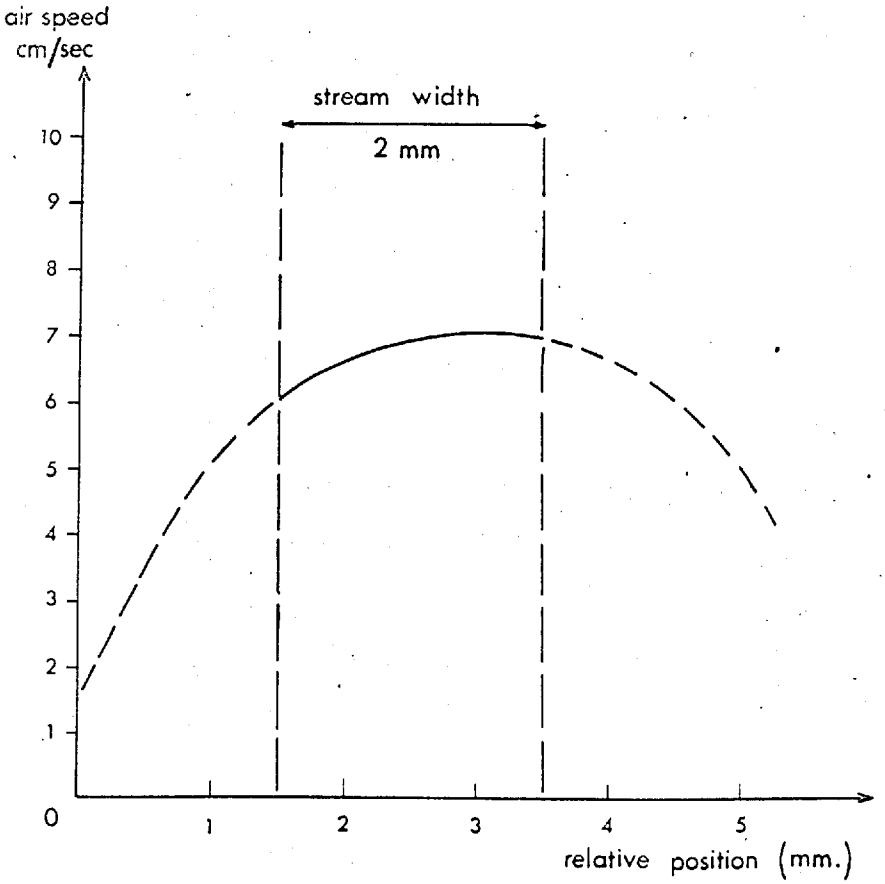

of only 0.2 cm/sec. across two grazing 50μ radius drops. This is an order of magnitude smaller than the relative velocity caused by their hydrodynamic interaction and therefore it does not significantly affect the collision of drops in the stream.

Superimposed upon the steady downward airstream is a turbulent motion which causes the drop trajectories to make temporary deviations from the vertical. This effect is particularly clear in Fig. 4.14 which shows a stream of 30μ radius drops. The period of the deviations is approximately $^1/_{50}$th second and the horizontal displacements are approximately one drop diameter. Drops within a few millimetres of each other suffer a similar displacement. These observations indicate that the turbulent eddies are a few millimetres across and have maximum velocities of a few millimetres per second. These conclusions were confirmed by studying the motion of particles in a fine aerosol injected into the vicinity of the stream.

It was necessary to distinguish between these turbulent motions and accelerations caused by the interaction of two drops. For example, the divergence of the trajectories at the top of Fig. 4.10 b may be interpreted

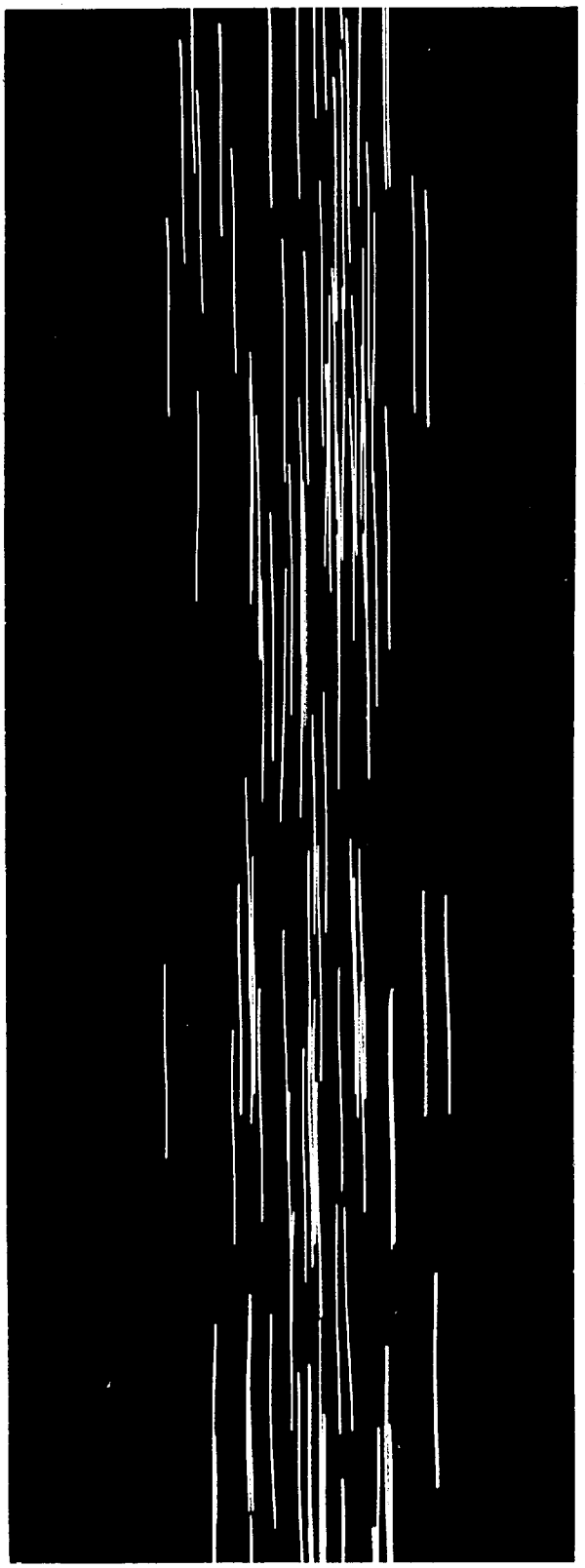

Fig. 4.14

Turbulent perturbations to the trajectories of 30μ drops in a narrow stream.

Each streak corresponds to 20 milliseconds.

as the successive response of the drops to an eddy. The streak on the left of the picture exhibits a similar disturbance.

Vertical accelerations accompany the horizontal displacements. The vertical velocities of the 62μ radius drops plotted in Fig. 4.11 oscillate about the smooth curve with an amplitude of $\frac{1}{2}$ cm/sec. and a period of about 5 msecs.

Occasionally the turbulent motions in the airstream caused two drops to collide at an angle, as shown in Fig. 4.15. The collection efficiency data given in Section 4.4 was based upon streak photographs in which the drops appeared to be relatively free from turbulent motion. This was verified by examining the tracks of drops which fell alongside the pair in collision. However, collisions between equal drops in the range $35\mu < R < 40\mu$ were nearly always associated with turbulent motions. It is concluded that equal drops in this size range do not collide in still air but require the assistance of some external air motion. They are examples of <u>turbulent capture</u>.

B. <u>Collisions caused by an artificial wind shear</u>

In all the collisions described above, in which turbulence played some part, if not a necessary one, the

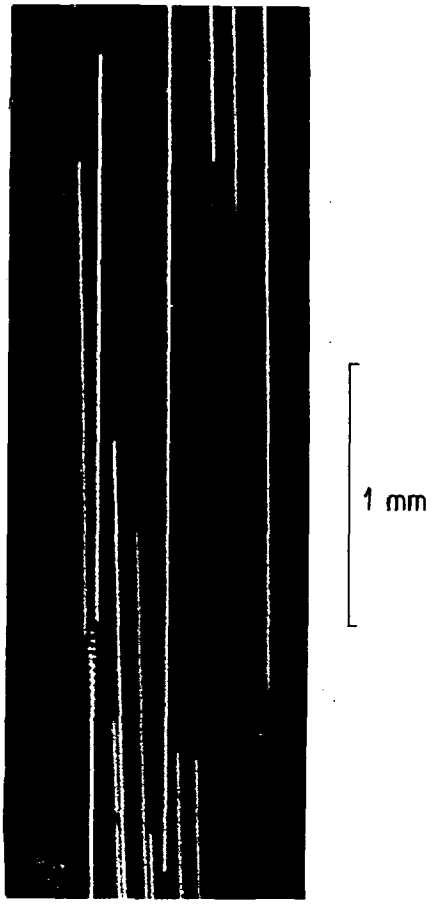

Fig. 4.15 Two 36μ drops coalesce after colliding at an angle.

drops collided at an angle, rather than one behind another. An experiment was designed to test whether drops which do not coalesce spontaneously could be made to do so by inclining their trajectories to one another. A wide horizontal jet of air was directed across a stream of drops, through the illuminated working area and orthogonal to the optic axis.

Streak photographs of 35μ drops, taken on 16 mm. film using the Bolex camera, were inspected for coalescence events. Despite the increased separation of the drops caused by the air stream, several coalescences were found. An example is shown in Fig. 4.16. In every case coalescence followed the collision of two drops approaching at a considerable angle after originating in different parts of the airstream. No coalescence events were recorded in control photographs of the same drop stream in the absence of the horizontal air jet.

The maximum horizontal velocity of the air jet was about 10 cm/sec. and the maximum velocity shear was about 10 sec^{-1}. The constant temperature probe of a hot-wire anemometer was used to investigate the structure of the air jet. With this instrument it was possible to demonstrate that turbulent fluctuations in the air jet

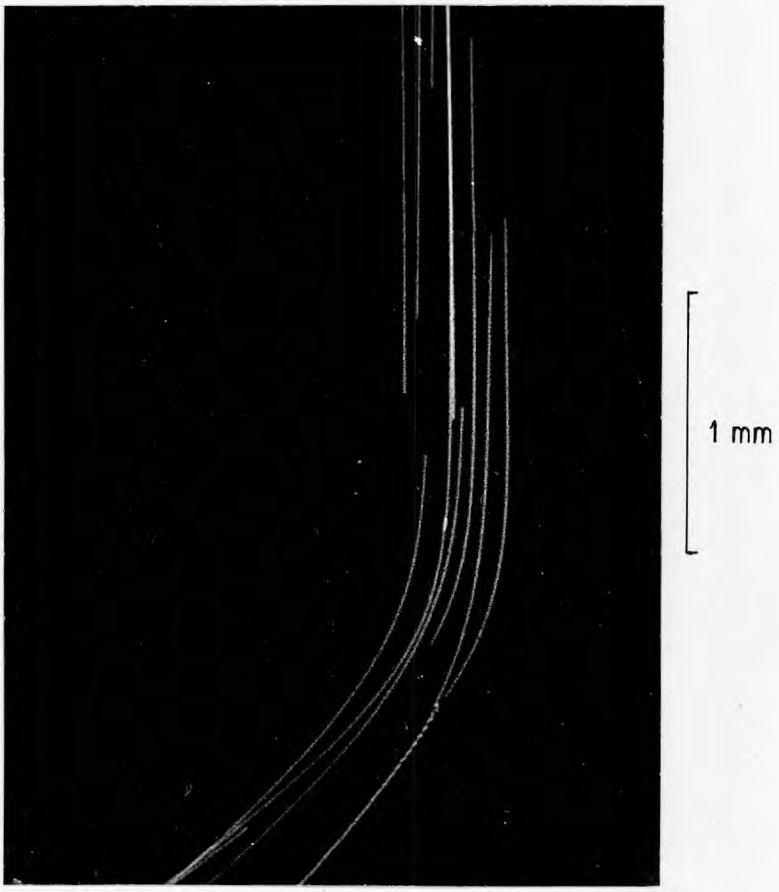

Fig. 4.16 A collision between two equal drops of radius 35μ caused by their falling into a horizontal air jet of maximum speed 10 cm/sec.

had a root-mean-square amplitude of less than 3% of the steady velocity. It may therefore be concluded that the reason for the different drop trajectories was spatial variations in the stream velocity and not time variations.

Many of the coalescence events occurred after the individual drops had nearly stopped turning. Thus coalescence was not caused by the centrifugal acceleration, but by either the velocity shear across the drops or by the angle between their trajectories. The experiment did not differentiate between these two effects.

This investigation of the effect of microturbulence upon the collision and coalescence of identical drops was not completed at the time of writing. Further experiments, involving the study of a drop stream in controlled homogeneous turbulence are planned. The conclusion based on the present very limited investigation is that equal drops colliding at an angle coalesce quite readily, even though they are too small to coalesce spontaneously in still air. The turbulence in the stream of drops from a vibrating needle is sufficient to cause identical drops of between 35 and 40μ to coalesce. Smaller drops require a more violent air motion.

4.7 THE EFFECT OF ELECTRIFICATION

The importance of electrification as a possible additional cause of drop coalescence has already been discussed in Section 2.3A. Previous workers have demonstrated that an increase in the coalescence rate is observed when drops fall in an electric field or carry electric charges. The experiment of Telford, Thorndike and Bowen was repeated incorporating the improved techniques described in 4.2.

Drop charging

The drops from the vibrating needle apparatus may be charged by applying a D.C. potential to the steel needle. The magnitude of the charge carried by each drop is then measured by collecting the stream of drops in a metal can connected to a vibrating reed electrometer. The average charge, q, on each drop is equal to the steady current, i, measured by the electrometer, divided by the frequency of drop production, f.

$$\text{i.e.} \quad q = {}^{i}/_{f}$$

In practice the charges carried by the satellite drops were usually about a quarter of that which would be carried by a conducting sphere of the same size when raised to the needle.

potential.

In the experiment, successive drops were charged alternately to equal positive and negative values by applying a square wave potential to the needle at half the frequency of drop production. This signal was obtained from an Eccles-Jordan ("flip-flop") circuit triggered by pulses obtained by differentiating the square wave signal used to drive the vibrating needle apparatus. The amplitude of the drop-charging signal was varied by changing the supply voltage to the "flip-flop".

Experiment and results

The procedure followed that described in Section 4.2. Streak photographs of a single stream of satellite drops (radius 36μ) were taken in rapid succession on a 100-foot length of 16 mm film using the Bolex camera. The film was divided into seven sequences of five hundred frames each. For the first sequence the vibrating needle was maintained at earth potential; for the following five sequences a square wave signal of $\pm$ 16 V , $\pm$ 32 V. , $\pm$ 48 V. , $\pm$ 64 V. and finally $\pm$ 70 V. was applied to the vibrating needle; for the final sequence a D.C. potential of 63 V was applied to the needle. The complete film was exposed in under five

minutes during which time the drop stream remained steady and with drops of constant size.

The 3,500 streak photographs were subsequently examined for evidence of coalescence, as revealed by the oscillatory streak of the coalesced drop. No attempt was made to analyse the individual collisions, but as the drop size and charge remained constant throughout each sequence of five hundred photographs, each frame was treated as a typical random sample. The variation in the frequency of coalescence events (coalescence rate) with drop charge is plotted in Fig. 4.17 together with similar curves for R = 40μ and R = 16μ. The D.C. potential of 63 V was sufficient to prevent all coalescences in the case of 36μ and 16μ drops, and reduced the coalescence rate of the 40μ drops by a factor of five below the rate for uncharged drops.

Those photographs which did include a coalescence event were inspected carefully. In many cases the two colliding drops were observed to draw together just before they collided, as shown in Fig. 4.18a. This detectable attraction confirmed that the coalescing drops carried opposite charges. On occasions, however, drops with like charges were brought together by disturbances in the airstream. These were marked by a pair of streaks which

Fig. 4.17 INCREASE IN FREQUENCY OF COALESCENCE BETWEEN IDENTICAL DROPS CARRYING ELECTRIC CHARGES OF OPPOSITE SIGN.

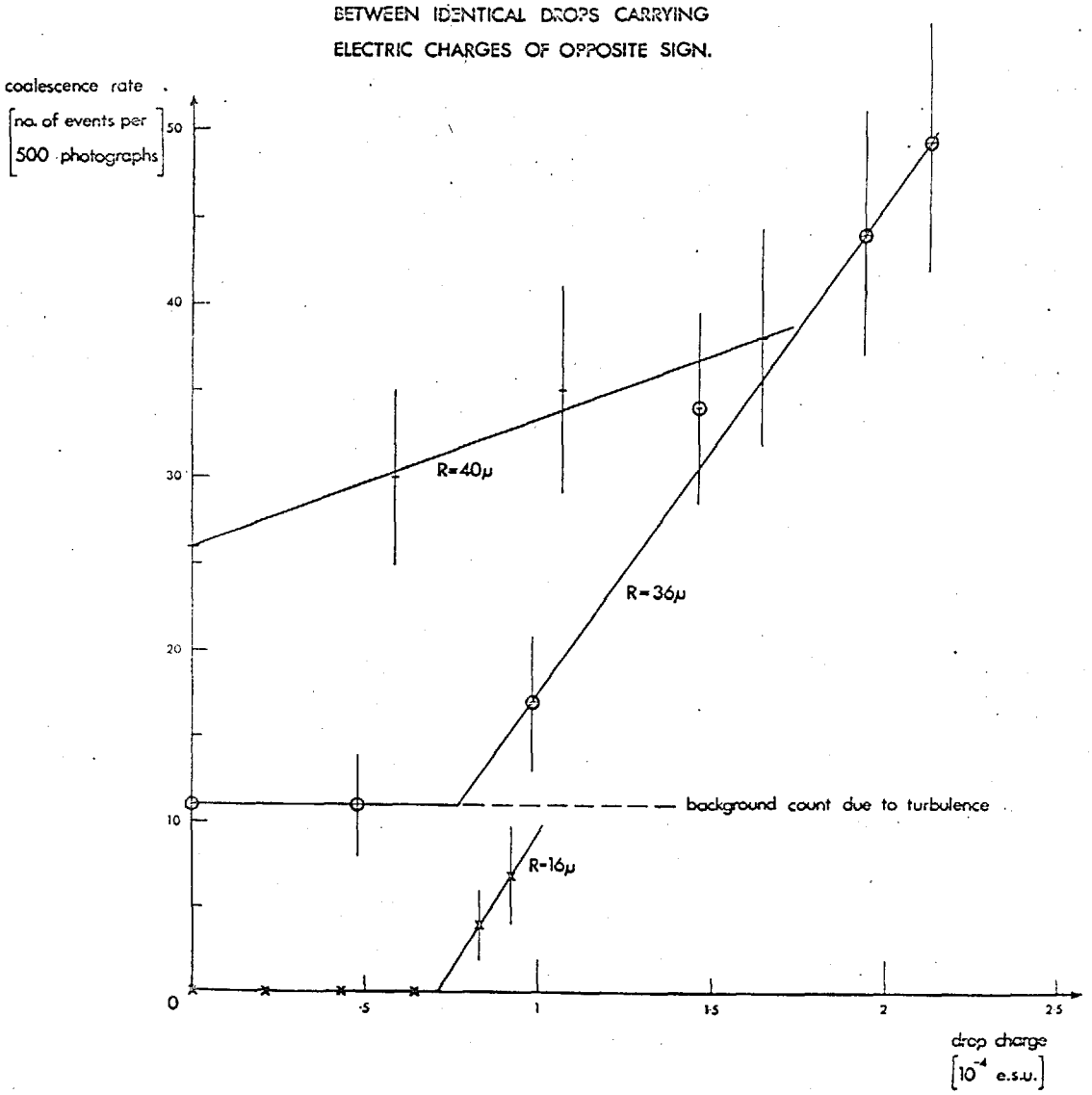

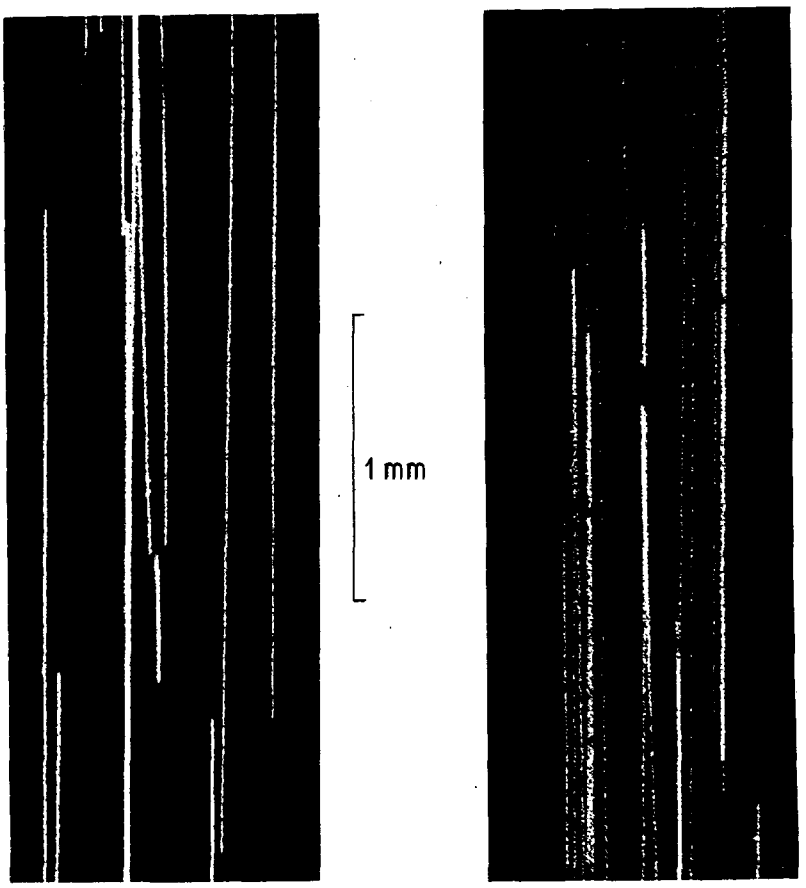

Fig. 4.18 The effect of electrification

(a) Two 36μ radius drops carrying opposite charges of 2×10^{-4} e.s.u. are attracted into coalescence.

(b) Two 16μ radius drops carrying like charges of 10^{-4} e.s.u. repel one another.

curved away from each other, corresponding to the drops repelling each other, a phenomenum which was much more frequently observed in the last sequence, when the drops all carried the same charge (i.e. when a D.C. potential was applied to the needle.) An example of repulsion is shown in Fig. 4.18b.

The magnitude of the charges carried by the drops was measured by applying to the needle a D.C. potential equal to the half wave amplitude of the charging signal. The stream was then collected and the charge measured with the vibrating reed electrometer as described above. The measured value for the 36μ radius drops was $q = \pm 0.3 \times 10^{-5}$ e.s.u./volt, for R = 40μ , $q + \pm 0.35 \times 10^{-5}$ and for R = 16μ $q = \pm 0.13 \times 10^{-5}$ e.s.u./volt.

Discussion

The slopes of the curves in Fig. 4.17 represent the effect of the electrical forces upon the collection efficiency for pairs of identical drops.

Uncharged drops of R = 16μ do not collide unless they carry equal and opposite charges in excess of $q_{min} = 7 \times 10^{-6}$ e.s.u. This charge provides sufficient electrical force to cause the collision of two 16μ radius

drops that approach one another slowly with an impact parameter, $b > 0$. Larger charges cause collision for progressively increasing values of b. Here, the experimental curve shows a linear relationship between the coalescence rate and the drop charge, i.e. between E and q.

For drops of $R = 36\mu$ the minimum charge required for collision, $q_{min} = 8 \times 10^{-6}$ e.s.u. This is the value of the charge at which the coalescence rate starts to rise about the initial constant value of 11 events per 500 photographs. This constant "background" coalescence rate is caused by turbulent accretion, which can occur between drops which originally had large separations in the stream, i.e. large values of b ($>> R$). The result of this turbulent accretion is to reduce, by a very small fraction, the number of drops in the stream available for coalescence by other causes.

Uncharged drops of radius 40μ collide with a finite collision efficiency by "wake capture". The smallest charge is capable of increasing this value of E and again the increase in coalescence rate and therefore collection efficiency, E, varies linearly with the drop charge, q.

The slope of the coalescence rate: drop charge curve for drops of $R = 65\mu$ obtained by Telford et al (1955) is shown in Fig. 2.15 for comparison. It is very similar to the

slope of the R = 40μ curve.

The constancy in the coalescence rate for R = 36μ before the threshold charge $q_{min} = 8 \times 10^{-5}$ e.s.u. is reached, supports earlier evidence (Section 4.4) that the coalescence efficiency, E, is unity for cloud drop collisions. Extrapolation of Jayaratne's investigation of water drops bouncing on a large water surface suggests that drop charges of considerably less than q_{min} are sufficient to ensure coalescence. If the coalescence efficiency were less than unity for uncharged 36μ drops a small charge, less than q_{min}, would have raised ϵ to unity with a corresponding rise in the turbulent accretion rate. This was not observed and it is therefore correct to assume that collision efficiency and collection efficiency are identical for cloud drop collisions.

In Table 4.2 are listed the observed values of coalescence rate with increasing drop charge along with the electrical forces calculated on the basis of Davis' (1962) theory. In the last column is listed the vertical electric field which, by polarizing neutral drops of the same size, would produce approximately the same forces. It is interesting to note that this is similar to the field at the surface of the charged drop in the absence of an external

Table 4.2

Forces on the charged drops and the vertical field which would give approximately the same forces.

(Computed from formulae by Davis 1962)

Experimental data				Calculated from Davis theory			
Radius (μ)	Charge 10^{-5} esu	Field at drop surface (Kv/cm)	Relative coalescence	Force between drops at separation of:- R (10^{-5} dynes)	0.1R (10^{-5} dynes)	0.01R (10^{-5} dynes)	Approximately equivalent vertical polarizing field (Kv/cm)
16	0	0	0	0	0	0	0
	2.1	2.4	0	2	14	70	2.4
	4.2	4.8	0	8	56	280	5.4
	6.3	7.2	0	18	126	630	7.8
	8.4	9.6	4	32	224	1120	10.2
	9.1	10.5	7	38	266	1330	11.5
36	0	0	11	0	0	0	0
	4.8	1.15	11	2	14	70	1.6
	9.6	2.3	17	8	56	280	2.4
	14.4	3.45	34	18	126	630	3.5
	19.2	4.6	44	32	224	1120	4.5
	21.0	5.0	49	38	266	1330	5.1
40	0	0	26	0	0	0	0
	5.6	1.05	30	2	14	70	1
	11.2	2.1	35	8	56	280	2.1
	16.8	3.15	39	18	126	630	3.1

field.

In a fair weather cumulus drops carry charges of the order of 10^{-8} e.s.u. and the large-scale electric field is of the order of 10 volts/cm. Clearly this degree of electrification will not materially affect the collection efficiencies of identical drops of $R = 40\mu$ and below that size there will be no charge at all as the threshold electrification is not reached. It may be argued that a similar situation exists at the other two cut-off values in the collection efficiency diagram, i.e. for $R = 20\mu$ and $r = 5\mu$ or for $R < 18\mu$ and $r/R = 0.5$. Calculations based on a combination of Davis' electrical forces and Hocking's hydrodynamic forces (these may be combined linearly in the Stokes region, $Re \ll 1$) may be used to estimate the effect of electrification at all three cut-off values (see Davis and Sartor, 1960). The experimental values given above for the variation of E with q will provide a test for the theory at $r/R = 1$.

CHAPTER 5

CONCLUDING DISCUSSION

The experiments described in the preceding chapters have been designed to test theoretical values of collision efficiency for cloud drops. The theoretical analyses of Hocking and of Shafrir and Neiburger have been considered the best available. They make three predictions, namely

(a) Drops smaller than 18μ radius cannot collect droplets of any smaller sizes.

Larger drops can only capture droplets that are

(b) larger than a certain minimum radius,

(c) smaller than a certain maximum radius.

The experimental results are in good agreement with prediction (a), but give slightly smaller values for the minimum droplet radius than predicted by Shafrir and Neiburger. There is no maximum droplet radius for collector drops of greater than 40μ radius.

The major meteorological significance of the experiments is contained in the confirmation of Hocking's cut-off for collector drops at 18μ radius and the confirmation that coalescence efficiency is unity for cloud drops. The former provides the fundamental limitation to the coalescence

mechanism; until drops of greater than 18μ radius are formed by condensation the mechanism cannot contribute to the development of precipitation. The latter conclusion confirms that cloud drops always coalesce after colliding.

The slight discrepancy between theoretical and experimental values for the minimum droplet size is less significant. While the cloud contains a large concentration of drops in this size range ($r \sim 4\mu$) the collection efficiency is small, so a large fraction of those encountered by a collector drop will not be captured. Furthermore, it is necessary for the collector drop to capture very many of these small droplets before it increases its radius appreciably.

The effect of wake capture is very strikingly presented on the collection efficiency diagram, but the concentration of drops greater than 40μ occurring in natural clouds is quite small, so they will encounter one another relatively infrequently. The role of development of a cloud will probably not be appreciably faster than that predicted on the basis of Shafrir and Neiburger's collision efficiency data, which do not account for wake capture.

The final question is whether electrification or turbulence, the two major perturbing influences in natural

clouds, might relax the limits on collector and droplet sizes discussed above. The experiments have shown that a high degree of electrification is required to increase significantly the collection efficiency of identical drops. It is not likely that the necessary electrification would occur in the early stages of cloud development when the coalescence mechanism is beginning to contribue. In well developed thunder clouds the large electric fields required to increase collection efficiency are present, but the precipitation process is already well advanced. However, some increase in the precipitation rate may be expected when large electric fields are present.

The effect of turbulence is less easy to study. A few preliminary experiments suggest that if the eddy field in clouds can cause the cloud drops to collide at an angle rather than one behind the other, then the collection efficiency may be raised considerably. This aspect of turbulent accretion has not been discussed before. Further experiments and computations will be needed to estimate the degree of turbulence necessary for a significant increase in the coalescence rate. This value must then be compared with estimates of turbulence in natural clouds. Unfortunately no measurements are available in the required range

of eddy sizes.

REFERENCES

Berg, T.G.O., Fernish, G.C. and Gaukler, T.A.	1963	J. Atmos. Sci. 20, 153.
Bergeron, T.	1935	Proc. 5th Assembly U.G.G.I., Lisbon 2, 156.
Bowen, E.G.	1950	Austr. J. Sci. Res. A, 3, 193.
Collison, W.E.	1935	"Inhalation therapy technique" Heineman, London.
Das, P.K.	1950	Ind. J. Met. Geophys. 1, 137, 90.
Davis, M.H.	1962	Rand. Corp. Rep. No. RM. 2607 -1 - PR.
Dessens, H.	1955	Bull. Inst. Puy de Dome. No. 3.
East, T.W.R. and Marshall, J.S.	1954	Q.J. Roy. Met. Soc., 80, 26.
Findeisen, W.	1932	Beitr. Geophys. 35, 295.
Fonda, A. and Hearne, H.	1957	Nat. Coal Board, Rep. No. 2068.

Goldstein	1929	Proc. Roy. Soc. A, 123, 225.
Gunn, K. and Hitschfeld, W.	1951	J. Met. 8, 7.
Gunn, R.	1952	J. Met. 9, 397.
Hocking, L.M.	1958	Ph.D. Thesis, London University.
Hocking, L.M.	1959	Q.J. Roy. Met. Soc., 85, 44.
Hocking, L.M.	1960	"Aerodynamic capture of particles", Pergamon.
Jayaratne, O.W.	1964	Ph.D. Thesis, University of London.
Jenson, V.G.	1959	Proc. Roy. Soc., A, 249, 346.
Kinzer, G.D. and Cobb, W.E.	1956	J. Met., 13, 295.
Lamb, H.	1879	"Hydrodynamics", Cambridge.
Langmuir, I. and Blodgett, K.B.	1945	U.S.A.A.F. Rep. No. RL -224.
Langmuir, I.	1948	J. Met. 5, 175.

Linblad, N.R. and Semonin, R.G.	1963	J. Geophys. Res., 68, 1051.
Ludlam, F.H.	1951	Q.J. Roy. Met. Soc., 77, 402.
Mason, B.J.	1957	"Physics of Clouds" Oxford.
Mason, B.J.	1960	Unpublished computations.
Mason, S.G. and Charles	1960	J. Colloid Sci. 15,
Mason, S.G. and Manley	1952	J. Colloid Sci., 7,
Mason, S.G. and Manley	1955	J. Colloid Sci. 10,
May, K.R.	1950	J. Sci. Instruments 27, 128.
Oseen, C.W.	1910	Arkiv. fur Matermatik, Astronomic och Fysik, Stokholm, 6, 29.
Pearcey, T. and Hill, G.W.	1957	Q.J. Roy. Met. Soc., 83, 77.
Pearcey, T. and McHugh	1955	Phil. Mag. 46, 787.
Picknett, R.G.	1960	"Aerodynamic capture of particles", Pergamon.

Plumlee, H.R., Linblad, N.R., and Semonin, R.G.	1964	Report to AMS Conf. on Cloud Phys., Chicago.
Proudman, I. and Pearson, J.R.A.	1957	J. Fluid Mech. 2, 237.
Rayleigh, Lord	1879	Proc. Roy. Soc. A, 28, 406.
Rayleigh, Lord	1896	"Theory of Sound", Dover.
Saffman, P.G. and Turner, J.S.	1956	J. Fluid Mech. 1, 17.
Sartor, J.D.	1954	J. Met. 11, 91.
Sartor, J.D.	1956	Q.J. Roy. Met. Soc. 82,
Sartor, J.D.	1957	Rand. Corp. Rep. No. 1824.
Sartor, J.D. and Davis, M.H.	1960	J. Geophys. Res. 65, 1953.
Schotland, R.M.	1957a	"Artificial stimulation of rain", Pergamon.
Schotland, R.M.	1957b	J. Meteor. 14, 381.

Schotland, R.M. and Kaplin, E.J.	1956	New York Univ., Dept. Met. Rep. AFRC-TH-55-867.
Shafrir, U.	1962	Ph.D. Thesis, U.C.L.A.
Shafrir, U.	1964	Unpublished report.
Shafrir, U. and Neiburger, M.	1963	J. Geophys. Res. 68, 4141.
Simpson, G.G.	1941	Q.J. Roy. Met. Soc., 67, 99.
Stokes	1851	Trans. Camb. Phil. Soc. 9, 8.
Taylor, G.I.	1952	Proc. Roy. Soc. A
Telford, J.W.	1955	J. Met. 12, 436.
Telford, J.W., Thorndike, N.S. and Bowen, E.G.	1955	Q.J. Roy. Met. Soc., 81, 241.
Telford, J.W. and Thorndike, N.S.	1956	Bull. Inst. Puy de Dome, No. 1, 1.
Telford, J.W. and Thorndike, N.S.	1961	J. Met. 18, 382.
Telford, J.W. and Cottis, R.E.	1964	J. Atmos. Sci. 21, 549.

Appendix A

"An improved vibrating capillary device for producing uniform water droplets of 15 to 500μm radius."

from

Journal of Scientific Instruments
May 1963.

Appendix B

"Experimental determination of collection efficiencies for small water droplets in air."

from

Quarterly Journal of the Royal Meteorological Society. October 1964.

(*From the* QUARTERLY JOURNAL OF THE ROYAL METEOROLOGICAL SOCIETY, Vol. 90, No. 386, October 1964)

Experimental determination of collection efficiencies for small water droplets in air

By J. D. WOODS and B. J. MASON

Imperial College, London

551.578 11 : 551.574.12

Experimental determination of collection efficiencies for small water droplets in air

By J. D. WOODS and B. J. MASON
Imperial College, London

(Manuscript received 21 April 1964)

SUMMARY

This paper describes measurements of collection efficiencies for gravitational collisions between water drops of radius $R = 30$ to 55 μ and saline droplets of radius $r = 1$ to 12 μ. The results agree quite well with those obtained earlier by Picknett for drops of $R = 30$, 40 μ and also with the collision efficiencies computed by Hocking, Mason and Shafrir and Neiburger except that, for values of $r/R < 0{\cdot}1$, the experimental values are consistently higher than the calculated values and fail to show the sharp cut-off predicted by theory. The experiments support Hocking's prediction that drops of $R \leqslant 18$ μ will fail to collect droplets of smaller size.

INTRODUCTION

This paper describes the experimental determination of collection efficiencies for water drops of radius $R = 30$-55 μ coalescing with droplets of radius $r = 1$-12 μ falling in air. Collisions between droplets of different radii are caused by their differential rates of fall under gravity and precautions are taken to eliminate other effects such as turbulence and electrical forces. Since the droplet size and concentration in the apparatus is of the same order as that occurring in natural clouds, the results should be applicable to problems in cloud physics and also stand comparison with computed values of collision efficiencies obtained by Langmuir (1948), Pearcey and Hill (1957), Hocking (1959), Mason (1960), Shafrir and Neiburger (1963).

Of the theoretical values, Hocking's are the most accurate in that he determined the forces on the spheres from the solution of the Stokes equations for two moving spheres making full allowance for their mutual influence, although the Stokes approximation limits the size of the drops to 30 μ radius. Also, his computations are not very reliable for values of $r/R < 0{\cdot}2$. Mason (1960) interpolated between Hocking's values for drops of $R \leqslant 30$ μ and those of Langmuir for drops of $R \leqslant 200$ μ and values of $r/R \leqslant 0{\cdot}5$. Shafrir and Neiburger (1963) obtained collision efficiencies for water drops of radius up to 136 μ (Reynolds number $\simeq 19$) by an approximate but more reliable method than used before for drops of this size. They used an accurate numerical solution of the equations of fluid motion around one sphere, including all the non-linear terms, and evaluated the approximate drag force on the other sphere in a relatively simple form. This procedure led to values of collision efficiency that were not very different from the more accurate values of Hocking for drops of $R \leqslant 30$ μ, and not very different from Mason's values for larger drops (see Fig. 5).

Turning to experimental data on collision efficiencies for drops of $R < 100$ μ, experiments by Schotland and Kaplin (1956) and by Sartor (1954), in which aerial collisions were modelled by solid spheres falling in a liquid, failed to provide quantitative confirmation of calculated values, probably because it was impossible to model simultaneously both the Reynolds number of the drops and the ratio of the densities of the sphere and the surrounding fluid. Kinzer and Cobb (1958) supported small water drops

by a vertical airstream in a narrow tube of 8 mm diameter and measured the growth rate of an individual drop by the changes in the air velocity required to keep it stationary in the tube. Collisions between droplets were caused not only by gravitational settling but also by turbulence, and the drop growth was also affected by evaporation-condensation processes. Because of these factors, and undesirable velocity gradients and wall effects in the tube, these results cannot be regarded as reliable. Telford and Thorndike (1961) allowed their drops to fall down a vertical tunnel and observed the close approach of pairs of nearly equal-sized drops by photographing their trajectories. A few collisions and coalescences were observed between drops of diameter 45 μ, but none was observed between drops of $d = 30\text{-}35\ \mu$ although, in this case, coalescence could be induced by electric fields of 1,000-3,000 V/cm. These results were interpreted by their authors as being in accord with the theoretical calculations of Hocking but contrary to those of Pearcey and Hill (1957). The first really satisfactory experiment on drops of dissimilar size was carried out by Picknett (1960) who obtained good agreement with the calculated values of collision efficiency for collector drops of $R = 30\ \mu$ and $40\ \mu$ colliding with droplets of $r \leqslant 9\ \mu$. The present experiment, employing improved techniques, confirms and extends the results obtained by Picknett.

2. Principle of the experiment

Several thousands of identical water drops, produced by a vibrating hypodermic needle, are allowed to fall through a one-metre depth of cloud composed of droplets of salt solution maintained at their equilibrium radii in an ambient humidity of 84 per cent. A small fraction of the water drops collide with and capture a salt droplet on their way through the cloud, and arrive at the bottom of a 3-metre settling column with a mass of salt that indicates the size of the captured cloud droplet. The number concentration of salt droplets in the cloud is sufficiently small that only a negligible fraction of the collectors collide with more than one salt droplet. The proportion of collector drops ultimately containing salt is, of course, the proportion that has undergone coalescence. Examination of a large number of collector drops therefore determines the fraction of these coalescing with each size of salt droplet. It will be shown in Section 3 that this information, together with the characteristics of the salt-droplet cloud, is sufficient to evaluate collection efficiencies.

3. Theory of the experimental method

We consider a drop of radius R falling through a tranquil cloud of smaller droplets of radius r. Those droplets whose centres lie inside a vertical cylinder of radius $(R + r)$ concentric with the collector drop are considered to lie in its fall path. Only a fraction of these will be captured by the collector drop, and this fraction is defined as the collection efficiency $E(R, r)$*.

In our experiment, the collector drop falls through a cloud of smaller droplets of a range of sizes. On the assumption that these droplets are distributed at random horizontally, Poisson's Law may be applied to give the probability of finding a given number of droplets in a vertical column of cross-sectional area, A, passing right through the cloud. For droplets in the size range r to $r + dr$, where $n(r)\,dr$ is the average number in this range in a vertical column of unit cross-sectional area, we have :

p_0, the probability of finding no droplets is $\exp[-An(r)\,dr]$

p_1, the probability of finding 1 droplet is $[An(r)\,dr]\exp[-An(r)\,dr]$

p_2, the probability of finding 2 droplets is $\dfrac{[An(r)\,dr]^2\exp[-An(r)\,dr]}{2!}$ etc.

With $A = \pi(R + r)^2 E(R, r)$, p_0, p_1, p_2, ... become the probabilities that a collector drop R will collide with 0, 1, 2, ... droplets in this size range.

* We follow Picknett in using this definition of E which has the advantage that it has a maximum possible value of unity. It differs from that of some other workers by the factor $R^2/(R + r)^2$.

As described in the previous section, the experiment measures the fraction $F(r)\,dr$ of a large number of identical drops, R, which suffer coalescence with one or more salt droplets in the size range r to $r + dr$. This can now be written as :

$$F(r)\,dr = (1 - p_0) = 1 - \exp[-An(r)\,dr] = 1 - \exp[-\pi(R + r)^2 E(R, r)\, n(r)\, dr] \quad (1)$$

or

$$E(R, r) = -\frac{\ln[1 - F(r)\,dr]}{\pi(R + r)^2 n(r)\,dr} \quad . \quad . \quad . \quad (2)$$

Eq. (2) expresses $E(R, r)$ in terms of the experimentally-determined parameters $F(r)\,dr$, $n(r)\,dr$, R and r.

To fulfil the requirement that the number of multiple coalescences shall be negligible it is necessary to make $p_1 \gg p_2, p_3 \ldots$. etc.

i.e.,

$$\int_{r=1\mu}^{r=12\mu} \pi(R + r)^2 E(R, r)\, n(r)\, dr \ll 1 \quad . \quad . \quad . \quad (3)$$

4. Experimental procedure

The experimental arrangement is shown diagrammatically in Fig. 1. The glass tube, A, 1 m long and 8 cm in diameter, was filled with a cloud of droplets produced by atomizing sodium chloride solution, 270 g/l, with a modified Collison spray. The cloud droplets, whose size distribution extended to $r = 15\,\mu$ with a peak at about $r = 1{\cdot}5\,\mu$, rapidly attained their equilibrium sizes in the ambient humidity of 84 per cent maintained by flushing the inner walls of the glass tubes with the salt solution. The collector drops were

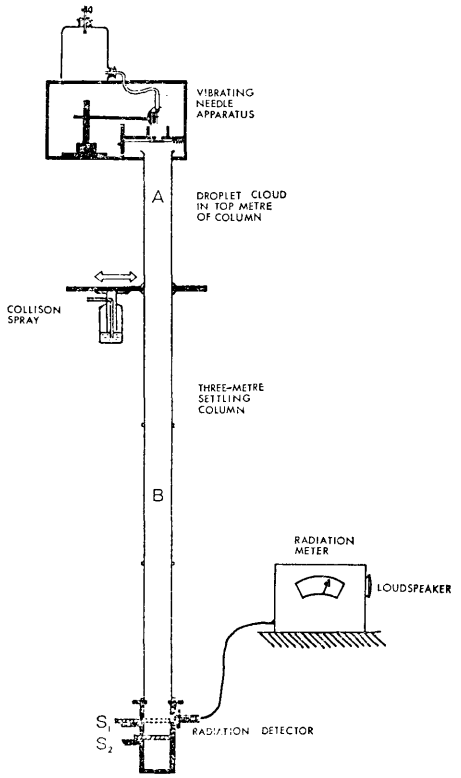

Figure 1. The experimental arrangement of apparatus used.

produced at the rate of about 800 per second by the vibrating-capillary device described by Mason, Jayaratne and Woods (1963) and which was located in a draught-proof box at the top of the cloud column. A droplet stream, composed of uniform drops of the required size, was directed through a $\frac{1}{4}$-inch hole in the floor of this box and was admitted to the cloud column by a spring-loaded shutter for a known period, usually 10 seconds. The drops consisted of a radioactive orthophosphate solution, concentrations of up to 1 mc ml^{-1} being used. The radioactivity served to discharge the drops and allowed their passage down the column to be traced. After passing through the cloud, the drops fell through a 3-metre settling column of air maintained at 84 per cent humidity, and finally landed on a 2 in. $\times$ 2 in. glass slide coated with a thin, smooth layer of Apiezon M grease.

Immediately before each experiment, the size of the drops leaving the needle was determined from measurements of the craters they produced in the magnesium oxide slide. Evaporation of the drops was measured in subsidiary experiments; drops of radius 30 μ evaporated to 29 μ during the 3-metre fall but those of $R > 40$ μ suffered no detectable loss.

The operational procedure was as follows : the inner walls of the glass tubes were washed with salt solution, and then, at the bottom of the sedimentation column B, a glass slide coated with magnesium oxide was placed in the upper sampling position S1 (see Fig. 1) and a greased slide in the lower position, S2. The Collison spray was swung into position beneath the upper tube and operated for 60 seconds. The upper tube was then sealed for 60 seconds to allow the turbulence to die down and the droplets to attain their equilibrium size. Having adjusted the vibrating needle to give a stream of drops of the required size, the settling column was then swung into position under the cloud column, the magnesium-oxide slide removed, and the collector drops injected into the cloud for 10 seconds. A radiation monitor, placed at the level of the greased sampling slide, was closely watched for a rise in the count that heralded the arrival of the collector drops. Precise timing was necessary to prevent contamination of the slide by the cloud droplets, which fell faster in bulk than the terminal velocity of individual drops. 10 seconds later, the magnesium-oxide slide was reinserted to cut off the cloud from the greased slide which was then removed to a humidity chamber for examination under the microscope. After a further 30 seconds, the magnesium-oxide slide was removed and examined, the absence of drop impressions serving as a check that all the collector drops had arrived at the grease slide before it was covered. A second grease slide was then inserted in place of the oxide slide, and left there overnight to collect all of the slowly-falling cloud droplets. All experiments were carried out at room temperature which was approximately 20°C.

The grease slides were transferred to a small humidity chamber mounted on the stage of a binocular microscope. This box contained a small dish of saturated potassium bromide solution and, by vigorous stirring of the air with a small electrically-driven fan, the relative humidity over the surface of the slide was maintained at 84 per cent. The collector drops evaporated before the slide was examined but they left behind salt crystals that grew in the chamber to equilibrium-sized hemispheres in a few minutes. The diameter of each hemisphere was measured with a Vernier eyepiece, the hemisphere diameter being $2^{\frac{1}{3}}$ times the diameter of the original cloud droplet that had coalesced with the collector drop. Fig. 2 shows the size distribution of the droplets captured by collector drops of three different sizes. This provides the data for evaluating the parameter $F(r)\,dr$ in Eq. (2), because if $n'(r)\,dr$ is the number of the captured droplets of radius between r and $r + dr$.

$$F(r)\,dr = \frac{n'(r)\,dr}{N},$$

where N is the total number of collector drops. Tests showed that the saline cloud droplets reached the grease slide only as the result of coalescence. When dye was added to the collector drops it was established that each salt particle on the slide was surrounded by a ring of dye left by the evaporated drop.

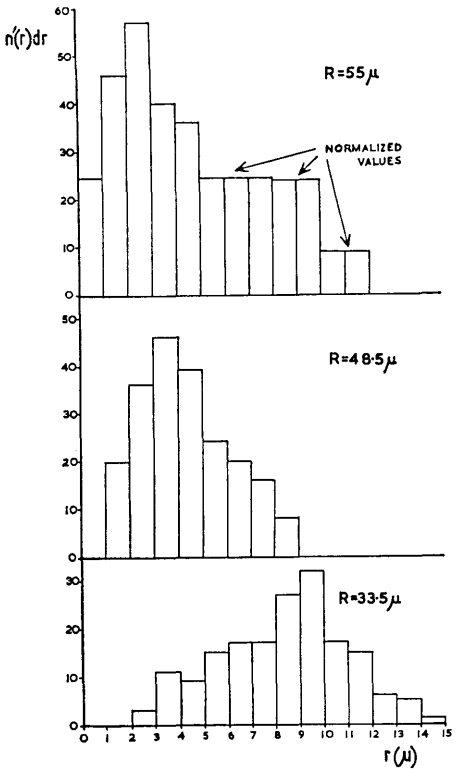

Figure 2. Size distributions of cloud droplets captured by drops of three different sizes.

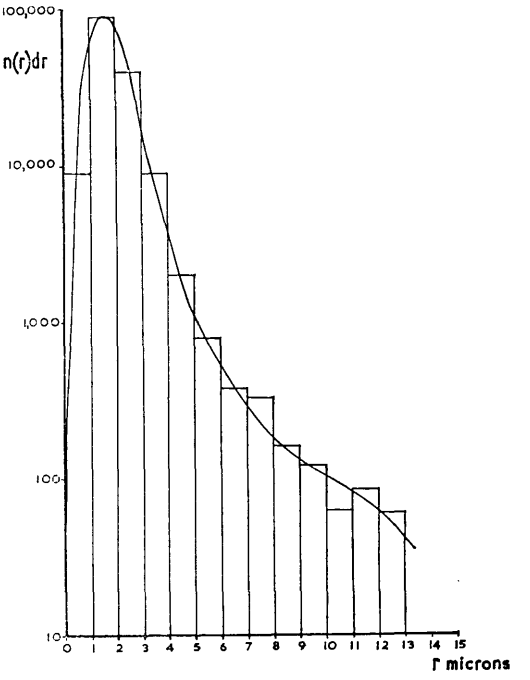

Figure 3. A typical distribution of cloud-droplet sizes.

The cloud droplets, collected on the second grease slide, were analysed in the same manner but, having established that the deposition was uniform, instead of evaluating the whole slide, a sufficient number of random samples were made to ensure representative results. A separate analysis of the cloud droplet spectrum was carried out for each experimental run. A typical spectrum of cloud-droplet sizes is shown in Fig. 3. From such a distribution, one may compute the number of droplets in a given size range falling on unit area of the slide and hence evaluate the term $n(r)\,dr$ in Eq. (2). In all the experiments the value of $n(r)\,dr$ was such that Eq. (3) was satisfied and so multiple collisions were rare.

Evaluation of the collection efficiency, $E(R, r)$, involves four measured quantities. Random errors arise in determining the size distributions of the cloud droplets and of the captured droplets because of local random fluctuations in the constitution of the 5 litres of cloud. The standard deviation in the value of $n(r)\,dr$ is estimated to be about 2 per cent for droplets of $r = 2\,\mu$ and 10 per cent for droplets of $r = 12\,\mu$. The standard deviation in $n'(r)\,dr$ for the captured droplets (Fig. 2) is estimated at 15 per cent at the centre of the distribution and 25 per cent at the extremes. The combined effect of these two errors on the values of collection efficiency is indicated by the lines drawn through the individual points of Fig. 4. The curves represent the lines of best fit through these points but further uncertainty in the positions of these curves arises from errors in determining the radius, R, and the number, N of the collector drops.

The radii of the collector drops were determined from the diameters of the craters produced in the magnesium-oxide film, the error in an individual reading being estimated at $\pm 1\,\mu$. The number of collector drops, as estimated from the frequency of drop production (determined stroboscopically) and the exposure time of the shutter, had

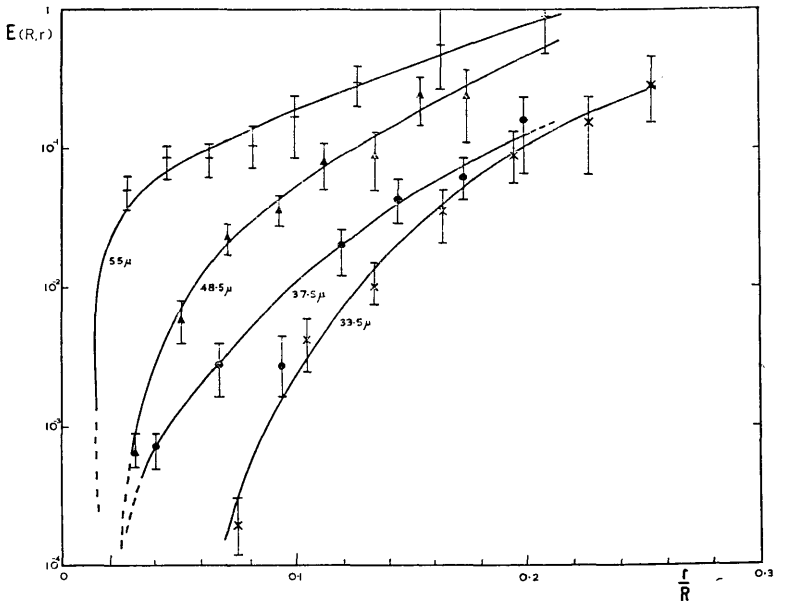

Figure 4. Experimental values of collection efficiency, E, plotted as a function of r/R, for collection drops of radius R between 33·5 and 55 μ.

—, $R = 55\ \mu$; ▲, $R = 48{\cdot}5\ \mu$; ●, $R = 37{\cdot}5\ \mu$; ×, $R = 33{\cdot}5\ \mu$.

an estimated error of $\pm$ 5 per cent. An independent check with a magnesium-oxide slide placed at the bottom of the column showed that no appreciable loss of drops occurred during their journey in the tube.

The number of coalescences might be effectively reduced if successive drops sweep through the same volume of cloud but, except for a small area in the centre of the slide, the drops were always more than four diameters apart. The maximum systematic error introduced in this way is estimated at 3 per cent.

It is difficult to arrive at a reliable estimate for the effect of these last three types of error on the derived values of collection efficiency but it would imply the same percentage error in the E value of each point on a given curve in Fig. 4 and this is estimated not to exceed 10 per cent.

5. Comparison of experimental and theoretical results

In Fig. 5 are plotted the results of the present experiments together with the earlier results of Picknett and the values of collision efficiency computed theoretically by various authors. Selected values of collection efficiencies taken from the smoothed curves are given in Table 1.

In general, and considering the experimental errors involved, our results agree quite well with those of Picknett for drops of $R = 30$-$40\ \mu$, and fit in fairly well with the theoretical values of Hocking, of Mason, and of Shafrir and Neiburger, except that for values of $r/R < 0{\cdot}1$, the experimental values of E are consistently higher than the calculated values and fail to show the sharp cut-off predicted by theory. This discrepancy at low values of r/R, which was also observed by Picknett, is unlikely to be due to experimental error because the technique is most reliable for small droplets of $r = 1$-$3\ \mu$. There is more reason for suspecting the theory because, as pointed out in the Introduction, Hocking's values are unreliable for values of $r/R < 0{\cdot}2$, and a more accurate evaluation of the drag forces on a pair of dissimilar drops at small separations would probably lead to higher values of the collision efficiency.

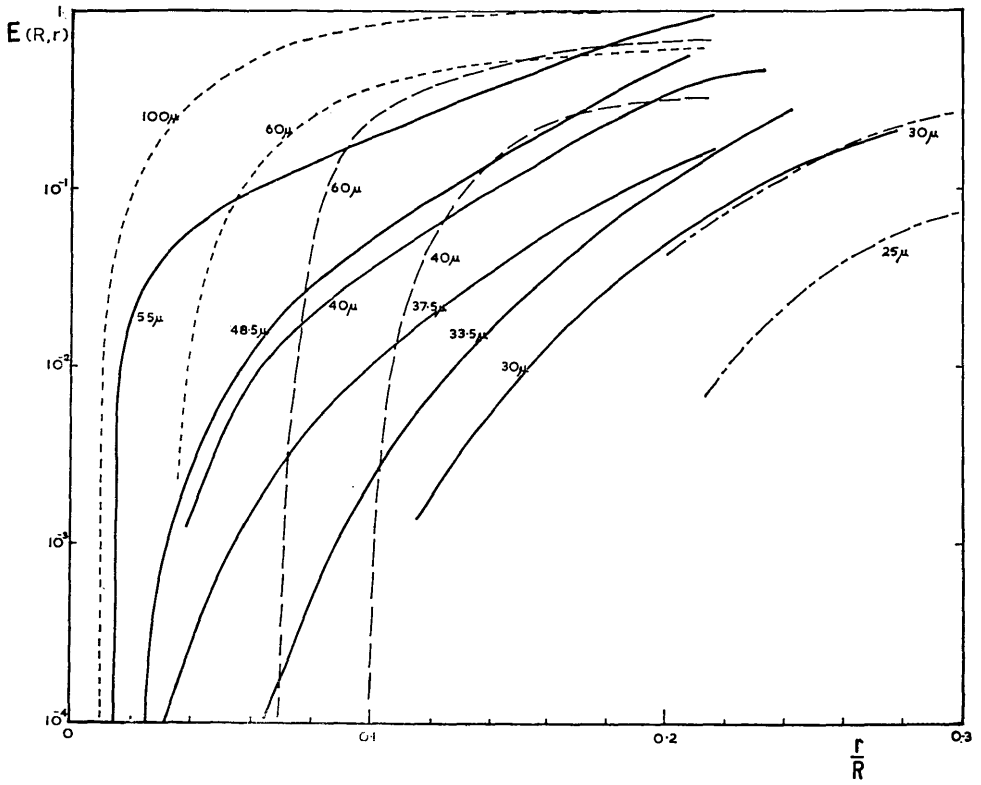

Figure 5. Comparison of experimental collection efficiencies and computed values of collision efficiency.

Experimental : ———— Picknett $R = 30\ \mu$, $40\ \mu$
Woods and Mason $R = 33{\cdot}5$, $37{\cdot}5$, $48{\cdot}5$ and $55\ \mu$

Computed : — - — - Hocking $R = 25\ \mu$, $30\ \mu$
— — — Shafrir and Neiburger $R = 40\ \mu$, $60\ \mu$
- - - - - Mason $R = 60\ \mu$, $100\ \mu$

TABLE 1. SMOOTHED EXPERIMENTAL VALUES OF COLLECTION EFFICIENCY

r/R	$R = 33{\cdot}5$	37·5	48·5	55 μ
0·02	—	—	—	0·02
0·04	—	0·0003	0·003	0·07
0·06	—	0·001	0·01	0·09
0·08	0·001	0·005	0·03	0·13
0·10	0·003	0·01	0·05	0·18
0·12	0·008	0·02	0·09	0·25
0·14	0·02	0·04	0·14	0·34
0·16	0·03	0·06	0·21	0·45
0·18	0·06	0·08	0·34	0·60
0·20	0·10	0·12	0·48	0·70

— signifies $E < 10^{-4}$

It is possible, however, that another mechanism, perhaps residual small-scale turbulence in the air column, was responsible for the enhanced collection of the very small droplets. It is unlikely that electrical forces were responsible. The collector drops carried only a few hundreds, and the cloud droplets only a few tens, of elementary charges, so the electrical forces must have been negligible compared with the hydrodynamic forces. From the practical point of view, the discrepancy at low values of r/R may not be very important because, in any case, the collection efficiencies are very low (mostly $< 0{\cdot}05$) in this regime. On the other hand, it seems possible that the growth rate of 30 μ drops by coalescence could be increased appreciably in a moderately turbulent atmosphere, and this could be very important in accelerating the early stages of precipitation development in clouds.

The fairly good agreement between the experimentally-determined *collection* efficiencies and the computed *collision* efficiencies, at least for values of $r/R > 0{\cdot}1$, suggests that the *coalescence* efficiency for drops of $R < 60$ μ is practically unity. Certainly our experiments provide no evidence that such small drops separate after colliding at their terminal velocities.

Appendix

Experimental test of whether $E = 0$ for drops of $R < 18$ μ

Hocking (1959) predicted that drops of radii less than 18 μ cannot collide in still air with smaller drops of any size. This cut-off has important consequences in cloud physics because it implies that cloud drops must attain a radius of at least 18 μ by condensation before they can grow by the accretion of smaller drops.

In an attempt to test this prediction, we modified our experiment to investigate the collection efficiencies of drops of radius about 18 μ.

Since drops of radius 20 μ evaporated completely while falling through the 4-metre column maintained at 84 per cent relative humidity, it was clearly necessary to use much higher humidities of about 98 per cent. But, while at 84 per cent humidity the equilibrium radius of salt droplets varies very little with small variations in humidity, much larger changes are produced at 98 per cent and the cloud droplet spectrum is much less stable. We therefore had to accept the fact that the size distribution of the cloud droplets would not be well defined. Furthermore, it is difficult to maintain and measure such a high humidity accurately. In practice, the inner walls of the column were washed with tap water at room temperature and this raised the humidity of the air to near 98 per cent.

The cloud droplets were produced by atomizing an aqueous solution containing now only 50 g/l of sodium chloride. Having grown to equilibrium size, the largest droplets attained radii of about 14 μ. Because the cloud droplet spectrum could not be accurately maintained and measured, no attempt was made to obtain complete curves of E *vs* r/R for the small collector drops. Instead the experiment was designed only to detect coalescences between drops of $R \simeq 18$ μ and droplets of $r = 10\text{-}14$ μ that appeared on the sampling slide in concentrations of about 300/cm^2.

The results of five experiments are summarized in Table 2. In four of these, no salt droplets were collected, which implies that the actual collection efficiencies were very probably lower than those corresponding to the capture of a single droplet, i.e., smaller than the values listed in the fourth column of Table 2. For comparison, the fifth column contains the values of E computed by Hocking. In these four cases, the experiment appears to demonstrate that drops of $R < 19$ μ do have very small collection efficiencies as predicted by Hocking. In the fifth experiment, 7 salt droplets with $r = 10\text{-}14$ μ were collected on the slide but these may well have been deposited directly from the cloud because only 10 sec separates the arrival of the last collector drops and the first cloud droplets.

TABLE 2. SUMMARIZED RESULTS OF EXPERIMENTS

Collector radius, R (μ)	No. of collectors	Fraction of collectors that captured a droplet	Collection efficiency corresponding to a single capture	Theoretical collision efficiency (Hocking)
17·0	8,000	0	0·03	0·0
17·5	8,000	0	0·03	0·0
18·5	6,000	0	0·07	0·015
19·0	15,000	0·0045	0·08*	0·03
19·5	7,000	0	0·02	0·04

* In this case, with $R = 19\ \mu$, 7 droplets were captured, and the corresponding collection efficiency is 0·08.

A further experiment, with drops of $R = 30\ \mu$, produced the range of collected droplets expected on Hocking's calculations, but again these were not analysed in detail to give a curve of collection efficiency because of the errors inherent in using such a high relative humidity.

REFERENCES

Hocking, L. M. 1959 *Quart. J. R. Met. Soc.*, **85**, p. 44.
Kinzer, G. D. and Cobb, W. E. 1958 *J. Met.*, **15**, p. 138.
Langmuir, I. 1948 *Ibid.*, **5**, p. 175.
Mason, B. J. 1960 Unpublished.
Mason, B. J., Jayaratne, O. W. and Woods, J. D. 1963 *J. Sci. Instr.*, **40**, p. 247
Pearcey, T. and Hill, G. W. 1957 *Quart. J. R. Met. Soc.*, **83**, p. 77.
Picknett, R. G. 1960 *Aerodynamic capture of particles*, Pergamon Press (London), p. 160.
Sartor, D. 1954 *J. Met.*, **11**, p. 91.
Schotland, R. M. and Kaplin, E. J. 1956 *Report* AFCRC-TH-55-867, New York Univ.
Shafrir, U. and Neiburger, M. 1963 *J. Geophys. Res.*, **68**, p. 4141.
Telford, J. W. and Thorndike, S. C. 1961 *J. Met.*, **18**, p. 382.

(*From the* QUARTERLY JOURNAL OF THE ROYAL METEOROLOGICAL SOCIETY, Vol. 91, No. 387, January 1965)

The wake capture of water drops in air

By J. D. WOODS and B. J. MASON

Imperial College, London

551.501.45 : 551.574.12 : 532.6 : 778.534.8

The wake capture of water drops in air

By J. D. WOODS and B. J. MASON
Imperial College, London

(Manuscript received 26 June 1964)

SUMMARY

A technique is described for evaluating directly from a single streak photograph the impact parameter for a collision between two falling water drops of similar size. Collision results from one member of a pair of drops being accelerated in the wake of the other. An analysis of many such photographs allows the collection efficiency to be determined. No coalescences were observed between droplets of radius $R \leqslant 35\ \mu$. Droplets of $40\ \mu < R < 100\ \mu$ had well-developed wakes, and coalescences occurred relatively frequently, the collection efficiencies being close to unity. No evidence is found for the much larger values of collection efficiency reported by other workers. Collisions between droplets of this size appear always to be followed by coalescence.

1. INTRODUCTION

In a recent paper (Woods and Mason 1964), a description is given of the experimental determination of collection efficiencies for small, unequal water droplets of up to 60 μ radius, colliding in air. Droplets of $R < 35\ \mu$ (Reynolds number $Re < 1$) do not develop wakes and the relative trajectory of two dissimilar droplets is largely determined by the flow conditions at the leading surface of the larger drop. The flow around drops with $Re > 1$ becomes markedly asymmetrical and a wake develops in the rear. The possibility now arises that the wake may influence a larger overtaking drop and effect its capture. This may occur even with two droplets of the same size if they approach each other within a few drop diameters.

This problem was investigated theoretically by Pearcey and Hill (1957) who used Oseen's approximate solution of the hydrodynamic equations to compute the velocity field around a water droplet falling at terminal velocity. This solution, which possesses the correct asymptotic form at large distances from the sphere but fails close to it, predicts a parabolic wake for spheres of $Re > 1$ in which the velocities increase rapidly with increasing Re, the width of the wake being proportional to $Re^{-\frac{1}{2}}$. In estimating the relative motions of two drops, Pearcey and Hill assumed that their individual flow patterns could be superposed linearly to give the total flow. Collisions between droplets of $Re > 1$ and of nearly equal size could then conceivably occur in two different ways, both depending upon the flows within the wakes. Collision could occur *directly*, the larger droplet (drop) falling and colliding with the smaller (droplet) as it becomes accelerated in the wake of the latter. Alternatively, the drop may pass the droplet so closely as to engage the latter within its wake and eventually make an *indirect* collision with it. In considering direct collisions, Pearcey and Hill deduce that the forces of attraction between the two drops increase rapidly with the radius, r, of the droplet. Moreover, if drop and droplet are of equal or nearly equal size, their velocity of approach is small, the drop spends a long time in the wake of the droplet, its trajectory is strongly affected and consequently its collision cross-section may be many times the geometrical cross-section.

This deduction appeared to be confirmed by the experimental observations of Telford, Thorndike and Bowen (1955), who took streak photographs of groups of interacting, nearly equal-sized drops of radius about 75 μ while they moved slowly upwards in a vertical wind tunnel. Coalescences produced drops of double mass which fell downwards. The number concentration, n, of original drops moving upwards and that, N, of the coalesced drops moving downwards were determined by photographing a known volume of the upward-moving air stream. The relative velocities of pairs of

neighbouring but not interacting drops were measured from streak photographs and plotted in a histogram. The average relative velocity, Δv, for approaching pairs was then calculated, separating pairs being ignored. This average value of Δv, together with values of N and n, were then substituted in the equation

$$NV = \tfrac{1}{2}n^2 E' \pi R^2 \Delta v H, \quad . \quad . \quad . \quad . \quad (1)$$

where V is the settling velocity of the coalesced drops, R the radius of the original drops, and H the height of the settling column, to give a computed value of collection efficiency $E' = 12{\cdot}6 \pm 3{\cdot}4$.* This procedure appears sound provided that the values of Δv given by Telford *et al.* in their histogram were measured when the neighbouring drops were far apart and represented differences in terminal velocity between drops of slightly different sizes, and provided also that the coalescence events were produced entirely by gravitational settling.

In a later experiment, Telford and Thorndike (1961) studied collisions between freely-falling drops of $d = 20$-$60\ \mu$. Coalescence was occasionally observed to occur between nearly equal drops of diameter about $45\ \mu$ but no values were given for the collection efficiency. When smaller drops, of diameter 30-35 μ, came close together, they fell with greatly increased velocity but later separated and coalescence was never observed.

In this paper, we shall describe how the impact parameters, and hence the collection efficiencies, for pairs of equal or nearly equal-sized drops may be measured *directly* from streak photographs.

2. Experimental technique

A stream of identical water drops spaced about ten radii apart is allowed to fall vertically at terminal velocity in a closed transparent chamber in which draughts are reduced to a minimum. A small section of the stream is illuminated from behind by a parallel beam from a tungsten lamp and also by a focused beam from a stroboscopic point source. On still photographs of this illuminated section the trajectories of the drops appear as vertical streaks produced by the highlights of the falling drops, while the highlights produced by the stroboscopic flash appear as a series of dots that provide time markers. Coalescence between two neighbouring drops is marked by the sudden disappearance of their highlight streaks and the appearance instead of a single oscillatory streak in which the oscillations die out after several milliseconds and leave a single, continuous streak. The time markers allow the velocities and accelerations of the drops to be determined, and the impact parameters can be deduced from measurements on the streaks of a single photograph. The frequency of oscillation of the streak provides quite an accurate measurement of the size of the drop produced by the coalescence of two smaller ones.

The general layout of the apparatus is shown in Fig. 1. The droplet stream was produced by the vibrating-needle device described by Mason, Jayaratne and Woods (1963). This was mounted on a universal head that permitted translational movements in three mutually perpendicular directions and rotation about a vertical axis. The drops were ejected horizontally from a position about 10 cm above and to one side of the illuminated area; by the time they passed through the optic axis they had lost their initial horizontal momentum and were falling downwards at their terminal velocity. The drop size was most conveniently varied by varying the amplitude of the oscillation of the needle, the diameter of the drops being determined by allowing them to fall on to a slide coated either with oil or magnesium oxide. The whole assembly was placed in a draught-free perspex box lined with earthed brass foil to eliminate stray electric fields.

* Telford *et al.* define collection efficiency E' as the fraction of droplets, of radius r, lying in a cylinder having the same radius, R, as the collector drop, that are actually captured by it. We shall define it in terms of the fraction of droplets removed from a cylinder of radius $(R + r)$ to give a parameter E such that $E = E'(R^2/(R + r)^2)$ and Telford's value of $E' = 12{\cdot}6$ would correspond to $E = 3{\cdot}15$.

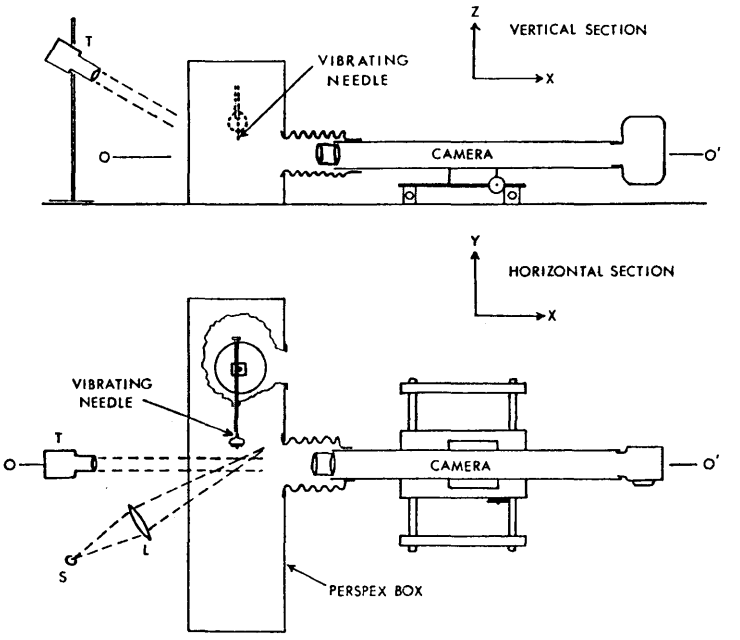

Figure 1. The experimental arrangement; vertical and horizontal sections through the optic axis 00′.

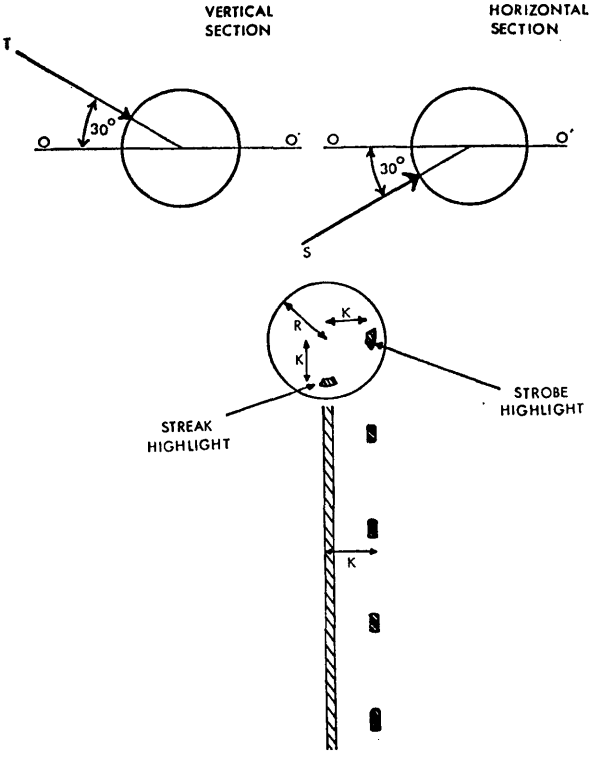

Figure 2. The illumination of the falling drops.

A section of the droplet stream was illuminated by two light sources. A parallel beam from the tungsten lamp, T, was directed downwards at an angle of 30° to the horizontal and in the vertical plane through the optic axis, 00′. This produced an intense highlight below the centre of each water drop as shown in Fig. 2. Light from the stroboscopic lamp, S, producing 1,000 flashes/sec, each of duration $\frac{1}{2}$ μsec, was focused on to the drops by the lens, L. This interrupted beam was directed along the horizontal plane through the optic axis and at 30° to it, and so produced a highlight that was level with the centre of the drop. This arrangement gave two highlights equally displaced from the centre of the drop; the vertically-displaced highlight from the tungsten lamp produced a continuous vertical streak on the photograph, while the horizontal one from the stroboscopic lamp produced a line of dots parallel to, but horizontally displaced from, the continuous streak – (see Fig. 2). The drops were photographed through an f/4·5 Dallmeyer lens of 8 in. focal length, placed at a distance of 120 cm from a 16 mm Bolex ciné camera with the lens removed, to give an overall magnification of X6 on the film. With this arrangement it was possible to take several hundreds of photographs in rapid succession with exposure times of about 15 m sec. With the lens set at f/16, the depth of focus was sufficient to accommodate a lateral spread of up to 2 mm in the droplet stream.

3. Analysis of the photographs

We shall show that, provided the drop sizes are known, a single streak photograph such as Fig. 4 (Plate I) provides information sufficient to compute the impact parameter of a collision between two drops and also the actual motion of the drops in space during a period of about 15 m sec, (~ 10 drop radii) prior to the collision.

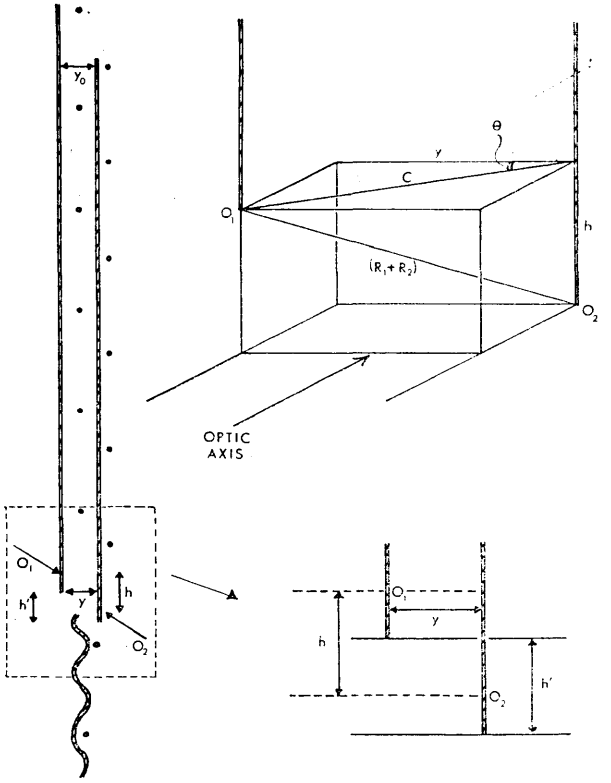

Figure 3. The geometry of a coalescence event.

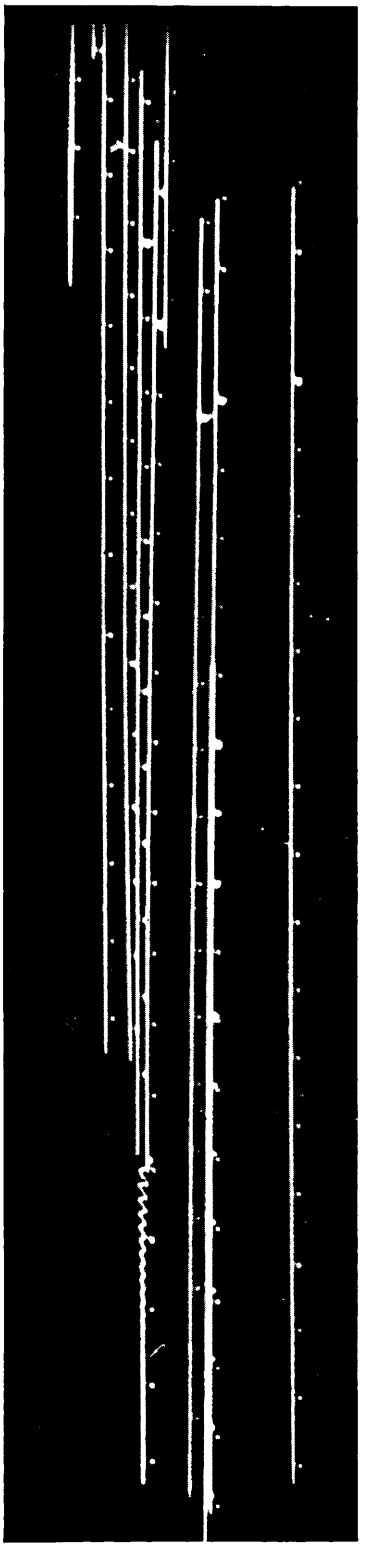

Figure 4. A streak photograph showing the coalescence of two drops of 62 μ radius.

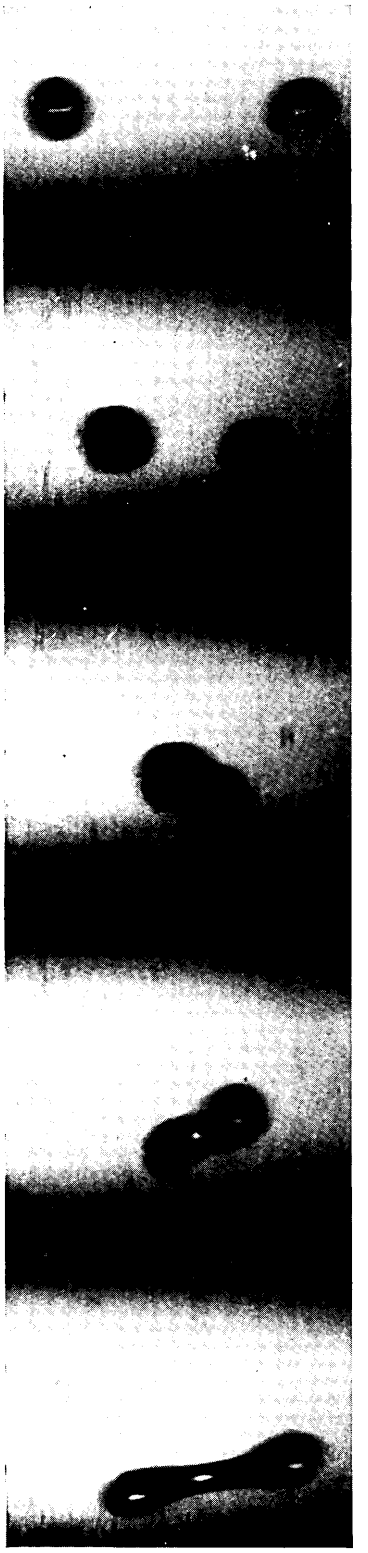

Figure 5. The coalescence of two drops of radius 120 μ impacting at a relative velocity of 3 m sec^{-1}. Photographs taken at 7,000 frames/sec.

Photographs such as Fig. 5 (Plate I) taken at 7,000/sec showed that, when two droplets of $R \simeq 50\ \mu$ collide, coalescence follows within $< 100\ \mu$ sec, and this is consistent with the fact that the period of oscillation of the resultant drop, as measured from the streak photographs, was 85 μ sec. The initial stages of coalescence therefore occur too rapidly to be recorded on the streak pictures and so the disappearance of the highlights may be taken as coincident with the onset of coalescence. Moreover, when the streaks disappear, the droplet centres, 0_1 and 0_2, are separated exactly by $(R_1 + R_2)$, the sum of their radii, the distortion of the drops being negligible before the onset of coalescence.

Referring to Fig. 3, we see that the parameter, c, defined as the horizontal separation of the droplet centres, is determined uniquely by this separation $(R_1 + R_2)$ and the vertical separation, h, of their centres at the moment of impact, i.e.,

$$h^2 + c^2 = (R_1 + R_2)^2, \quad . \quad . \quad . \quad . \quad (2)$$

If the drop sizes are unequal, Fig. 2 shows that

$$h = h' + (k_1 - k_2), \quad . \quad . \quad . \quad . \quad (3)$$

where h', and k_1, k_2, the displacements (vertical or horizontal) of the highlights from the drop centres, can all be measured directly from the photograph. If both drops are of the same size, $h = h'$. Now the impact parameter, c_0, for a collision is defined as the horizontal distance which separated the droplets when they started on their collision course at large vertical separations. Assuming that the relative horizontal orientation, θ, of the drops remains constant during their approach, c_0 is given by

$$\frac{c_0}{c} = \frac{y_0}{y} \quad , \quad . \quad . \quad . \quad . \quad . \quad (4)$$

where y is the projection of c on a plane normal to the optic axis (and is the horizontal separation of the streaks at the instant of their disappearance on the photographs), and y, is the corresponding separation of the streaks when the drops have large vertical separation. The collision efficiency, E*, may be defined as

$$E = \frac{{c_0}^2{}_{\max}}{(R_1 + R_2)^2} = \frac{{y_0}^2}{y^2}\left[1 - \frac{h^2{}_{\min}}{(R_1 + R_2)^2}\right] \quad , \quad . \quad . \quad (5)$$

where $c_{0\max}$ corresponds to $h_{\min}$, the minimum observed value of h. Now $h_{\min}$, y_0 and y may be measured from the photographs so that if R_1 and R_2 are known, E may be evaluated. Even for two identical drops, E is uniquely defined in terms of $c_{0\max}$ measured at the largest vertical separation at which interaction just becomes detectable. In practice the wake behind a drop has a finite effective length which, in the atmosphere, will be limited by random motions of the air and of neighbouring droplets.

The 1 m sec time markers allow the velocity of each drop and also the period of oscillation, τ, of a drop produced by coalescence to be measured. Using Rayleigh's formula

$$\tau = (3\pi\rho V/8\gamma)^{\frac{1}{2}} \quad . \quad . \quad . \quad . \quad . \quad (6)$$

where ρ and γ are respectively the density and surface tension of the drop, it was possible to determine its volume, V. This provided a useful check on the drop size and allowed us to distinguish between drops resulting from double and triple coalescences.

4. Evaluation of collection efficiencies

The main results may be stated very briefly. Drops of $R < 35\ \mu$ ($Re < 1$) did not appear to have wakes that were strong enough to attract identical drops into collision and coalescence. Many thousands of photographs of streams of droplets of $R \leqslant 35\ \mu$

* Experimentally we measure the collection efficiency = colllision efficiency × coalescence efficiency, but since we observe the coalescence efficiency to be unity (see later), the collection and collision efficiencies are numerically equal.

were examined without once finding the unmistakable oscillatory trace of a coalesced drop. To check that hydrodynamic attraction was not being counterbalanced by repulsive forces due to electric charges on the drops, 10 volt square-wave pulses were applied to the needle at half the frequency of droplet production, giving opposite charges to successive drops that were 100 times larger than those normally present. Although the electrostatic forces of attraction should now have overwhelmed the repulsive forces due to the original charges, the streak photographs showed no discernible changes in the droplet trajectories.

With drops of $35\ \mu < R < 40\ \mu$, occasional coalescences were observed, probably when two drops were brought into unusually close alignment as the result of small-scale eddying in the droplet stream.

Droplets of $40\ \mu < R < 100\ \mu$ had well-developed wakes and coalescences between pairs of equal-sized drops were relatively frequent. As the upper drop closed from 10 to within about 3 radii of the lower drop, it approached at nearly constant velocity, but, thereafter, showed a marked acceleration and nearly doubled its velocity of approach during the final stages. This is illustrated in Fig. 6, which shows velocity-time curves for a pair of drops of radius $62\ \mu$ and $Re = 3$. The velocity of the lower drop is unaffected by the interaction until 4 m sec (one diameter) before impact, when it increases noticeably, but not as rapidly as that of the upper drop. Theoretically, one should measure the initial horizontal separation, y_0, of the drops at very large vertical separations, i.e. at the very limit of the wake interaction. In practice, the field of view of the camera was limited by the minimum magnification required for adequate resolution of the streaks, so y_0 was measured when the drops were 10 radii apart. However, the photographs revealed that the trajectories of two interacting drops are nearly always accurately parallel right up to the moment of impact; in other words, within the limits of resolution of the photographs ($\sim 10\ \mu$), $y = y_0$ and $c_0 = c$, and so no serious error was introduced by the restricted field of view.

The values of E obtained from determinations of $c_{0\,\max}$. on about 30 pairs of drops of a given size are listed in Table 1. Because they are based on a limited sample of observations, these highest observed values of c_0 may not be identical with the maximum

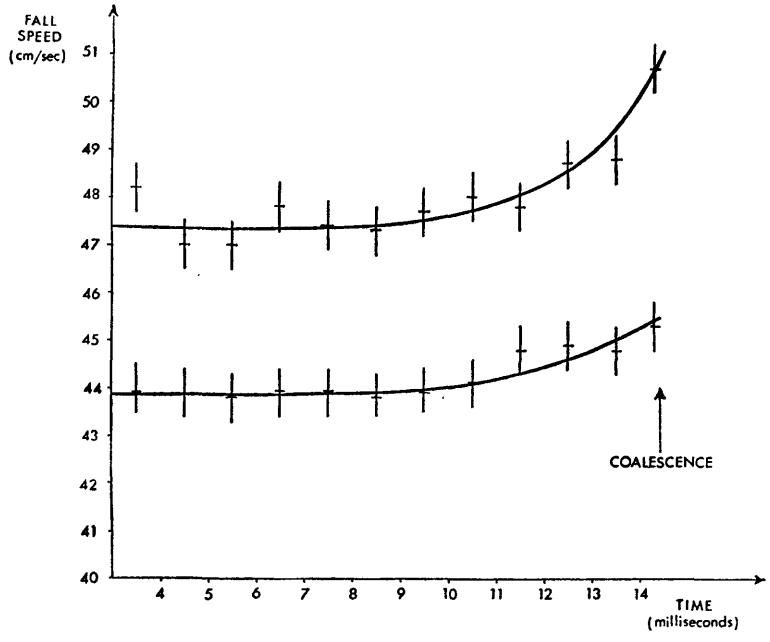

Figure 6. The fall-speeds plotted as a function of time for the two colliding drops of Figure 4.

possible values but, for a set of 20 observations, there is an 88 per cent probability that the tabulated values lie within 10 per cent of those that would be given by an infinite set of observations if all values of the initial horizontal separation are equally probable.

TABLE 1. EXPERIMENTAL VALUES OF COLLECTION EFFICIENCY

(a) Pairs of equal-size drops

$R_1 = R_2$ (μ)	E (highest value)	No. of events
35-45	0·5	14
45-55	0·7	30
55-65	0·85	34
65-75	0·9	36
75-85	0·95	8
85-95	0·9	2

(b) Pairs of unequal drops

R_1	R_2	E	No. of events
113	90	0·9	7
68	47	0·9	12
60	47	0·8	8
50	30	0·5	6

Because the highest observed impact parameters are, in fact, very close to the sum of the droplet radii, the collection efficiencies are close to unity. Drops resulting from a coalescence event were sometimes observed to take part in a second collision, the collection efficiency again being close to unity. Coalescence always followed collisions between drops of equal or non-equal size; we never observed a sharp divergence of the trajectories that would have indicated separation.

5. DISCUSSION OF RESULTS

Hundreds of collisions have been observed between drops of radius 35-100 μ, when the members of a colliding pair are either of equal size, or one has twice the mass of the other, and one member enters the wake of its partner. In no case has the measured collection efficiency exceeded unity and we find no evidence for one droplet being sucked laterally into the wake of the other. Consequently, our findings do not support the high values of collection efficiency ($E = 3{\cdot}15$ according to our definition) reported by Telford, Thorndike and Bowen. We acknowledge that our technique allows us to study the interaction between two droplets only when these are less than 10 radii apart. Although it seems likely that the probability of a collision will be largely determined by strong interactions between the drops at small separations, one cannot exclude the possibility that weaker interactions acting at larger distances for longer times may be decisive. On the other hand, the relative motion of the two drops is more likely to be influenced at large separations by fortuitous eddies in the air stream. Herein may be the reason for the difference between our results and those obtained by Telford *et al.* It appears that their ingenious method would be particularly valid if applied to the interaction of two classes each composed of drops of very uniform sizes. The present authors have set up such an experiment using two vibrating needles to produce drops of radius 50 μ and 30 μ. Using Eq. (1) with Δv set equal to the difference in the terminal velocities of the two classes of drops, we obtained a value for the collection efficiency of $E = 0{\cdot}65$, which is in good agreement with the value found by measurement of streak photographs.

Since in our experiments, the droplets in the stream are separated by only about ten drop radii, each drop lies in the wake of the preceding one. Although each drop falls at its terminal velocity relative to the air, interactions between neighbouring drops cause the air in the stream as a whole to move downwards at a rather greater velocity. However, if the velocity gradients across the air stream are not large enough to disturb the relative motions of two neighbouring drops, their collision behaviour should be the same as for two similar drops falling in still air. The velocity profile across the air stream carrying the drops was determined by measuring the fall speeds of equal-size drops falling through the stream. The velocity gradients were such that the maximum velocity difference likely to be imposed across two grazing drops each of radius 50 μ was 0·2 cm sec^{-1} or only 3 per cent of their relative velocity on impact.

The introduction of a fine aerosol into the chamber revealed the presence of eddies of order 1 cm in diameter in which the particles moved with a maximum velocity of only 5 mm sec^{-1}. Streak photographs showed that drops of $R \leqslant 40\ \mu$ moving in these eddies sometimes had slightly curved trajectories but, since two adjacent drops suffered similar displacements, the effect on their relative motion was probably negligible.

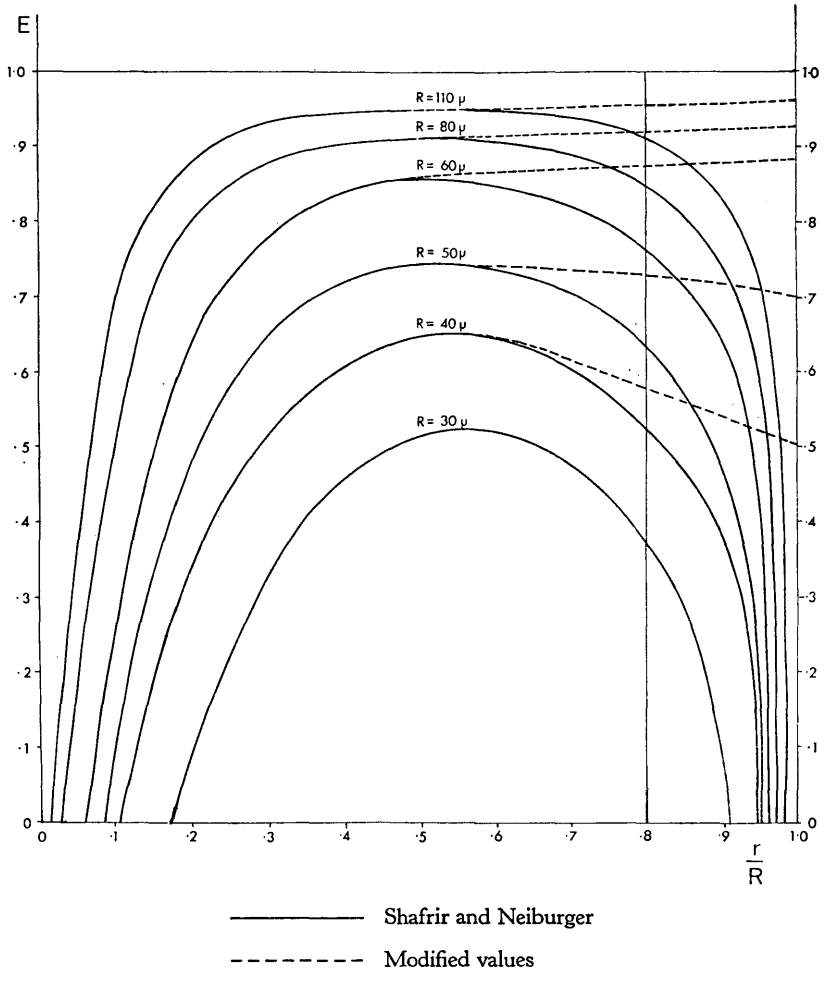

Figure 7. Tentative modification of the Shafrir and Neiburger plot of collection efficiency to show the effect of wake capture for drops of comparable size.

The values of collection efficiency E, in Table 1, are sketched in Fig. 7 to provide a tentative indication of how the curves of E against r/R are modified when wake capture is taken into account. For drop radii $40 < R < 100\ \mu$ and r/R ratios $> 0{\cdot}5$, collection efficiencies now assume values of between 0·5 and 1·0 instead of falling to zero as predicted theoretically by Shafrir and Neiburger (1963).

In natural clouds, identical drops having no difference of terminal velocity could collide only if brought one into the wake of the other, for example, by random motions of the air; even slightly dissimilar drops may interact more frequently through turbulent motions than by gravitational settling. Hence the frequency of such collisions cannot be calculated from the usual formula involving E and Δv (Δv being zero for identical drops); here one is concerned with the probability of one drop encountering the wake of a similar drop. However, in a non-precipitating cloud, the spatial concentration of drops of $R > 40\ \mu$ is so low, usually < 1/litre, that such droplet interactions will be very rare. Consequently, wake capture is unlikely to be of much importance in cloud physics.

References

Mason, B. J., Jayaratne, O. W. and Woods, J. D.	1963	*J. Sci. Instr.* **40**, p. 247.
Pearcey, T. and Hill, G. W.	1957	*Quart. J. R. Met. Soc.*, **83**, p. 77.
Shafrir, U. and Neiburger, M.	1963	*J. Geophys. Res.*, **68**, p. 4141.
Telford, J. W., Thorndike, S. C. and Bowen, E. G.	1955	*Quart. J. R. Met. Soc.*, **81**, p. 241.
Telford, J. W. and Thorndike, S. C.	1961	*J. Met.*, **18**, p. 32.
Woods, J. D. and Mason, B. J.	1964	*Quart. J. R. Met. Soc.*, **90**, p. 373.

Reprinted from the *Journal of Scientific Instruments*, VOL. 40, pp. 247–249, MAY 1963

An improved vibrating capillary device for producing uniform water droplets of 15 to 500μm radius

B. J. MASON, O. W. JAYARATNE and J. D. WOODS
Physics Department, Imperial College, London
MS. received 2nd January 1963, *in revised form 1st February* 1963

A vibrating capillary device, consisting of a hypodermic needle vibrated at its resonant frequency by an electromagnetically driven diaphragm, produces controllable and very uniform streams of drops of radius down to 15 μm. The size and frequency with which the droplets are produced depend upon the flow rate of the liquid through the needle, the needle diameter, its resonant frequency and the amplitude of oscillation of the needle tip. The device is being used to study the collision and coalescence of small water drops in air.

1. Introduction

In studying the collision, coalescence and rebound of small water droplets it is necessary to produce directed streams of water drops of very uniform size with radii in the range 15 to about 500 μm.

The most promising method involves the break-up of a mechanically vibrated jet of liquid, the theory of which was given by Rayleigh (1879). A device based on this principle was described by Dimmock (1950). The liquid flowed through a vertical glass capillary tube carrying a small steel armature which was moved to and fro by a small electromagnet energized by a 50 c/s alternating current. The length of the capillary was adjusted until it resonated at the applied frequency and then several streams, each composed of uniform size droplets, were flung off the tip in different directions.

Our experience with such a device is that it is very difficult to obtain reproducible and stable modes of vibration and that the sizes and directions of the streams are very variable and difficult to control; in effect, one has to take whatever streams are being produced at the time. Schotland (1960) reports that he has used a vibrating hypodermic needle to produce drops in the radius range 150 to 500 μm, but gives no further details. We now describe a sharply tuned, stable, vibrating needle device capable of producing controllable streams of droplets of radius down to 15 μm.

2. Construction and operation

A general view of the device is shown in figure 1 and the details of construction in figure 2. A stainless-steel hypodermic needle N, through which water is forced at a constant rate, fits snugly into a small central hole in the cylindrical spigot S, which is cemented to the centre of an iron diaphragm D of an electromagnetically driven earphone. The energizing coil C of the electromagnet M is connected to an audio-frequency oscillator and causes the needle to be vibrated

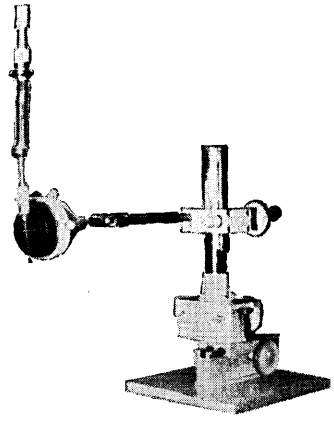

Figure 1. A general view of the vibrating capillary apparatus.

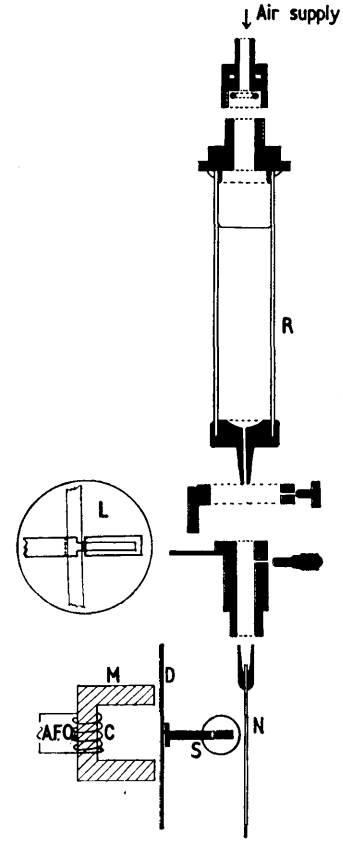

Figure 2. Constructional details of the vibrating capillary device.

mechanically by the movement of the diaphragm and spigot. The frequency of the oscillator is varied until the tip of the needle vibrates in a resonant mode with an amplitude of several millimetres. The resonance frequency, which is determined not only by the characteristics of the needle but also by the masses and dimensions of the diaphragm and

spigot, is quite sharp. For example, a 4 cm, 30 gauge Record needle driven at a point 3 cm from its tip resonated at about 300 c/s, a change of ± 10 c/s being sufficient to damp the oscillations completely.

The stability of the droplet stream is particularly dependent upon the flow rate of the liquid and it is essential to keep this constant. Instead of using a large constant head, the water is forced from the reservoir R by compressed air. The air supply is maintained at constant pressure, short-term fluctuations being minimized by the use of a large buffer vessel. A pressure head of 5 lb in^{-2} produces a flow rate of about 50 ml. h^{-1}.

To ensure that the needle vibrates in the same stable mode for long periods it is necessary to prevent it moving in the spigot; this is achieved by the small locking device L shown inset in figure 2.

Observation through the microscope of the needle tip, when it is illuminated by a stroboscopic lamp flashing at near the resonance frequency, reveals that for a given needle and amplitude of vibration, a critical volume of liquid has to accumulate before it is flung off by a change in direction of the needle. At low flow rates the needle may execute several oscillations before the critical volume is reached and there is a tendency for this to be ejected as a single drop. As the flow rate is increased, a single drop may be ejected at each turning point of the needle and finally, at high flow rates, the issuing liquid is drawn out into a thread by the receding tip and this usually breaks up into a series of progressively smaller masses. For a given orifice diameter, the length of the thread increases with the pressure head and, for a given pressure head, the length of the thread increases with increasing diameter of the orifice. After travelling only about 1 cm through the air, the drops assume a spherical shape. Drops of differing sizes are projected in different directions and produce separate streams the number of which may also be controlled by the frequency and amplitude of the vibrations.

When the frequency of the stroboscope is adjusted to that of the needle vibrations, the tip of the needle and all the droplet streams appear stationary indicating that all the droplets in any one stream are of uniform size, see figure 3. If the needle vibrates in only one plane, the major and satellite streams are almost coplanar but, more usually, the tip executes a circle, ellipse or figure of eight, and then the droplets are flung off in different directions as the tip makes sharp changes of direction.

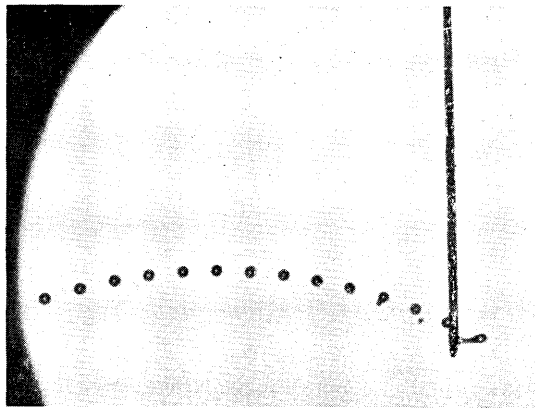

Figure 3. A thread of liquid issuing from the tip of the hypodermic needle and breaking up into a main stream of uniform droplets and a stream of satellite droplets which, in this case, are coalescing with the larger ones.

3. Control of droplet size and frequency

We have seen that the size and frequency with which droplets are produced depend critically upon the flow rate of the liquid. Other factors which influence the mode of disintegration of the liquid thread are the needle diameter, its resonant frequency and the amplitude of vibration.

3.1. *Needle tip diameter*

A standard 30 gauge hypodermic needle (bore diameter 140 μm) with a 30° chamfered tip was used to produce drops of radius 80 to 200 μm at frequencies of about 300 per second. By adjusting the amplitude of vibration and the flow rate of the liquid it was possible to obtain a single stable droplet stream of any desired radius between 140 and 200 μm. Smaller droplets were obtained by selecting a stable satellite stream.

To produce even smaller droplets the needle tip was modified by grinding it square, redrilling the bore with a 0·2 mm drill and inserting a 5 mm length of 0·1 mm inside diameter steel tube which protruded about 2 mm from the tip. In this way it was possible to produce stable streams of droplets of radius as small as 15 μm, at resonance frequencies of between 500 and 1000 c/s.

Drops of radius greater than 200 μm are readily produced with needles of larger gauge.

3.2. *Resonance frequency*

This can be varied to some extent by varying the length of the needle and the thickness, diameter or loading of the diaphragm and, in some cases, by using the second harmonic of the fundamental frequency. In tuning the device it is necessary to avoid frequencies that set up sympathetic vibrations in the supports and cause instability.

3.3. *Amplitude of vibration*

It is often convenient to fix the flow rate of the liquid and to vary the drop size slightly by adjusting the output of the audio-frequency oscillator and hence the amplitude of the needle oscillation.

4. Some applications of the device

The vibrating capillary is being used to study the coalescence of water droplets falling on a plane water surface. The droplets are first rendered uncharged by applying a suitable neutralizing voltage to the needle. The droplet stream is allowed to fall into an insulated induction can connected to a sensitive electrometer and the voltage adjusted until zero current is recorded. Figure 4(*a*) shows a stream of droplets, of 100 μm radius, bouncing three times on a plane water surface. When, however, an electric field of only 20 v cm^{-1} is applied normal to the surface, attraction between the induced charges on the drops and their image charges in the earthed water surface ensures coalescence as shown in figure 4(*b*).

The vibrating head is mounted on a universal rotating joint and attached to a three-way carriage that allows translational movements in three mutually perpendicular directions. In this way the droplet streams from two needles

can be brought into alignment. Figure 5 shows two such streams colliding and coalescing to form one single stream.

These experiments will be described in more detail elsewhere.

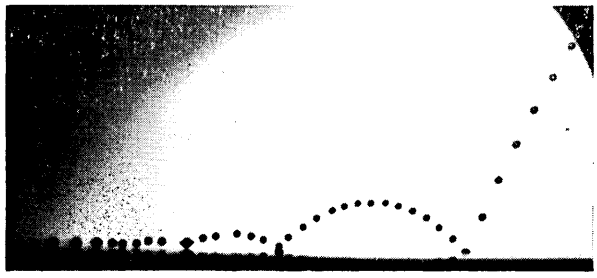

Figure 4. (*a*) A stream of 100 μm radius water drops making three successive bounces on a plane water surface.

(*b*) The drops coalesce with the water surface when a vertical electric field of 20 v cm^{-1} is applied.

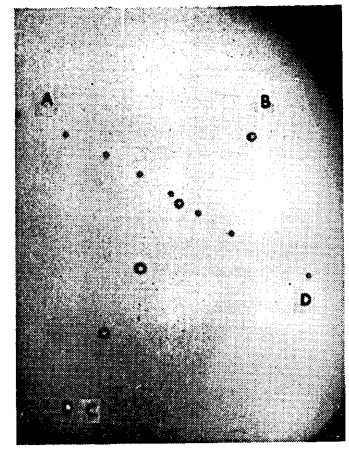

Figure 5. Two interacting streams A, B of drops from two separate needles. The drops coalesce to produce stream C, leaving gaps in stream D.

Acknowledgments

We are grateful to Mr. B. Dahlbom for suggesting that we use an earphone to drive the needle.

References

DIMMOCK, N. A., 1950, *Nature, Lond.*, **166**, 686.
RAYLEIGH, LORD, 1879, *Proc. Roy. Soc.*, A **29**, 71.
SCHOTLAND, R. M., 1960, *Disc. Faraday Soc.*, No. 30, 72.

UNWIN BROTHERS LIMITED, WOKING AND LONDON